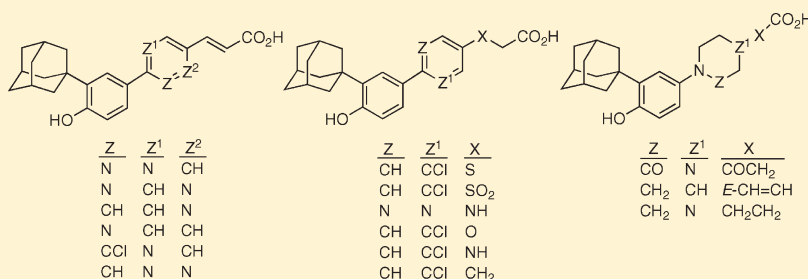# Heteroatom-Substituted Analogues of Orphan Nuclear Receptor Small Heterodimer Partner Ligand and Apoptosis Inducer (*E*)-4-[3-(1-Adamantyl)-4-hydroxyphenyl]-3-chlorocinnamic Acid

Zebin Xia,[†] Lulu Farhana,[‡] Ricardo G. Correa,[†] Jayanta K. Das,[‡] David J. Castro,[†] Jinghua Yu,[†] Robert G. Oshima,[†] John C. Reed,[†] Joseph A. Fontana,[‡] and Marcia I. Dawson*,[†]

[†]Cancer Center, Sanford-Burnham Medical Research Institute, La Jolla, California 92037, United States
[‡]Department of Veterans Affairs Medical Center and Wayne State University School of Medicine, Detroit, Michigan 48201, United States

S *Supporting Information*

ABSTRACT:

Z	Z¹	Z²
N	N	CH
N	CH	N
CH	CH	N
N	CH	CH
CCl	N	CH
CH	N	N

Z	Z¹	X
CH	CCl	S
CH	CCl	SO₂
N	N	NH
CH	CCl	O
CH	CCl	NH
CH	CCl	CH₂

Z	Z¹	X
CO	N	COCH₂
CH₂	CH	E-CH=CH
CH₂	N	CH₂CH₂

(*E*)-4-[3′-(1-Adamantyl)-4′-hydroxyphenyl]-3-chlorocinnamic acid (3-Cl-AHPC) induces the cell cycle arrest and apoptosis of cancer cells. Because its pharmacologic properties—solubility, bioavailability, and toxicity—required improvement for translation, structural modifications were made by introducing nitrogen atoms into the cinnamyl ring and replacing its *E*-double bond with XCH₂ (X = O, N, and S) with the objective of enhancing these properties without impacting apoptosis-inducing activity. Analogues having nitrogen atoms in heterocyclic rings corresponding to the cinnamyl phenyl ring displayed equal or higher biological activities. The pyrimidine and pyridine analogues were more soluble in both phosphate-buffered saline and water. While the 2,5-disubstituted pyridine analogue was the most potent inducer of KG-1 acute myeloid leukemia cell apoptosis, on the basis of apoptotic activity in KG-1 cells and solubility, the 2,5-disubstituted pyrimidine proved to be the more promising candidate for treatment of acute myeloid leukemia.

■ INTRODUCTION

Several classes of retinoid-related small molecules—peptidomimetic analogues of *N*-(4-hydroxyphenyl) all-*trans*-retinamide (4-HPR) and its β-glucuronide, diaryl-substituted thioureas such as SHetA2, and analogues of the parent phenol of the 1-adamantyl-substituted retinoid and antiacne drug adapalene—are undergoing development as promising apoptotic agents for treatment of cancer and leukemia.[1−9] In the 1-adamantyl (1-Ad)-substituted series, the prototype 6-[3′-(1-adamantyl)-4′-hydroxyphenyl]-2-naphthalenecarboxylic acid (AHPN∞/CD437[3] **1** in Figure 1), while originally reported as a retinoic acid receptor (RAR) γ-selective transcriptional agonist,[10] was first identified by the Fontana and Dawson groups as an inducer of apoptosis of cancer and leukemia cell lines regardless of their sensitivity to growth inhibition by all-*trans*-retinoic acid (ATRA).[1,11] On this basis, analogues of **1** were synthesized and evaluated to optimize apoptosis-inducing activity, while reducing that associated with RAR transactivation, which is associated with the hypervitaminosis A syndrome.[12] Results from structure—activity studies using

assays for reversal of keratinization in vitamin A-deficient hamster trachea in culture (TOC assay)[13] and inhibition of tumor promoter-induced ornithine decarboxylase activity in mouse epidermis (ODC assay)[14] led us to mimimize retinoid activity by substituting the *E*-cinnamic acid moiety for the naphthalene-2-carboxylic acid ring of **1** in the design of (*E*)-4-[3′-(1-adamantyl)-4′-hydroxyphenyl]cinnamic acid (AHPC, **4**) in 1997. Unfortunately, administration of **1** or **4** to mice caused adverse systemic effects.[4] The synthesis and apoptosis-inducing activity of **4** were reported in the open literature by Sigma-Tau Pharmaceuticals in 2003.[15]

This group also reported the transcriptional activation of the retinoic acid nuclear receptor (RAR) subtypes α, β, and γ on an RARE reporter construct by **1** and **4**. RAR α, β, and γ activations induced by 0.1 μM **1** were approximately 10-, 20-, and 50-fold, respectively, above basal levels, and those induced by 0.1 μM **4**
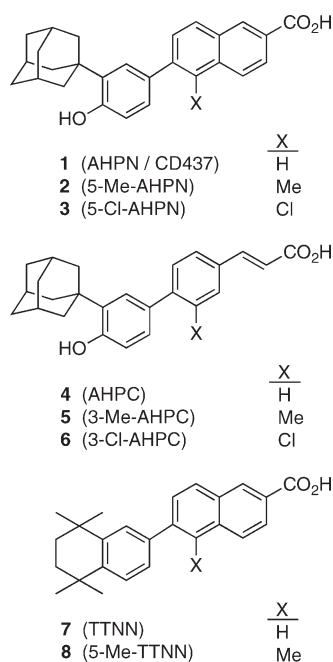
Figure 1. Structures of 1-Ad-substituted retinoid-related compounds **1**−**6** and their retinoid precursors tetrahydronaphthyl-substituted **7** and **8**.

were 6-, 6-, and 25-fold, respectively, above basal levels.[15] On the $(TREpal)_2$-tk-CAT reporter, the transcriptional activations of RARs α, β, and γ induced by 1.0 μM **1** were 21, 78, and 88%, respectively, of those induced by 1.0 μM ATRA, while those by 1.0 μM **4** were 8, 85, and 103%, respectively.[5] Despite having reduced ability to activate RARα, **4** retained its apoptotic activity (Table 1).

Earlier collaborative structure−activity studies with the Pfahl, Schiff, and Sani groups established that introducing a methyl group at the 5-position of the naphthalene ring of the retinoid **7** resulted in decreased retinoid activity in the 5-methyl analogue **8** so that the EC_{50} values in the TOC, ODC, and F9 teratocarcinoma cell assays, which are commonly used to measure retinoid activity, were 11-, 33-, and 3-fold, respectively, higher than those displayed by **7**. This methyl substitution strategy was based on the 1983 report by Strickland et al.[16] that the retinoid activity profile of 3′-methyl-TTNPB was differentially modified as compared to that of TTNPB by the addition of the 3′-methyl group. In terms of their EC_{50} values, 3′-Me-TTNPB was 15-fold more potent than TTNPB in inhibiting the growth of HL-60 myeloid leukemia cells but had 1.5% of the activity of TTNPB in inducing the differentiation of F9 cells.

Subsequently, the introduction of halogen on the tetrahydronaphthalene ring or a nitrogen into the benzoic acid ring ortho to the 1,1-ethenyl bridge of the retinoid X receptor (RXR) ligand bexarotene was also observed to diminish RAR transactivation activity in bexarotene analogues.[17,18] While the methyl-substituted analogues **2** and **5** exhibited diminished retinoid activity as compared to **1** and **4**, introducing a chloro group at the same position in **3** and **6** robustly impaired their interaction with RARα and RARβ as demonstrated by substantially reduced binding affinities and also inhibited RARγ transactivation. Although **3** bound weakly to the RARγ ligand-binding domain (LBD), it was unable to induce the LBD to assume the compact conformation that is characteristic of transcriptional agonist binding,

as we first demonstrated by time-dependent proteolysis.[5] In contrast, the proteolysis of the RARγ LBD complexed with the RAR transcriptional agonist 9-cis-retinoic acid was substantially reduced as compared to that of the apo-LBD.[5] Crystallography has shown that the binding of a transcriptional agonist such as ATRA to the RARγ LBD produced shifts in the positions of helices H3 and H11 that allowed helix H12 to move from an extended position to the LBD surface to form the activation function (AF)-2 groove with helices H3 and H4.[19] Generation of the AF-2 groove induced by agonist binding then permits coactivator recruitment by the LBD leading to gene transcription. Such helical shifts caused the RARγ LBD to become more compact and, therefore, more resistant to time-dependent proteolysis.[20]

Computational studies employing density functional theory revealed that the favored torsion angles (10−30°) for the diaryl bonds of free **1** and **4** oriented their 1-Ad groups in positions that were nearly planar with the aromatic rings of their carboxylate termini.[5] In contrast, molecular dynamics studies suggested why chloro-substituted **3** did not function as an RARγ agonist. The most highly preferred poses for **3** in docking to the RARγ LBD favored larger diaryl bond torsion angles (30−50°). With the position of the carboxylate group of **3** constrained by ionic and hydrogen bonding with the guanidinium group of arginine (R) 278 in helix H5 of the LBD, the larger torsion angles oriented the bulky 1-Ad group of **3** in positions that blocked helix H11 from assuming an agonist orientation that would allow helix H12 to shift to form the AF-2 groove.[5] The results of the proteolytic studies and docking were supported by the inability of **3** to transcriptionally activate the RARs α, β, and γ on the $(TREpal)_2$-tk-CAT reporter construct. The transactivations of these RAR subtypes induced by 1.0 μM **3** and **6** were within experimental error of 0%, namely, −3, −7, and 8% and 0, 5, and 10%, respectively, of the levels (100%) induced by 1.0 μM ATRA. The lack of RAR activation activity accompanied by the retention of apoptotic activity demonstrated that apoptosis induction by these 1-Ad-substituted retinoid-related compounds (ARRs) was independent of RAR activation.[5−7]
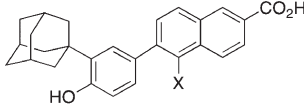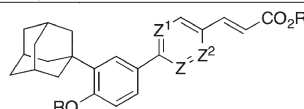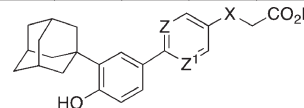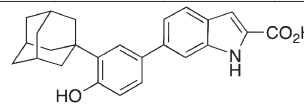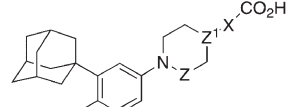
Although the signaling pathway by which these ARRs induce apoptosis remains to be fully discerned, their therapeutic potential as anticancer agents is promising because of their ability to induce apoptosis of a wide variety of cancer and leukemia cell lines[21−25] and that of leukemia cells from patient samples.[4] Moreover, the ARRs offer the advantage of inducing apoptosis independent of the pathways activated by the tumor suppressor protein p53, the activity of which is lost in approximately 50% of cancers.[26,27] By functioning independently of the RARs, adverse effects associated with administering retinoids for cancer therapy[28] would also be minimized.[1,11] Although the therapeutic index (efficacy vs toxicity dose ratio) of **6** was improved in an acute myelogenous leukemia (AML) murine model as compared to **1** or **4**; at higher doses, **6** retained some toxicity.

To further improve pharmacologic properties such as toxicity, solubility, and bioavailability to permit lower dosing, three strategies were employed, namely, (i) introducing N atoms into the cinnamyl ring of the scaffold of **4**, (ii) replacing its cinnamyl ring with a saturated heterocyclic ring, and (iii) replacing its cinnamyl E-double bond by XCH_2 (X = O, N, S). Below, we report the syntheses of these heteroatom-substituted analogues of **4** and **6** and their effects on inhibiting cancer cell proliferation and inducing apoptosis.

■ RESULTS

Chemistry. In Schemes 1−3 are illustrated the routes used for the syntheses of 17 heterosubstituted analogues having

Table 1. Effects of Heteroatom Substitution in the AHPC Cinnamyl Phenyl Ring and Side Chain on Inhibition of Acute Myeloid Leukemia Cell Proliferation and Induction of Apoptosis as Compared to 1, 4, and Their Chloro-Substituted Analogues 3 and 6

Scaffold (naphthalene, CO₂H, substituent X):

compound	X	growth inhibition (%) KG-1 AML at 48 h 1.0 µM	5.0 µM	apoptosis (%) KG-1 AML at 48 h 1.0 µM	5.0 µM	HL-60R leukemia at 24 h 0.1 µM	1.0 µM
1 (AHPN / CD437)	H					73	98
3 (5-Cl-AHPN)	Cl					62	94

Scaffold (propenoate side chain; variables Z, Z¹, Z², R, R¹):

compound	Z	Z¹	Z²	R	R¹	1.0 µM	5.0 µM	1.0 µM	5.0 µM	0.1 µM	1.0 µM
4 (AHPC)	CH	CH	CH	H	H					90	98
6 (3-Cl-AHPC)	CCl	CH	CH	H	H	44	67	30	55	51	94
34	N	CH	CH	H	Et	0	45	0	0		
38	CCl	N	CH	H	H	41	47	56	65		
39	CH	CH	N	H	H	48	58	36	52		
40	N	CH	CH	H	H	85	90	68	84		
41	CH	N	N	H	H	44	61	39	50		
42	N	N	CH	H	H	100	100	40	50		
43	N	CH	N	H	H	70	80	48	59		
44	N	CH	CH	Ac	H	46	54	52	67		

Scaffold (X–CH₂CO₂H side chain; variables Z, Z¹, X):

compound	Z	Z¹	X	1.0 µM	5.0 µM	1.0 µM	5.0 µM		
74	N	N	NH	0	0	0	0		
75	CH	CCl	NH	30	45	18	35		
76	CH	CCl	O	34	75	5	25		
77	CH	CCl	S	7	11	2	5		
78	CH	CCl	SO₂	7	13	2	6		
79	CH	CCl	CH₂	0	0	0	1		
83				1	8	1	3		

Scaffold (indole-2-carboxylic acid) for compound 83; piperazine scaffold (variables Z, Z¹, X):

compound	Z	Z¹	X	1.0 µM	5.0 µM	1.0 µM	5.0 µM
98	CH₂	CH	CHCH	1	2	1	1
99	CH₂	N	CH₂CH₂	−3	5	1	1
100	CO	N	COCH₂	−2	−5	1	2

modifications of the central cinnamyl rings and side chains of 4 and 6. The synthetic routes are straightforward and differ mainly in which of the two reactive groups on the 1,4-disubstituted central ring precursors was elaborated first to introduce the remainder of the scaffold. In cases where the central ring was aromatic (Schemes 1 and 2), the central diaryl bond was generated by a Suzuki—Miyaura palladium-catalyzed coupling reaction[29] using the arylboronic acid 25, which had been synthesized in three steps as we previously reported.[6] Either a Wittig olefination or a Heck coupling reaction was used to introduce the E-propenoate group.

In Scheme 1, the syntheses of pyridines 38—40, pyridazine 41, pyrimidine 42, and pyrazine 43 were undertaken to explore the effects of π-deficient mono- and diaza-substituted heteroaromatic rings on cell cycle arrest and apoptosis induction. Analogues 40 and 43 have one N atom adjacent to the diaryl bond to reduce interaction with the RARs, whereas 42 has two such adjacent N atoms, and 38 has both an adjacent N atom and an ortho Cl ring substituent. In contrast, 39 has its N atom on the ring meta to the diaryl bond.

In this series, the side chain was introduced prior to the diaryl bond. Wittig reaction of heteroaryl aldehydes 10—12 and 14 with

carboxymethylene(triphenylphosphorane) introduced the *E*-3-propenoate group of **19**−**22** in yields of >94%. Yields of the *Z* isomer were <10% as determined by HPLC and NMR. The *E* isomer was readily isolated by crystallization from hexane (62−89% yields). Use of the Heck coupling of heteroaryl halides with ethyl (*E*)-propenoate to introduce the side chain in **22**−**24** was less successful. Only the 2-chloropyrimidine **16** effectively coupled to produce **23** in 74% yield, whereas despite attempts to enhance reactivity by using an arylbromide (**15**) or replacing the chloro group of **17** with the more reactive iodo group (**18**), both **15** and **18** only afforded coupling products **22** and **24** in 8 and 8.5% yields, respectively, and byproduct. A review of the chemical literature did not indicate a precedent for Heck coupling on 2,5-dibromopyrazine or 3-chloro-6-iodopyridazine. However, a high yield (83%) of a 2,3-disubstituted pyrazine was obtained in the Heck coupling of 2,3-chloropyrazine with ethyl acrylate using palladium diacetate and dicyclohexyl (2,4,6-triisopropylbiphen-2-yl)phosphine at 90 °C.[30] Use of higher temperatures produced reduced and dehalogenated byproduct. Diaryl coupling of intermediates **19**−**24** with **25** resulted in **26**−**31**, from which **38**−**43** were produced by a two-step deprotection sequence (BBr₃-mediated benzyl ether cleavage at −78 °C followed by ester hydrolysis). Unoptimized diaryl coupling yields varied from 8 to 96%, and as expected, the heteroaryl bromides produced higher yields than the corresponding chlorides with the exception of the activated 2-chloro-1,3-pyrimidine **23**, which gave **30** in 96% yield. The overall optimized yield for preparation of the 2,5-disubstituted pyrimidine **42** from **16** (four steps) was 61%. Acetylation of the 2,5-disubstituted pyridine **40** provided **44**.

In Scheme 2 are presented the syntheses of side chain-modified analogues having the *E*-double bond of **6** or **42** replaced by (CH₂)₂ (**79**), NHCH₂ (**74** and **75**), OCH₂ (**76**), SCH₂ (**77**), or SO₂CH₂ (**78**). In addition, the effect of tethering the double bond to the central phenyl ring was explored in benzimidazole **83**, in which the indole ring N atom was used as the tether. Although we previously determined that introducing a Cl or Me group at the 2-position of the cinnamyl ring led to loss of apoptotic activity,[31] we speculated that including the tether in a 5-membered ring might ameliorate bulk so as to permit some activity. In addition, we had observed that this strategy had reduced retinoid activity in the benzothiophene analogue of the retinoid (*E*)-6-[2-(2,6,6-trimethylcyclohexenyl)ethenyl]-2-naphthalenecarboxylic acid.[32] Their respective EC₅₀ values in the TOC assay for retinoid activity were 1.0 and 0.1 nM.

Suzuki coupling of **45**, **47**, and **48** with **25** was used to form the diaryl bond in three intermediates—the 2-phenyl-4-nitropyrimidine **49**, 2-chloro-4-nitrobiphenyl **51**, and 2-chloro-4-phenylphenol **53**—before the heteroatom-substituted and alkyl side chains were introduced. The side chain of **64** was directly introduced by alkylation of the phenolate of **53** with ethyl bromoacetate, whereas the nitro groups of **49** and **51** were first reduced to give the corresponding amines **50** and **52**, which were then alkylated to provide **62** and **63**, respectively.

In contrast, the side chains of **65**−**67** were introduced first. Compound **54** was converted to the thiophenol **55** by diazotization followed by treatment with potassium ethyl xanthate and hydrolysis.[33] Akylation of the thiophenolate of **55** with bromoacetate produced **60**. Compound **56** was diazotized using a procedure suitable for hydrophobic compounds and then treated with cuprous bromide to introduce the bromo group of **57**,[6] the cyano group of which was then reduced using DIBAL to provide the benzaldehyde **58**. The Wittig reaction of Scheme 1 was used to elaborate **58** to the cinnamate **59**. Hydrogenation of its double

bond produced the 3-phenylpropanate **61**. Suzuki coupling of **60** and **61** with **25** afforded **65** and **67**, respectively. Oxidation of the thioether bond of **65** afforded sulfone **66**. Deprotection of **65**−**67** produced the side-chain modified series **77**−**79**.

In Scheme 3 are shown the syntheses of the aza-substituted saturated cyclic ring series comprised of piperidine **98** and piperazines **99** and **100**. Computational studies suggested that the low-energy conformers of **98**−**100** would have interatom distances between their 4′-C atom bearing the phenolic OH and the carboxylate C atom of 10.8, 10.8, and 10.0 Å, respectively, as compared to 12.0 Å for **6**. These distances suggested that **98**−**100** could occupy the small heterodimer partner (SHP) ligand-binding pocket (LBP) if the increased bulk of the chair forms of their saturated rings and increased electronegativities did not preclude binding. Although **98**−**100** only have slightly larger overall volumes (respective increases of 2.0, 0.27, and 0.87%) than **6** (366.7 Å³), only **98** having the *E*-propenoic acid terminus of **6** was capable of docking to the SHP homology model.[34]

The first step in the synthetic sequences for **98**−**100** was introducing their central anilino-N bonds. These bonds in precursors **89**, **92**, and **93** were generated in respective yields of 78, 65, and 69% by the palladium-catalyzed coupling[35] of **84** and **85** with **86** (the precursor of **25**) and the copper(I)-catalyzed coupling[36] of **87** with the phenyl iodide **88**, respectively. The side chains of **98** and **100** were introduced next. The carbethoxy group of **89** was reduced by DIBAL at −78 °C to the piperidinecarboxaldehyde **90**, which was then elaborated to the *E*-propenoate **91** by a Wittig olefination. Piperazine **93** was acylated with ethyl 3-chloro-3-oxopropanoate to produce **94**. Deprotection of **91**, **92**, and **94** afforded **98**, **99**, and **100**, respectively.

Biological Studies. *Apoptotic and Antiproliferative Activities.* The 17 analogues were first evaluated for their abilities to inhibit the proliferation and induce the apoptosis of human KG-1 AML cells in culture in comparison with **6** as a positive control (Table 1). KG-1 cells are known to express wild-type p53 but are resistant to such chemotherapeutic drugs as etoposide and daunorubicin, and the antibody—drug conjugate gemtuzumab ozogamicin.[37,38] In contrast, HL-60R human myelocytic leukemia cells, in which p53 is null,[39] are resistant to the growth inhibitory effects of ATRA. The apoptosis-inducing activities of **1**, **3**, **4**, and **6** against HL-60R cells have also been included in Table 1 for comparison purposes. The most potent inhibitor of HL-60R cell growth after treatment for 24 h was **4** and was followed in potency by **1**, **3**, and then **6**. In this series, however, the severity of adverse effects on systemic administration to the mouse did not correlate with HL-60R growth inhibition so that **6** had the most favorable therapeutic ratio.

The analogues with the highest apoptotic activity after 48 h of treatment of KG-1 AML cells were the nitrogen-containing aromatics having *E*-propenoic acid side chains. The most potent in this series was the 2,5-disubstituted pyridine **40**, probably due, in part, to its increased solubility as compared to that of **6**. The relative aqueous solubilities of **6**, **40**, and **42** were assessed in phosphate-buffered saline (PBS) and in distilled water. In PBS (physiologic pH of 7.2) at room temperature (22 °C), **6** could not be detected by UV measurement at its absorption maximum, whereas **40** and **42** produced maximum concentrations of 14 μM and 0.44 mM, respectively. In water at room temperature (pH 5), the respective maximum concentrations of **6**, **40**, and **42** were 4.5, 7.0, and 54 μM.

Dose−response curves for **6**- and **40**-mediated growth inhibition and apoptosis induction over 24 and 48 h time periods, which are shown in Figure 2A,B, indicate that **40** was more efficient at inhibiting growth and inducing apoptosis of KG-1 cells. Moreover, efficacy at 48 h was higher than that observed

Scheme 1. Synthesis of 38−44[a]
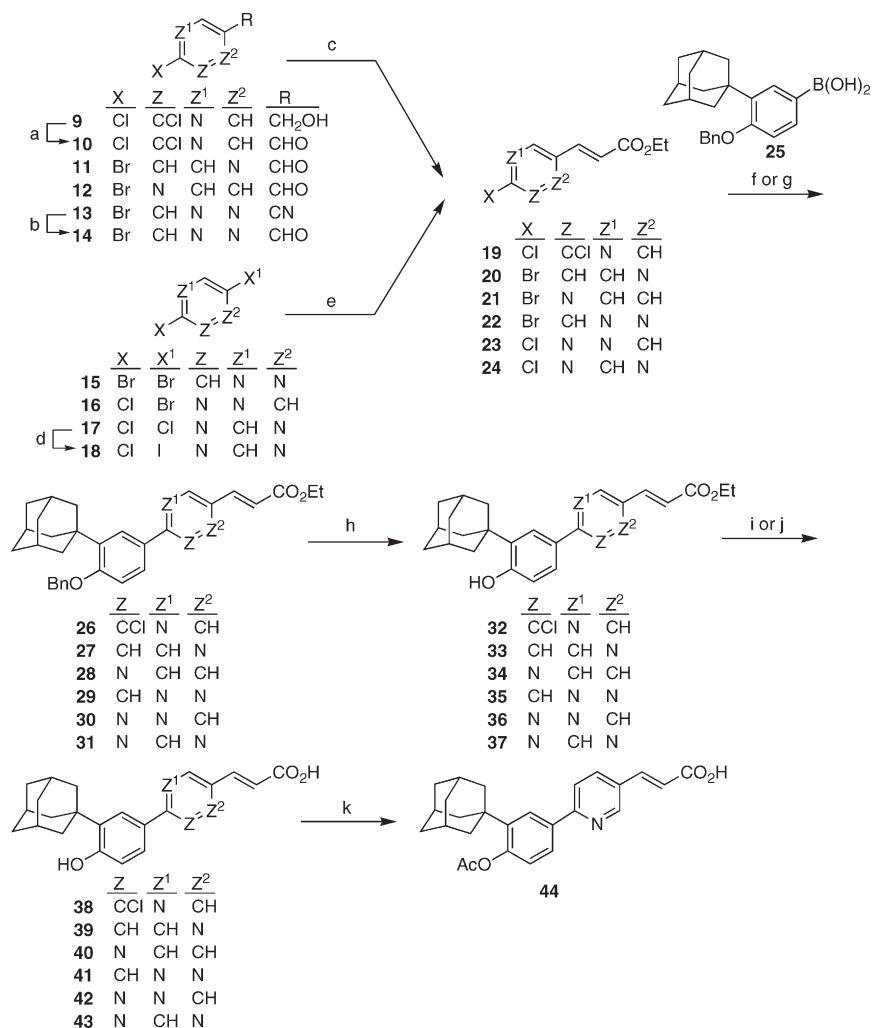
[a] Reagents and conditions: (a) 5,6-Dichloro-3-(hydroxymethyl)pyridine, MnO_2, CH_2Cl_2, hexane. (b) DIBAL, MePh, −78 °C to room temperature; MeOH; 10% H_2SO_4. (c) Compounds 10−12 and 14: (carbethoxymethylene)Ph_3P, MePh, reflux. (d) NaI, HI, 44 °C. (e) Compounds 15, 16, and 18: CH_2=$CHCO_2Et$, Pd(OAc)$_2$, DMF, (i-Pr)$_2$EtN, (o-MePh)$_3$P, 115 (15 and 16) or 111 °C (18). (f) Compound 19: 3-(1-adamantyl)-4-benzyloxyphenylboronic acid (25), 1,1′-(Ph$_2$P)$_2$ferrocenedichloropalladium(II)·CH_2Cl_2, DME, Cs_2CO_3, 75−90 °C. (g) Compounds 20−24: 25, Pd(PPh$_3$)$_4$, DME, 2 M aqueous Na_2CO_3, reflux. (h) BBr$_3$, CH_2Cl_2, −78 °C; H_2O. (i) Compound 32: LiOH·H_2O, THF/MeOH/H_2O, 0 °C; H_3O^+. (j) Compounds 33−37: aqueous NaOH, MeOH, reflux; H_3O^+. (k) Compound 40: Ac$_2$O, DMAP, THF.

after 24 h indicating a dose response. Evaluations were extended to the retinoid-resistant MDA-MB-231 human breast cancer cell line, which expresses p53 as a nonfunctional mutant and estrogen receptor (ER) β, but not ERα,[40,41] and has high levels of antiapoptotic Bcl-2 protein.[42] Again, 40 was more active than 6 in a dose- and time-dependent manner in inhibiting the growth and inducing apoptosis of MDA-MB-231 cells (Figure 2C,D). At 1.0 μM, 40 produced 86 and 85% growth inhibition at 24 and 48 h, respectively, whereas the respective levels of apoptosis as assessed by DNA fragmentation were 38 and 82%. In contrast, treatment with 1.0 μM 6 for 24 and 48 h inhibited proliferation by 8 and 43% and induced 3 and 7% apoptosis, respectively. Unfortunately, the higher apoptosois-inducing activity of 40 was accompanied by higher toxicity in the mouse.

Preliminary efforts at modifying 40 to attenuate toxicity included modulating systemic concentrations by derivatization of its carboxylic acid group as the ethyl ester (34) or its phenolic hydroxyl group to the acetate (44), either of which could

hydrolyze to release 40. In KG-1 AML cells in culture, the ethyl ester was inactive as an apoptosis inducer but did inhibit cell growth at 5 μM (45%), suggesting that its intracellular cleavage to 40 was low during the 48 h treatment period. We previously observed that free carboxylic acid and phenolic hydroxyl groups were required for maximal apoptosis induction.[6,7] The acetate 44 was active in both assays to suggest that the acetate group was cleaved and that esterification of the phenolic hydroxyl could be a suitable derivatization approach. Derivativization could also reduce metabolic deactivation of the two pharmacophoric groups. The 4-substituted cinnamic acid 4 was found to undergo metabolism during a clinical trial on patients with ovarian cancer.[43] In animal studies, the phenolic hydroxyl group of 4-HPR was found to be metabolized to both the glucuronide[44] and the methyl ether.[45]

Two analogues—the 3-chloropyridine 38 and 2,5-disubstituted pyrimidine 42—had KG-1 AML cell apoptosis-inducing activity comparable to that of phenyl acetate 44, whereas the

Scheme 2. Synthesis of 74−79 and 83[a]
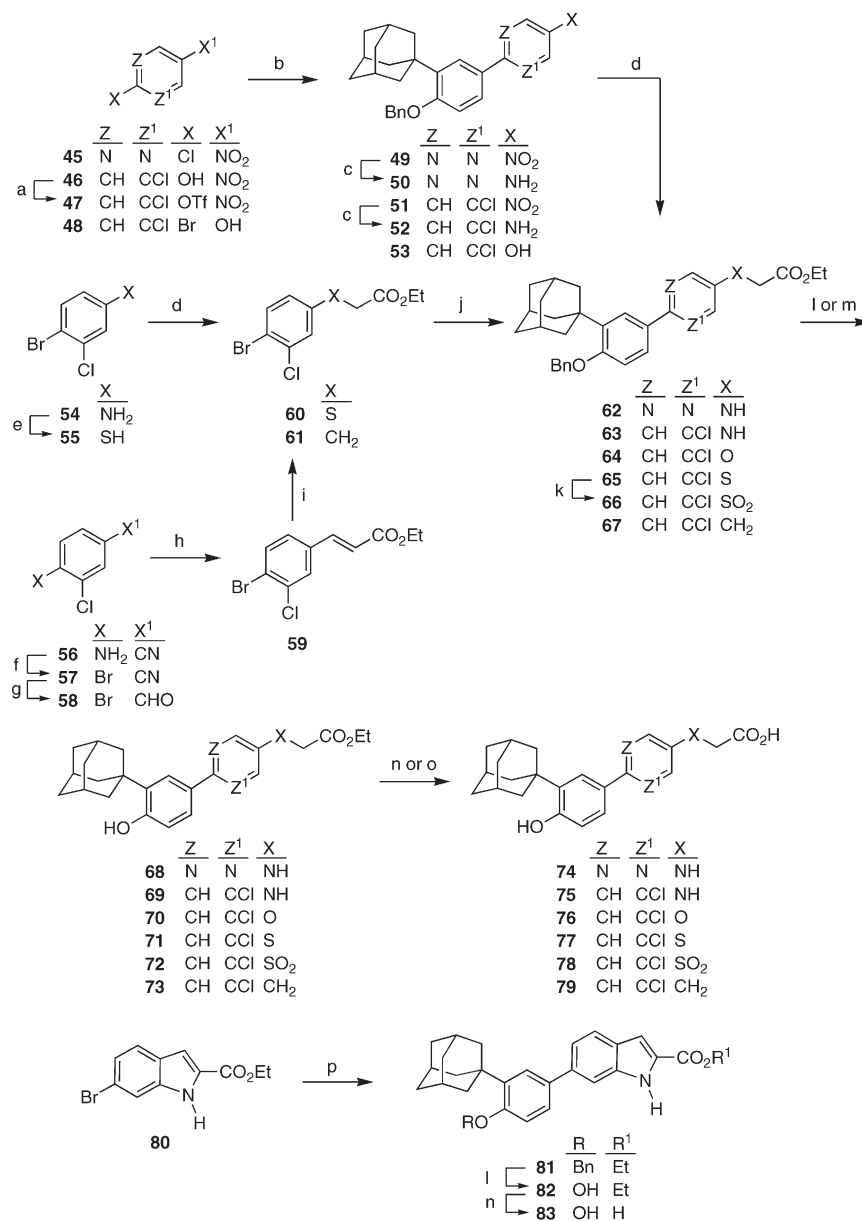
[a] Reagents and conditions: (a) Tf₂O, pyridine, CH₂Cl₂, 0 °C to room temperature. (b) Compound 25, Pd(PPh₃)₄, MePh, and NaHCO₃, H₂O, reflux (45); DME, K₃PO₄, reflux (47); or DME, 2 M Na₂CO₃, reflux (48). (c) SnCl₂·2H₂O, EtOH, reflux. (d) Compounds 50, 52, 53, and 60: BrCH₂CO₂Et, K₂CO₃, acetone, reflux. (e) NaNO₂, concentrated HCl, −5 to 0 °C; KSC(S)OEt, H₂O, 74 °C; KOH, EtOH, reflux. (f) CuBr₂, t-BuNO₂, CH₃CN, 0 °C to room temperature. (g) DIBAL, MePh, −78 °C to room temperature; MeOH; 10% H₂SO₄. (h) (Carbethoxymethylene)Ph₃P, MePh, reflux. (i) H₂, 10% Pd(C), EtOAc. (j) Compound 25, Pd(PPh₃)₄, and K₃PO₄, DMF, 93 °C (60) or DME, 2 M Na₂CO₃, reflux (61). (k) 3-Cl-C₆H₄-CO₃H, CH₂Cl₂. (l) Compounds 62, 63, 65−67, and 81: BBr₃, CH₂Cl₂, −78 °C. (m) Compound 64: H₂, 10% Pd(C), EtOH. (n) Compounds 68−72 and 82: LiOH·H₂O, THF/MeOH/H₂O; H₃O⁺. (o) Compound 73: 8.5 N NaOH, EtOH; H₃O⁺. (p) Compound 25, Pd(PPh₃)₄, saturated NaHCO₃, MePh, EtOH, 90 °C.

reversed 2,5-disubstituted isomer 39 of 40 and the 2,5-disubstituted pyrazine 41 were less active. In terms of proliferation inhibition, the most potent analogue was 42 followed by 40 and then 43.

The analogues in the series having modified side chains (Scheme 2) were not as active at inducing KG-1 AML cell apoptosis as those having *E*-propenoic acid side chains. The most active of this series was the carboxymethylaniline 75 followed by the carboxymethyl phenyl ether 76. Their orders of activity in terms of growth inhibition were reversed. Saturation of the

double bond of 6 or its replacement by the carboxymethyl thioether or carboxymethylsulfone led to loss of both growth inhibition and apoptosis induction activities by 79, 77, or 78, respectively. Like the 2-substituted cinnamic acids, the 2-indole-carboxylic acid 83 was inactive in both assays. The saturated heterocyclic ring analogues 98−100 (Scheme 3) were also inactive.

The effects of 6 and 40 on ATRA-sensitive human HeLa cervical cancer and estrogen receptor-negative SKBR-3 breast

Scheme 3. Synthesis of 98—100[a]
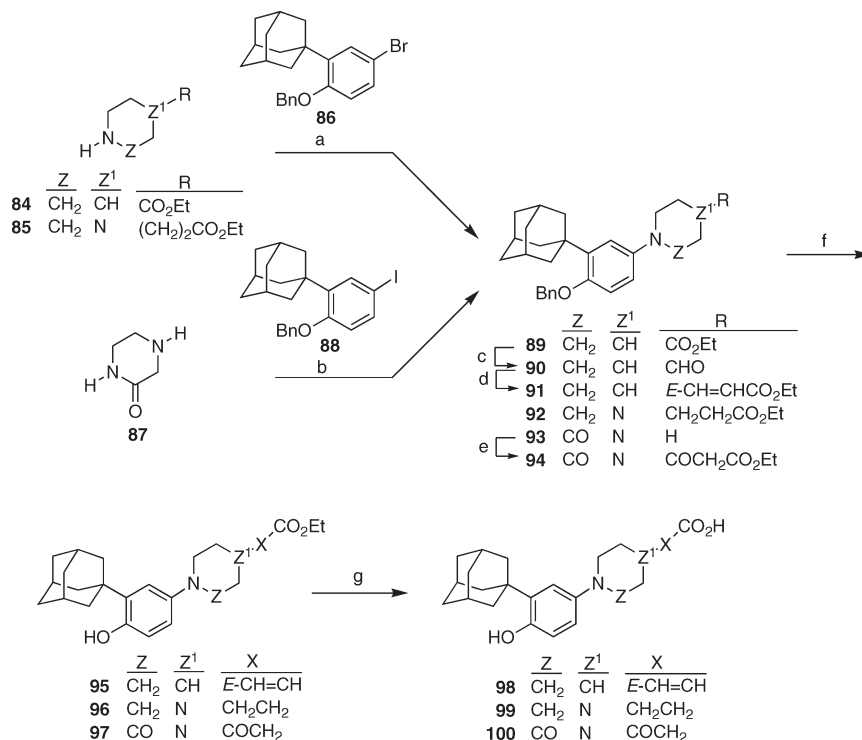
[a] Reagents and conditions: (a) 2-(1-Adamantyl)-1-benzyloxy-4-bromobenzene (**86**), 2,2′-bis(Ph$_2$P)-1,1′-binaphthyl, Pd(OAc)$_2$, Cs$_2$CO$_3$, MePh, 111 °C. (b) 2-(1-Adamantyl)-1-benzyloxy-4-iodobenzene (**88**), CuI, K$_3$PO$_4$, *trans-N,N′*-dimethylcyclohexane-1,2-diamine, 1,4-dioxane, 110 °C. (c) DIBAL, CH$_2$Cl$_2$, −78 °C; H$_3$O$^+$. (d) (Carbethoxymethylene)Ph$_3$P, MePh, 123 °C. (e) Ethyl 3-chloro-3-oxopropionate, Et$_3$N, CH$_2$Cl$_2$. (f) BBr$_3$, CH$_2$Cl$_2$, −78 °C; H$_2$O. (g) LiOH·H$_2$O, THF/MeOH/H$_2$O; H$_3$O$^+$.

cancer cells, which undergo apoptosis and differentiation on ATRA treatment, respectively, were examined next (Figure 3). HeLa cells are more sensitive to ATRA than SKBR-3 cells (Figure 3A). HeLa cell DNA contains integrated Herpes simplex virus 18 that causes the expression of E6 protein, which then inhibits p53 tumor suppressor activity by inducing p53 degradation by the ubiquitination pathway. HeLa cell growth was reported to be inhibited 71% at 96 h by 1.0 μM ATRA in medium containg 5% serum after a lag time of 48 h;[46] however, 87% apoptosis (caspase-3 cleavage) was induced by 10 μM ATRA after 12 h after the cells had first spent 24 h in serum-free medium.[47] Estrogen receptor-negative SKBR-3 cells overexpress Her2/ErbB2 tyrosine kinase[48,49] and lack functional p53.[50] Earlier, SKBR-3 cell proliferation relative to the control was found to be inhibited by 36% after 144 h and by 24% after 216 h treatments with 1.0 μM ATRA in medium containing 5% serum with changes of medium plus serum and compound every 2 days.[51] Analogue **40** at 0.5 μM induced time-dependent apoptosis of the cancer cell lines. HeLa cells were more sensitive with >60% cell apoptosis achieved after 48 h of treatment at 0.5 μM as compared to 1.9% SKBR-3 cell apoptosis. SKBR-3 cells required treatment at 1.0 μM for 72 h before apoptosis (15%) was noted. To answer the question of whether the leveling off of apoptosis at concentrations above 0.5 μM denoted cell resistance to treatment, the HeLa cell study at the same concentrations of **40** was extended for up to 72 h with compound and medium replaced every 24 h (Figure 3B). In this case, cell viability relative to the vehicle control was determined by the decrease in mitochondrial respiration as determined by ATP levels. In this case, viability decreased with treatment time and increasing concentrations with most cells nonviable at 1.0 μM after 72 h (2.6 ± 2.3% viability).

Three potent analogues of **6**—**40**—**42**—having one or two nitrogen atoms at various locations in their central heteroaromatic rings were compared with **6** for the ability to inhibit the proliferation of MMTV-Wnt1 mouse mammary cancer stem cells. After dispersion of their tumor spheroids, the cancer stem cells were treated for 72 h with **40**—**42**, or **6** at concentrations from 10 nM to 10 μM and then fixed and stained to generate dose—response curves (Figure 4). Analysis of DAPI-stained cells produced respective IC$_{50}$ values of 19, 316, 60, and 281 nM. Thus, these cells had 14.8- and 4.7-fold higher sensitivities to **40** and **42** than **6**, whereas the cells were 1.1-fold less sensitive to **41**. These values paralleled those observed for inhibition of KG-1 AML proliferation in which **40** and **42** were more potent than **6** and **41**. Most likely, the higher potencies observed in this stem cell assay were due to the evaluations being conducted in the absence of serum.

The analogues were next evaluated for activity against three ATRA-resistant solid tumor cell lines[52−55] that were selected to represent metastatic human lung, colon, and prostate adenocarcinoma cell lines that are often used to assess anticancer drug-signaling pathways and activities. These lines were also found to exhibit one or more changes in gene expression and mutations, some of which are listed in Table 2, that would support their abilities to proliferate, invade, and/or metastasize. Thus, tumor suppressor elements such as p16, p53, PTEN, and TRAIL were found to have been lost through gene deletion, mutation, or
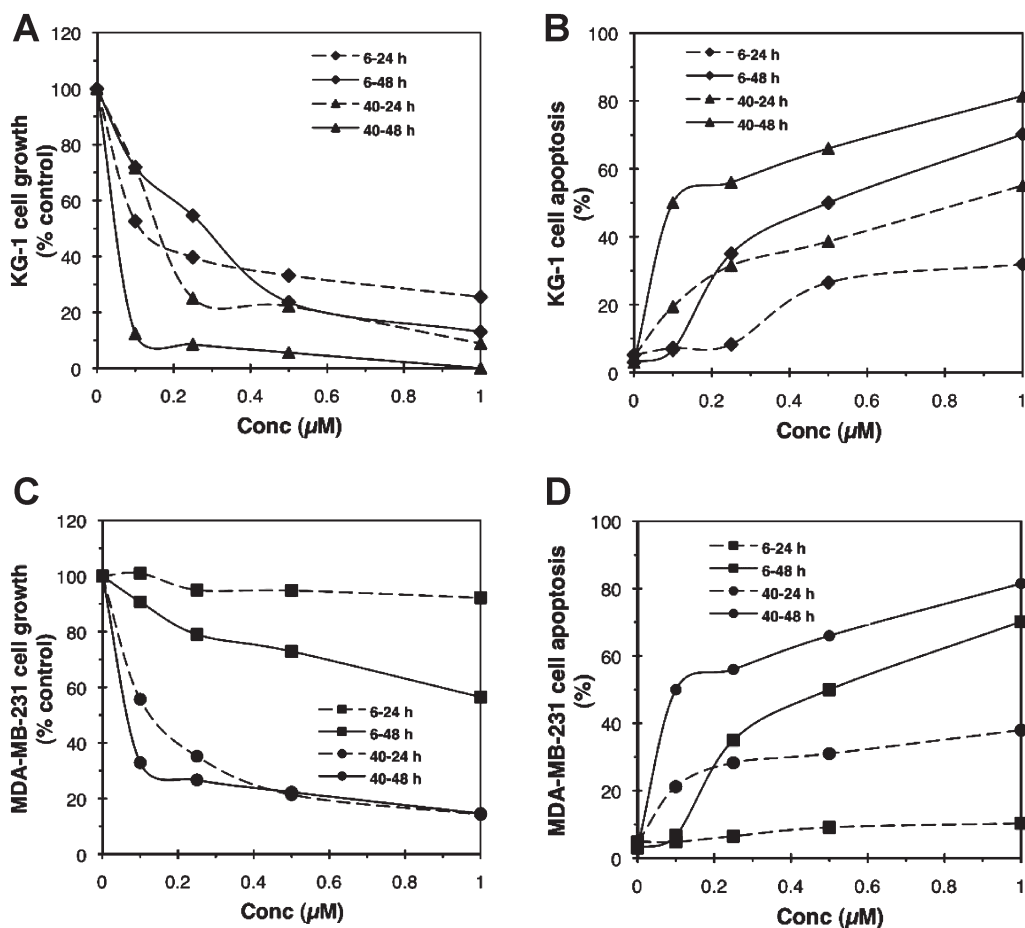
Figure 2. Human KG-1 AML and MDA-MB-231 breast cancer cell lines undergo growth inhibition and apoptosis on treatment with **6** or **40**. Cells were treated with each ARR at 0.1, 0.25, 0.5, or 1.0 μM or vehicle alone (Me$_2$SO control) for 24 or 48 h before cell growth (A and C) and apoptosis (DNA fragmentation) (B and D) relative to the controls were assessed by cell counting and acridine orange staining, respectively. Results shown are averages of triplicates $\pm$ SDs (<10%).
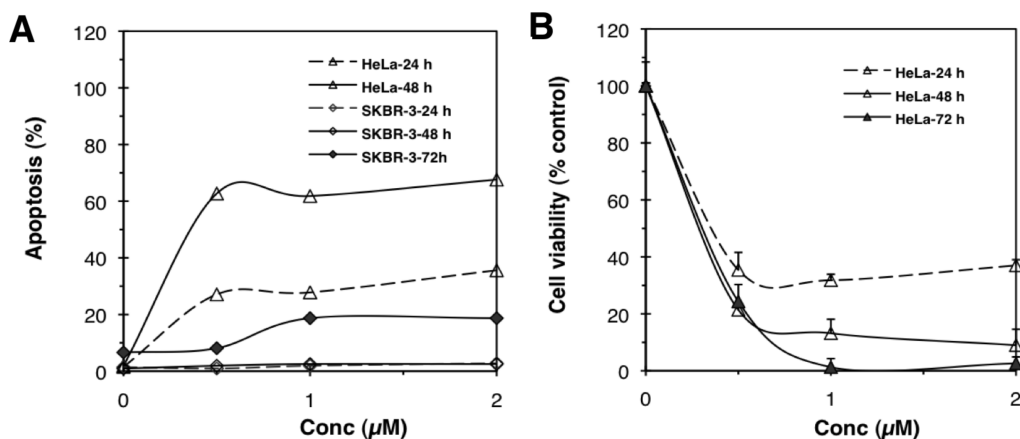

Figure 3. Pyridine analogue **40** induces apoptosis and inhibits viability of HeLa cervical cancer cells and weakly induces apoptosis of SKBR-3 breast cancer cells after treatments for 72 h. (A) Cells were treated with **40** at 0.5, 1.0, or 2.0 μM and with vehicle alone (Me$_2$SO control) for 24, 48, or 72 h before apoptosis levels were determined by acridine orange staining for DNA fragmentation. Results shown are averages of triplicates $\pm$ SDs (<10%). (B) HeLa cells treated at the same concentrations for up to 72 h before viability was determined by measurement of ATP levels using a luminescence assay. Results shown are means of triplicates $\pm$ SDs.

aberrant methylation. Oncogenic kinase K-Ras was found to be constitutively activated, and the secreted angiogenic growth factor VEGF was reported to be overexpressed. The transcription factor NFκB, which has been found to play either an antiapoptotic

or a proapoptotic role in cancer cells and is required for SHP-mediated apoptosis,[56] can also be constitutively activated. The A549 nonsmall cell lung, HT29 colon, and PC-3 prostate adenocarcinoma cell lines were treated for 72 h with the

Table 2. Properties of Three Adenocarcinoma Cell Lines Used To Evaluate Analogues 6, 34, 38−44, 74−79, 83, and 98−100

	human adenocarcinoma cell line		
property[a]	A549 lung	HT29 colon	PC-3 prostate
Origin	transformed pneumonocyte II	transformed epithelial cell	prostatic adenocarcinoma metastatic to bone
Metastatic potential	metastatic	high	high
VEGF (angiogenic growth factor)	expressed	expressed and secreted; EGFR2 overexpressed	expressed and secreted
p53 tumor suppressor	wild-type	mutant	mutated and not expressed
Ras oncogene	mutant K-Ras	wild-type K-Ras	wild-type K-Ras
Chemotherapeutic drug response	cisplatin-sensitive; adriamycin and etoposide-resistant	multidrug resistant (MRP1, BCRP); doxorubicin-sensitive	multidrug resistant (MRP1, LRP)
p16/INK4A (DNA damage response)	null	expressed	null
PTEN	methylated gene	wild-type	mutated and null
TRAIL	resistant	DR2 induced by hypoxia	sensitive
NFκB	constitutively high	constitutive, γ-radiation-induced	constitutive
Androgen receptor	AR-positive	dihydrotestosterone stimulates ornithine decarboxylase	AR-independent
Estrogen receptor	ERα$^-$/ERβ$^+$	ERα$^-$/ERβ$^+$	ERα$^-$/ERβ$^+$
Response to ATRA	5% growth inhibition at 10 μM after 72 h[b]	8% growth inhibition at 10 μM in medium containing 10% FCS after 72 h[c]	IC$_{50}$ = 7.6 μM for growth inhibition in medium after 120 h[d] 281% growth of control (100%) at 10 μM in serum-free medium after 12−14 days[e]

[a] AR, androgen receptor; BCRP, breast cancer resistance protein; DR2, death receptor 2; ER, estrogen receptor; GTP, guanidine triphosphate; LHRH, luteinizing hormone-releasing hormone; LRP, lung resistance-related protein; MRP1, multidrug resistance-associated protein 1; PTEN, phosphatase and tensin homologue deleted on chromosome ten; TRAIL, tumor necrosis factor-related apoptosis-inducing ligand; VEGF, vascular endothelial growth factor. [b] Ref 52. [c] Ref 53. [d] Ref 54. [e] Ref 55.

analogues at five concentrations from 1.25 to 25 μM. Cell inhibition was assessed by measuring the decline in intracellular ATP levels, which was determined by a fluorescence assay for luciferase activity. ATP functions as a luciferase cofactor in the oxidation of luciferin. Dose−response curves are shown in Figure S1 in the Supporting Information.

The three cancer cell lines exhibited various sensitivities to the analogues, which appeared to depend on both analogue and cell type. Thus, ATP levels in HT29 colon cancer cells were most sensitive to **6**, **40**, and **75** at 10 μM ($\geq$40% decrease) and more resistant to **38**, **41**, and **42**. Both A549 nonsmall cell lung cancer and PC-3 prostate cancer cell lines showed substantial decreases in ATP levels after treatment with **6**, **34**, **38−40**, and **42** at 10 μM. The dose−response profiles exhibited by A549 cells were highly similar to those of the PC-3 cells for most of the active analogues, except that the A549 cells were appreciably more resistant to **43**, **75**, **76**, and **99**. Interestingly, in contrast to HT29 and A549 cells, PC-3 cells were sensitive to **41**, **43**, and **99**. The responses of the A549 and PC-3 cell lines to the active analogues were characterized by a rapid decline in ATP levels in a dose-dependent manner from 1.25 to 5.0 μM, which then leveled off at 5−10 μM to about 60% of the control values. In contrast, the slopes representing the concentration-dependent decreases in ATP levels in the HT29 cells on treatment with **6** and **40** at 10 μM were not as steep but dropped appreciably below 60% of the control value.

The maximum-tolerated effects of escalated dosing of **6** and **42** were compared in mice. Mice (two/group) were treated intravenously once daily for 7 days with 25% incrementally increasing doses of **6** or **42** beginning at 20 mg/kg (303.4 mg or 0.744 and 0.806 mmol, respectively, total dose). Mice were weighed daily before dosing. Between days 1 and 4, mice gained weight (9.3% for **6** and 5.7% for **42**) after which time weight loss was noted in both groups. By day 7, the average weight in the **6** treatment group had dropped to 90.4% of the day 1 weight and that in the **42** treatment group was 100.9%. At day 8, their respective average weights were 62.7 and 100% of their original average weights. At day 9, one mouse survived in the group dosed with **6**, whereas both mice were alive and active in the group dosed with **42**. In another study, SCID mice (eight/group) bearing xenografts were injected intravenously a total of 15 times with **42** at 20 mg/kg once daily on alternate days (300 mg or 0.797 mmol total dose). The average weights of treated mice with time are shown graphically in Figure S3 in the Supporting Information. As compared to the vehicle alone-treated control, the **42**-treated mice did not exhibit any weight loss, decreased physical activity, or symptoms of dehydration, diarrhea, or scruffy coat.[57]

Binding to SHP. Previously, we demonstrated that **6** bound to the orphan nuclear receptor SHP by using a competitive binding assay with the SHP ligand [5,5′-^{3}H$_2$]6-[3-(1-adamantyl)-4-hydroxyphenyl]-2-naphthalenecarboxylic acid (41% displacement)

in MDA-MB-468 human breast cancer cells.[25] Ligand binding can also be established using NMR spectroscopy by measuring the loss or broadening of ligand signals caused by complexation of ligand with the protein, which would increase ligand signal relaxation times as compared to those of ligand alone.[58,59] To establish binding of **42** to SHP, one-dimensional ^{1}H NMR binding studies were conducted using the recombinant chimeric glutathione-*S*-transferase (GST)−SHP protein. Spectra were run at low temperature (11 °C) to maintain protein stability. Binding of **6** to SHP was used as a positive control. Comparisons were made by using the aromatic and olefinic proton signals in the ligand spectra, which had the least overlap with signals from the medium and protein. The low-field region from 6.3 to 7.6 ppm of the ^{1}H NMR spectrum of **6** showed signals for its six aromatic and two olefinic protons (a−h) (Figure 5A), whereas
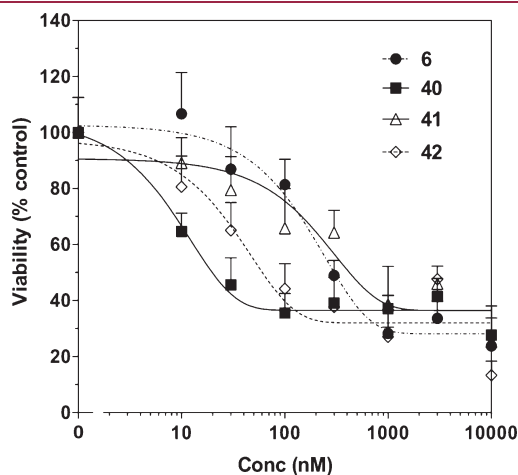

Figure 4. Effects of **6** and **40**−**42** on mammary cancer stem cell viability as measured by DAPI staining and cell counting. Cells were treated with each ARR at the indicated concentrations or with vehicle alone (Me$_2$SO control) for 72 h before viability of treated cells relative to vehicle-treated control was determined. Results represent the average of triplicates ± SDs.

the low-field region from 6.4 to 8.0 ppm in the spectrum of **42**, which has five aromatic and two olefinic protons, only showed five signals (a, b, and e−g) (Figure 5B) with signals for the remaining two protons (c and d) occurring at lower field and overlapped with non-**42** proton peaks. ^{1}H NMR signal intensities in these regions of the spectra that were obtained on solutions of **6** and **42** containing SHP protein displayed obvious decreases as compared with those of the ligands alone. These decreases in signal intensity indicate that both compounds interacted with SHP protein in a distinct manner that prevented rapid signal relaxation.

Computational Studies (Docking to the SHP Model). The ultraspiracle (USP) LBD (PBD 1g2n)-derived homology model for human SHP and its boat-shaped LBP were described previously.[7] In this model, portions of residues Q48, P52, T55, C56, and A59 in helix H3; F96, L97, and L100 in H5; G133, P139, P141, A144, and W148 in H7; L231, D234, L235, and R238 in H11; and I240 in the loop between helices H11 and H12 formed the putative LBP surface. Docking of energy-minimized conformers of the heterosubstituted analogues to the model was compared to that of **6** using the software program BioMedCAche 6.2. Generally, analogues having apoptotic activity (Table 1) docked in poses similar to that assumed by **6**. For example, the overlap of docked poses for **42** and **75** with that of **6** is shown in Figure 6A. The carboxylate groups of the docked conformers for **42**, **75**, and **6** resided in the bow of the boat-shaped LBP, where they could hydrogen bond and/or form a salt bridge with the positively charged guanidinium group of R238 located at the C terminus of helix H11. The measured interatom distances between their CO$_2$H C atoms and the R238 guanidinium carbon were 3.9, 4.5, and 4.0 Å, respectively, which suggest that forma-tion of a strong hydrogen bond and/or an ionic interaction could stabilize the binding of these ligands in the LBP. Treatment of KG-1 cells with 1.0 μM **42**, **75**, and **6** for 48 h induced apoptosis levels of 40, 18, and 30%, respectively. The lower apoptotic activity observed for **75** could be explained by its greater C−C interatom distance. The two aromatic rings of these analogues could make hydrophobic contacts with the alkyl side chains of L231, L235, and I240 that surround the hull region of the LBP,
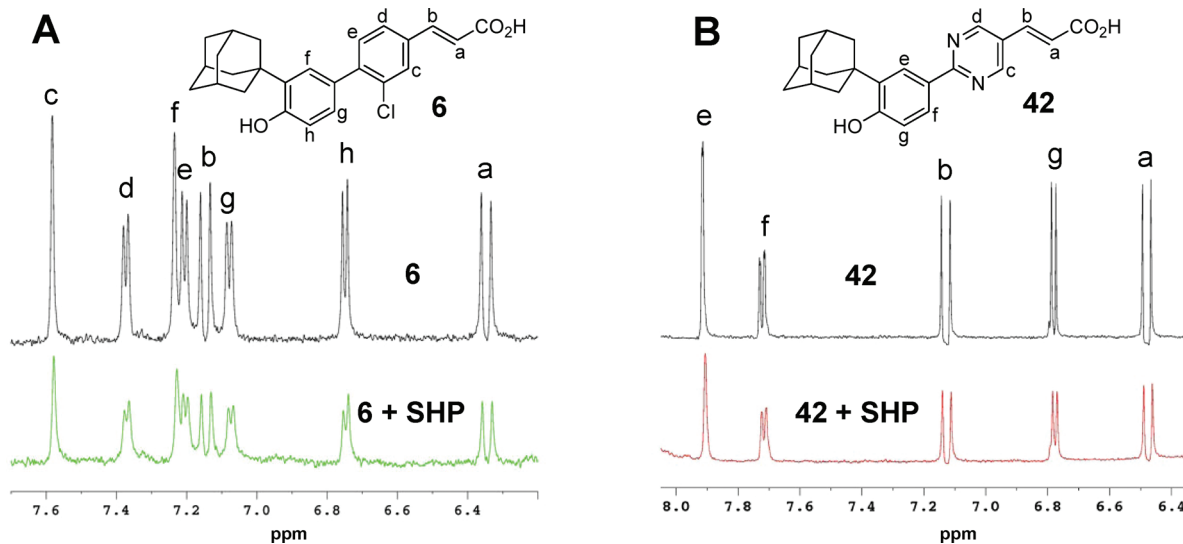

Figure 5. Comparison of the low-field regions in 1D ^{1}H NMR spectra of ARRs **6** and **42**. Spectra were taken on solutions of **6** (100 μM) (A) and **42** (100 μM) (B) at 11 °C in the absence (upper spectra) and presence (lower spectra) of 10 nM SHP protein.
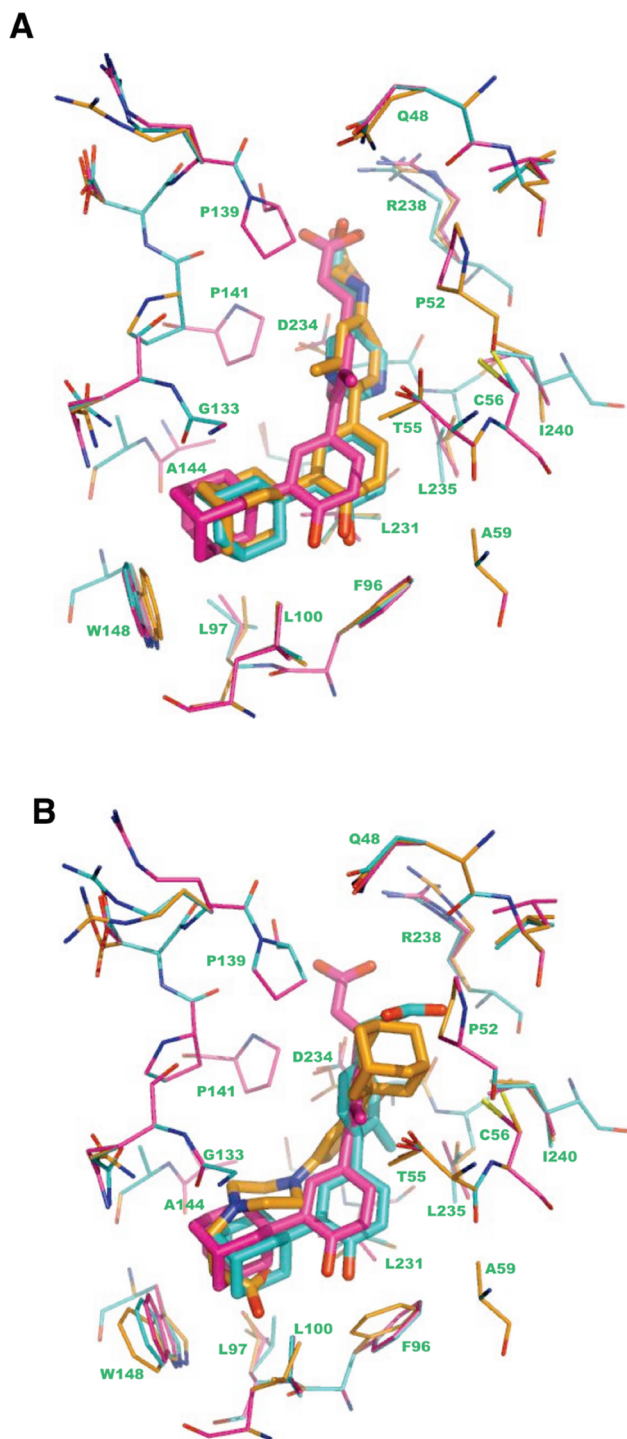
Figure 6. Poses assumed by **6**, **42**, **75**, **79**, and **99** on docking to the ultraspiracle-derived model of SHP. (A) Overlap of docking poses for **6**, **42**, and **75** shown in stick format with conformations of SHP LBP residues shown in line format. C atoms of **6**, **42**, and **75** and those of their corresponding LBP residues are colored magenta, cyan, and orange, respectively, with Cl in green; O, red; N, blue; S, yellow. (B) Overlap of docking poses for **6**, **79**, and **99** shown in stick format with LBP residues in line format. Cs of **6**, **79**, and **99** and their corresponding LBP residues in magenta, cyan, and orange, respectively, with other atoms as in A. Residue numbering is that for the SHP protein sequence. Docking studies were performed using BioMedCAche 6.2 with ligands and protein side chains flexible.

while their 3′-(1-Ad) and 4′-OH groups could interact with F96, L97, L100, and W148 located in the stern. The shortest distances between the 3′-(1-Ad) groups of **42**, **75**, and **6** and the indole ring of W148 were measured as 3.7, 3.3, and 3.0 Å, respectively, suggesting that the 1-Ad group could contribute strong van der Waals stabilizing interactions. The measured distances between the 4′-OH O atoms of **42**, **75**, and **6** and the center of the helix H5 F96 phenyl ring were 2.7, 3.0, and 3.5 Å, respectively and, therefore, could support the formation of a nonconventional hydrogen−π bond[7] between the 4′-hydroxyl H and the π-electron cloud of the phenyl ring that could enhance ligand−LBP interaction.[60] The docked poses also suggest that the 3-Cl atoms of **75** and **6** could form a H···Cl bond[61] with the hydrogen atom of the H3 T55 OH or the C56 SH group to further enhance binding.

In contrast, the inactive analogues generally either docked in poses similar to that of **6** but with their carboxylate groups farther from the R238 guanidinum group or in significantly different (orthogonal) poses. The docking poses for the inactive analogues **79** and **99** are shown superposed with that of **6** in Figure 6B. The pose for **79** was similar to that of **6** except for the position of its saturated side chain. The measured distance between its CO_2H C and the R238 guanidinium C being longer (5.4 Å) than that for **6** suggests that any stabilizing hydrogen bond and/or ionic interaction would be weaker.

The inactive piperazine **99** did dock to the SHP model but had a reversed pose as compared to that of **6** so that the CO_2H group of **99** was adjacent to the F96 phenyl ring rather than R238. No stabilizing interactions were observed for the 4′-OH group of **99**. Thus, the strong stabilizing ionic and H-bond interactions observed on docking of **6** were absent, although hydrophobic interactions could be possible and suggestive of only weak binding. Thus, the α-methylene of its saturated side chain, rather than the 1-Ad group of **6**, could have hydrophobic contacts with the W148 indole ring. The 3′-(1-Ad) group of **99** could form hydrophobic group contacts with such pocket residues as P52, T55, P139, L235, and I240 and the side chain carbons of R238. The positions of the piperazyl and phenyl rings of **99** suggest possible stabilizing contacts with hydrophobic residues P141, A144, A145, and L231. The proximity (4.6 Å) between the piperazyl N atom to which the side chain of **99** was linked and the Q134 amido N suggests that a hydrogen bond could stabilize this pose.

■ DISCUSSION

Incorporation of one or two N atoms in the central aromatic ring of the AHPC scaffold to give the aza-heteroaromatic analogues did not appreciably detract from their apoptotic activity against KG-1 AML cells, unlike replacement of the central phenyl ring by a saturated nitrogen-containing ring. Saturation of the side chain or replacement of the β-methylene group of **79** with a heteroatom also diminished apoptotic activity. The robustness of the correlation between apoptosis-inducing activity against KG-1 cells at 5 μM and that observed in reducing ATP levels at 5 μM in the three solid tumor cell lines (A549, HT29, and PC-3) varied among the active analogues. Thus, like **6**, **40** reduced ATP levels in the 30−40% range at 72 h, whereas **42** efficiently reduced ATP levels by approximately 35% in A549 and PC-3 cells but only by about 15% in HT29 cells. In contrast, **39** reduced ATP by only 10−20% and **43** reduced ATP by ≤5% in two of the lines, but both reduced ATP by >60% in the PC-3

cell line. The inhibition of MMTV-Wnt1 mammary cancer stem cell proliferation induced by **6, 40, 41**, and **42** correlated very well with inhibition of KG-1 AML cell growth. Analogues **40** and **42** with low IC_{50} values (19 and 60 nM, respectively) for inhibition of MMTV-Wnt1 mammary cancer stem cell proliferation displayed strong inhibition of KG-1 cell growth at concentrations 1.0 and 5.0 μM, whereas **6** and **41** with higher IC_{50} values (281 and 316 nM, respectively) were weaker inhibitors of KG-1 AML cell growth at 1.0 and 5 μM.

The ethyl ester **34** and acetate **44** derivatives of **40** were as capable as **40** of inhibiting KG-1 cell growth at 5 μM, but only **44** induced KG-1 apoptosis. Despite the fact that the A549 lung, HT29 colon, and PC-3 prostate cancer cell lines were only treated for 72 h with no alternate-day exchange of media or compound due to the small volumes used in the 384-well assay format, both derivatives decreased intracellular ATP. These lines were cultured under robust conditions in medium containing 10% fetal bovine serum, a condition under which we had previously observed that a longer treatment time (9 days) was necessary to achieve high inhibition of OVCAR-3 ovarian cancer cell growth by **1**, for which we obtained an IC_{50} value of 0.13 μM after that treatment period,[62] whereas the IC_{50} value achieved by **6** after only 3 days of treatment in the current assay was approximately 30-fold higher. To compensate for the shorter treatment time in the ATP assay, cells were treated at higher compound concentrations.

Analysis of plasma samples from ovarian cancer patients treated with **4** in a phase I clinical study suggested that β-glucuronidation of **4** had occurred because treatment of these samples with the glucuronide cleavage enzyme β-glucuronidase restored the levels of **4**.[43] The pharmacophoric element (OH or CO_2H) that was glucuronidated was not specified. We hypothesize that metabolic deactivation of the present analogues could be similar. Carboxylic acid groups have been metabolically converted to acyl β-glucuronides in such retinoids as ATRA, 9-*cis*-retinoic acid,[63−65] bexarotene,[66] and 9cUAB30[67] or to taurine conjugates as was observed for the RARα-selective retinoid Am80[68,69] and bexarotene.[66] The phenolic hydroxyl group of the retinoid derivative 4-HPR was converted in vivo to the methyl ether.[45] We undertook a produg approach to determine whether any possible metabolic deactivation of **40** could be delayed or prevented. Treatment of the three solid tumor cell lines with two derivatives of **40**—ethyl ester **34** and phenyl acetate **44**—led to a decrease in ATP levels to suggest that some cleavage to **40** had occurred. While the phenyl acetate **44** readily induced apoptosis of KG-1 AML cells, the ethyl ester **34** was inactive in these cells to suggest that this line was deficient in esterase activity. However, the esterases that are present in plasma[70] could circumvent this problem. Thus, the results showing that protecting either pharmacophoric element did not abolish cell growth inhibitory activity are encouraging and suggest that in vivo use of a prodrug could be a feasible approach to maintaining plasma levels of an analogue of **40** such as **42**.

To investigate whether analogues of **6** with high apoptotic activities also bound to SHP,[25] isothermal titration calorimetry (ITC) was investigated. However, the recombinant wild-type SHP that we expressed in *Escherichia coli* proved to be very unstable at ≥20 °C in the absence of glycerol and, thus, incompatible with ITC measurements. Therefore, 1D ^{1}H NMR spectra of **6** and **42** in the absence and presence of SHP protein were taken at low temperature to maintain protein stability. The proton signal intensities of the aromatic and olefinic

protons of **6** and **42** in the presence of SHP protein were obviously suppressed, thereby demonstrating direct interaction between ligand and protein.

Recently, we reported that **6** and (*E*)-3-{2-[3′-(1-adamantyl)-4′-hydroxyphenyl]-5-pyrimidyl}propenoic acid (AHP3) (**42**) induced apoptosis in FFMA-AML and TF(*v*-SRC) AML cell lines in culture after 96 h of treatment. Their IC_{50} values as determined by annexin V staining were submicromolar.[57] Apoptosis was accompanied by caspase-3 activation, PARP1 cleavage, and decreased levels of apoptosis inhibitors XIAP and c-IAP, phosphorylated Bad, and the NFκB p65 cytoplasmic sequestering protein IκBα. Both **6** and **42** extended the survival of NOD-SCID mice inoculated with FFMA-AML cells. Survival in NOD-SCID mice that had been injected intravenously with TF(*v*-SRC) AML cells was also extended by **42** without any decrease in body weight. These results suggest that **42** may have potential for the treatment of AML.

■ CONCLUSIONS

In summary, the results of these studies using cancer cell lines indicated that incorporating one or two nitrogen atoms in the central aromatic ring to give heteroaromatic analogues did not block their ability to induce apoptosis of KG-1 AML or three solid tumor cell lines or inhibit mammary cancer stem cell proliferation as compared to that of **6**. However, replacing the central aromatic ring with a saturated heterocyclic ring alone or combined with a saturated side chain abolished activity. Side chain modifications alone produced various results. In the analogues of **6**, saturation or replacement of the saturated side chain β-methylene group with sulfur abolished apoptotic activity, whereas replacement with oxygen or nitrogen decreased activity by approximately 50%. Most important, introducing nitrogen(s) in the central aromatic ring of the scaffold of **4** enhanced solubility with retention of apoptosis-inducing activity.

■ EXPERIMENTAL SECTION

Chemistry. Chemicals and solvents from commercial sources were used without further purification unless specified. The arylboronic acid **25** was synthesized using our reported procedure.[6] Abbreviations for solvents and reagents are as follows: BnBr, benzyl bromide; DIBAL, diisobutylaluminum hydride; DMAP, 4-(*N*,*N*-dimethylamino)pyridine; DMF, dimethylformamide; DME, 1,2-dimethoxyethane; NBS, *N*-bromosuccinimide; *tert*-Boc, *tert*-butoxycarbonyl; THF, tetrahydrofuran; and Tf$_2$O, trifluoromethanesulfonic anhydride. Experimental procedures were not optimized. Anhydrous and/or oxygen-sensitive reactions were carried out under argon gas. Reactions were monitored by thin-layer chromatography on silica gel (mesh size 60, F$_{254}$) with visualization under UV light. Unless specified, the standard workup involved washing the organic extract with water and brine and drying over Na$_2$SO$_4$ followed by concentration at reduced pressure. Chromatography refers to standard or flash column chromatography on silica gel (Merck 60, 230−400 mesh). Spectral characterization information about reported compounds has been included when that was absent from literature procedures. Melting points of samples were determined in capillaries using a Mel-Temp II apparatus and were uncorrected. Infrared spectra were obtained on powdered or liquid samples using an FT-IR Mason satellite spectrophotometer. UV absorbance was measured by using a NanoDrop ND-1000 spectrophotometer. ^{1}H NMR spectra were recorded on a 300 MHz Varian Unity Inova spectrometer, and shift values are expressed in ppm (δ) relative to CHCl$_3$ as the internal standard. Unless mentioned, NMR samples were dissolved in ^{2}HCCl$_3$.

High-resolution mass spectra were recorded on an Agilent ESI-TOF mass spectrometer at The Scripps Research Institute (La Jolla, CA). A Shimadzu HPLC system was used to analyze the purity of target molecules (Tables S1 and S2 in the Supporting Information). The purity of compounds used in the biological assays was ≥95%. The purity of **6** was 98% by HPLC analysis. SHP residue numbering in the model and protein followed that given in the Protein Data Bank SHP protein sequence. Thus, the reported SHP model residue numbers[34] were increased by 13.

2,3-Dichloro-5-formylpyridine (10)[71]. A reported method[71] was used. Briefly, a mixture of 5,6-dichloro-3-pyridinemethanol (**9**) (1.42 g, 8.00 mmol) and MnO_2 (13.9 g, 160 mmol) in CH_2Cl_2/hexane (1:1, 8 mL) was stirred for 1 h, diluted with 50% EtOAc/hexane (20 mL), and filtered (50% EtOAc/hexane wash). The filtrate was evaporated, and the residue was dried under vacuum to give **10** for use in the synthesis of **19**.

3-Chloro-6-iodopyridazine (18)[72]. A reported procedure[72] was followed. A suspension of 3,6-dichloropyridazine (**17**) (5.00 g, 33.6 mmol), NaI (6.75 g, 45.0 mmol), and hydroiodic acid (55−58%, 25 mL) was stirred at 44 °C (oil bath) under argon for 23 h, cooled to room temperature (room temperature), and quenched with concentrated NaOH to pH 12, then stirred for 10 min, and extracted with CH_2Cl_2. The extract was washed (H_2O) and dried. Solvent removal at reduced pressure gave 7.96 g (98%) of **18** as a pale-yellow solid, mp 114−116 °C (lit: 110−112 °C).[72] ^{1}H NMR δ 7.23 (d, J = 8.7 Hz, 1H, 4-ArH), 7.84 ppm (d, J = 8.7 Hz, 1H, 5-ArH) in agreement with that reported.[72]

General Procedure for Converting Aryl Cyanides 13 and 57 to Aryl Carboxaldehydes 14 and 58, Respectively. A reported procedure[73] was modified by changes in temperature, reaction time, and the acidic reagent. To a solution of the aryl cyanide (1.0 mmol) in anhydrous MePh (2.7 mL) at −78 °C was added 1.0 M DIBAL (1.5 mmol) in CH_2Cl_2 (1.5 mL). The reaction mixture was stirred at −78 °C for 15 min, warmed to room temperature with stirring, then quenched with MeOH (4 mL), and stirred for 30 min more before 10% H_2SO_4 (10 mL) was added with stirring, which was continued for 1.75 h more. Extraction with EtOAc (30 and 20 mL) and concentration of the extract at reduced pressure afforded the crude product, which was purified by chromatography.

5-Bromopyrazine-2-carboxaldehyde (14). 5-Cyano-2-bromopyrazine (**13**) (1.02 g, 5.54 mmol) after reaction for 26 h, workup, and chromatography (11−14% EtOAc/hexane) produced 289 mg (28%) of **14** as an orange solid, mp 56−58 °C. IR 2960, 1654, 1546, 1111 cm^{-1}. ^{1}H NMR δ 8.83 (d, J = 1.24 Hz, 1H, 6-ArH), 8.91 (d, J = 1.24 Hz, 1H, 3-ArH), 10.13 ppm (s, 1H). HRMS calcd $C_5H_3BrN_2O$ $[M + H]^+$, 186.9501; found, 186.9496.

4-Bromo-3-chlorobenzaldehyde (58)[7]. 4-Bromo-3-chlorobenzonitrile (**57**) (6.25 g, 28.9 mmol) after reaction for 4 h, workup, and chromatography (2−9% EtOAc/hexane) produced 5.04 g (80%) of **58** as an off-white solid, mp 46 °C (lit: 44−45 °C).[7] IR 2888, 1698, 1545, 1209 cm^{-1}. ^{1}H NMR δ 7.65 (dd, J = 1.8 Hz, 8.4 Hz, 1H, 6-ArH), 7.84 (d, J = 8.4 Hz, 1H, 5-ArH), 7.97 d, J = 1.8 Hz, 1H, 2-ArH), 9.97 ppm (s, 1H, CHO).

General Procedure for Heck Coupling of Ethyl Acrylate with Heteroaryl Halides 15, 16, and 18 To Afford Ethyl (E)-3-Heteroarylpropenoates 22−24, Respectively. A solution of the heteroaryl halide (1.0 mmol), ethyl acrylate (1.6−4.0 mmol), palladium-(II) acetate (0.015 mmol), and tri(o-tolyl)phosphine (0.1−0.12 mmol) in DMF (1.4 mL) and di(isopropyl)ethylamine (0.7 mL) was stirred with heating at 115 °C (oil bath), cooled to room temperature, diluted with brine, and then extracted with EtOAc. The extract was washed (brine) and dried. After solvent removal at reduced pressure, the residue was purified by chromatogaphy to give the coupled product.

Ethyl (E)-3-(5-Bromo-2-pyrazinyl)-2-propenoate (22). 2,5-Dibromopyrazine (**15**) (238.0 mg, 1.0 mmol) on coupling at 115 °C for 4.4 h, workup, and chromatography (11% EtOAc/hexane) produced 22 mg

(8.5%) of **22** as a cream solid, mp 70−71 °C. IR 2940, 1707, 1457, 1103 cm^{-1}. ^{1}H NMR δ 1.33 (t, J = 7.3 Hz, 3H, OCH$_2$CH$_3$), 4.28 (q, J = 7.3 Hz, 2H, OCH$_2$CH$_3$), 6.99 (d, J = 15.9 Hz, 1H, CH=CHCO), 7.62 (d, J = 15.9 Hz, 1H, CH=CHCO), 8.40 (d, J = 1.24 Hz, 1H, 6-ArH), 8.68 ppm (d, J = 1.24 Hz, 1H, 3-ArH). HRMS calcd $C_9H_9BrN_2O_2$ $[M + H]^+$, 256.9920; found, 256.9915. Propenoate **22** was also synthesized by the alternative method described below.

Ethyl (E)-3-(2-Chloro-5-pyrimidinyl)-2-propenoate (23). 5-Bromo-2-chloropyrimidine (**16**) (4.03 g, 20.8 mmol) on coupling at 115 °C for 3.5 h, workup, and chromatography (11% EtOAc/hexane) produced 3.26 g (73%) of **23** as a yellow solid, mp 125−127 °C. IR 2905, 1698, 1542, 1405, 1160 cm^{-1}. ^{1}H NMR δ 1.38 (t, J = 7.2 Hz, 3H, OCH$_2$CH$_3$), 4.32 (q, J = 7.2 Hz, 2H, OCH$_2$CH$_3$), 6.60 (d, J = 16.2 Hz, 1H, CH=CHCO), 7.61 (d, J = 16.2 Hz, 1H, CH=CHCO), 8.79 (s, 2H, 4-ArH, 6-ArH). HRMS calcd $C_9H_9ClN_2O_2$ $[M + H]^+$, 213.0425; found, 213.0428.

Ethyl (E)-3-(6-Chloro-3-pyridazinyl)-2-propenoate (24). 3-Chloro-6-iodopyridazine (**18**) (2.4 g, 10 mmol) on coupling at 111 °C for 3.5 h, workup, and chromatography (14−20% EtOAc/hexane) produced 174 mg (8%) of **24** as a brown solid, mp 106−110 °C. IR 2928, 1715, 1186 cm^{-1}. ^{1}H NMR δ 1.38 (t, J = 7.5 Hz, 3H, CH$_2$CH$_3$), 4.33 (q, J = 7.5 Hz, 2H, CH$_2$CH$_3$), 6.98 (d, J = 16.2 Hz, 1H, CH=CHCO), 7.57 (d, J = 8.4 Hz, 1H, 5-ArH), 7.63 (d, J = 8.4 Hz, 1H, 4-ArH), 7.86 ppm (d, J = 16.2 Hz, 1H, CH=CHCO). HRMS calcd $C_9H_9ClN_2O_2$ $[M + H]^+$, 213.0425; found, 213.0431.

General Procedure for Wittig Reaction of (Carbethoxymethylene)triphenylphosphorane with Heteroarylcarboxaldehydes 10−12, 14, and 90 and Arylcarboxaldehyde 58 To Afford Ethyl 3-Heteroarylpropenoates 19−22 and 91 and Ethyl Cinnamate 59, Respectively. A solution of the carboxaldehyde (1.0 mmol) and (carbethoxymethylene)triphenylphosphorane (1.2 mmol) in MePh (3.3 mL) was heated at reflux for 15.7−18 h. After solvent removal at reduced pressure, the residue was chromatographed to give the heteroarylpropenoate or cinnamate.

Ethyl (E)-3-(5,6-Dichloro-2-pyridinyl)-2-propenoate (19). 2,3-Dichloropyridine-5-carboxaldehyde (**10**) (crude) after reaction for 18 h, workup, and chromatography (9−10% EtOAc/hexane) produced 323 mg [16% from 5,6-dichloro-3-pyridinemethanol (**9**)] of **19** as a white solid, mp 102−103 °C. IR 2914, 1702, 1428, 1193 cm^{-1}. ^{1}H NMR δ 1.37 (t, J = 7.2 Hz, 3H, OCH$_2$CH$_3$), 4.31 (q, J = 7.2 Hz, 2H, OCH$_2$CH$_3$), 6.53 (d, J = 16.2 Hz, 1H, CH=CHCO), 7.62 (d, J = 16.2 Hz, 1H, CH=CHCO), 7.94 (d, J = 1.8 Hz, 1H, 4-ArH), 8.44 ppm (d, J = 1.8 Hz, 1H, 2-ArH). HRMS calcd $C_{10}H_9Cl_2NO_2$ $[M + H]^+$, 246.0083; found, 246.0086.

Ethyl (E)-3-(5-Bromo-2-pyridinyl)-2-propenoate (20). 5-Bromo-2-formylpyridine (**11**) (1.07 g, 5.58 mmol) after reaction for 17 h, workup, and chromatography (10−14% EtOAc/hexane) produced 1.42 g (97%) of crude **20** as a pale-yellow solid. Crystallization (hexane) yielded 1.28 g (89%) of pure E-isomer **20** as a white solid, mp 78−80 °C. IR 2978, 1710, 1468, 1180 cm^{-1}. ^{1}H NMR δ 1.35 (t, J = 7.3 Hz, 3H, OCH$_2$CH$_3$), 4.28 (q, J = 7.3 Hz, 2H, OCH$_2$CH$_3$), 6.91 (d, J = 15.9 Hz, 1H, CH=CHCO), 7.31 (d, J = 8.5 Hz, 1H, 3-ArH), 7.61 (d, J = 15.9 Hz, 1H, CH=CHCO), 7.84 (dd, J = 2.4 Hz, 8.5 Hz, 1H, 4-ArH), 8.69 ppm (d, J = 2.4 Hz, 1H, 6-ArH). HRMS calcd $C_{10}H_{10}BrNO_2$ $[M + H]^+$, 255.9968; found, 255.9967.

Ethyl (E)-3-(6-Bromo-3-pyridinyl)-2-propenoate (21)[74]. 6-Bromopyridine-3-carboxaldehyde (**12**) (3.06 g, 15.6 mmol) after reaction for 17.7 h, workup, and chromatography (16% EtOAc/hexane) produced 3.9 g (97%) of crude **21** as a pale-yellow solid. Crystallization (hexane) yielded 3.5 g (87%) of pure E-isomer **21** as a white solid, mp 79−80 °C (lit: 83.6−84.1 °C).[74] IR 2979, 1709, 1462, 1179 cm^{-1}. ^{1}H NMR δ 1.36 (t, J = 7.2 Hz, 3H, OCH$_2$CH$_3$), 4.31 (q, J = 7.2 Hz, 2H, OCH$_2$CH$_3$), 6.53 (d, J = 16.2 Hz, 1H, CH=CHCO), 7.55 (d, J = 8.1 Hz, 1H, 5-ArH), 7.68 (d, J = 16.2 Hz, 1H, CH=CHCO), 7.72 (dd, J = 2.1 Hz, 8.1 Hz, 1H, 4-ArH), 8.52 ppm (d, J = 2.1 Hz, 1H, 2-ArH).

Ethyl (E)-3-(5-Bromo-2-pyrazinyl)-2-propenoate (22). 5-Bromopyr-azine-2-carboxaldehyde (14) (284 mg, 1.52 mmol) after reaction for 18 h, workup, and chromatography (11−14% EtOAc/hexane) produced 369 mg (94%) of an E/Z mixture as a pale-yellow solid. Recrystallization (hexane) yielded 243 mg (62%) of pure E-isomer 22 as a cream solid, mp 70−71 °C.

Ethyl (E)-3-{1-[3′-(1-Adamantyl)-4′-benzyloxyphenyl]-4-piperidinyl}-2-propenoate (91). Compound 90 (86 mg, 0.20 mmol) after reaction for 15.7 h, workup, and chromatography (9% EtOAc/hexane) produced 78 mg (78%) of 91 as a white solid, mp 130−132 °C. IR 2902, 1716, 1478, 1218 cm^{-1}. ^{1}H NMR δ 1.33 (t, J = 7.2 Hz, 3H, OCH$_2$CH$_3$), 1.67 (m, 2H, N(CH$_2$CH$_2$)$_2$CH), 1.75 (bs, 6H, AdCH$_2$), 1.89 (m, 2H, N-(CH$_2$CH$_2$)$_2$CH), 2.07 (bs, 3H, AdCH), 2.17 (bs, 6H, AdCH$_2$), 2.26 (m, 1H, N(CH$_2$CH$_2$)$_2$CH), 2.71 (m, 2H, N(CH$_2$CH$_2$)$_2$CH), 3.57 (m, 2H, N(CH$_2$CH$_2$)$_2$CH), 4.23 (q, J = 7.2 Hz, 2H, OCH$_2$CH$_3$), 5.10 (s, 2H, ArCH$_2$), 5.88 (dd, J = 15.6 Hz, 1.2 Hz, 1H, CH=CHCO), 6.76 (dd, J = 8.7 Hz, 3.0 Hz, 1H, 6′-ArH), 6.89 (d, J = 8.7 Hz, 1H, 5′-ArH), 6.98 (d, J = 3.0 Hz, 1H, 2′-ArH), 7.01 (dd, J = 15.6 Hz, 6.9 Hz, 1H, CH=CHCO), 7.28−7.57 ppm (m, 5H, ArH). HRMS calcd C$_{33}$H$_{41}$NO$_3$ [M + H]$^+$, 500.3159; found, 500.3161.

Ethyl (E)-4-Bromo-3-chlorocinnamate (59). Compound 58 (4.91 g, 22.37 mmol) after reaction for 17 h, workup, and chromatography (2−9% EtOAc/hexane) produced 5.98 g (92%) of 59 as off-white needles, mp 67−69 °C. IR 3038, 1719, 1176 cm^{-1}. ^{1}H NMR δ 1.36 (t, J = 7.2 Hz, 3H, OCH$_2$CH$_3$), 4.29 (q, J = 7.2 Hz, 2H, OCH$_2$CH$_3$), 6.45 (d, J = 16.2 Hz, 1H, CH=CHCO), 7.28 (dd, J = 1.8 Hz, 8.4 Hz, 1H, 6-ArH), 7.58 (d, J = 16.2 Hz, 1H, CH=CHCO), 7.62 (d, J = 1.8 Hz, 1H, 2-ArH), 7.65 ppm (d, J = 8.4 Hz, 1H, 5-ArH). HRMS calcd C$_{11}$H$_{10}$BrClO$_2$ [M + H]$^+$, 288.9631; found, 288.9630.

General Procedure for Suzuki Coupling of 3-(1-Ada-mantyl)-4-benzyloxyphenylboronic Acid (25) with Heteroaryl Halides 19−24, 45, 48, and 60, Heteroaryl Triflate 47, Aryl Bromide 61, and 6-Bromoindole 80 To Afford Phenylhetero-aryl and Phenylaryl Conjugates 26−31, 49, 53, 65, 51, 67, and 81, Respectively. To a solution of 25 (1.2−1.3 mmol) and the heteroaryl halide (1.0 mmol) in the specified solvent (degassed under argon) was added 1,1′-bis(diphenylphosphino)ferrocenedichloropalla-dium(II)·CH$_2$Cl$_2$ (50 mg, 0.06 mmol) or (Ph$_3$P)$_4$Pd (151 mg, 0.12−0.13 mmol) and the specified base (solid or in degassed water). The reaction mixture was heated at reflux under argon, cooled to room temperature, diluted with EtOAc, washed (H$_2$O and brine), and dried. After solvent removal at reduced pressure, flash chromatography on silica gel yielded the purified coupling product.

Ethyl (E)-3-{2-[3′-(1-Adamantyl)-4′-benzyloxyphenyl]-3-chloro-5-pyridinyl}-2-propenoate (26). Compound 19 (123 mg, 0.500 mmol) in DME (6 mL), 1,1′-bis(diphenylphosphino)ferrocenedichloropal-ladium(II)·CH$_2$Cl$_2$ (25 mg, 0.03 mmol), and Cs$_2$CO$_3$ (652 mg, 2.00 mmol) on coupling at 75 °C for 17 h and then at 90 °C for 15 h, workup, and chromatography (9−11% EtOAc/hexane) gave 85 mg (32%) of 26 as a viscous pale-yellow oil. IR 2903, 1711, 1233, 1176 cm^{-1}. ^{1}H NMR δ 1.39 (t, J = 7.2 Hz, 3H, OCH$_2$CH$_3$), 1.76 (bs, 6H, AdCH$_2$), 2.08 (bs, 3H, AdCH), 2.23 (bs, 6H, AdCH$_2$), 4.33 (q, J = 7.2 Hz, 2H, OCH$_2$CH$_3$), 5.22 (s, 2H, C$_6$H$_5$CH$_2$), 6.57 (d, J = 16.2 Hz, 1H, CH=CHCO), 7.05 (d, J = 8.4 Hz, 1H, 5′-ArH), 7.28−7.57 (m, 5H, C$_6$H$_5$), 7.65 (d, J = 16.2 Hz, 1H, CH=CHCO), 7.66 (d, J = 8.4 Hz, 1H, 6′-ArH), 7.77 (s, 1H, 2′-ArH), 7.95 (s, 1H, 4-ArH), 8.71 ppm (s, 1H, 6-ArH). HRMS calcd C$_{33}$H$_{34}$ClNO$_3$ [M + H]$^+$, 528.2300; found, 528.2299.

Ethyl (E)-3-{5-[3′-(1-Adamantyl)-4′-benzyloxyphenyl]-2-pyridinyl}-2-propenoate (27). Compound 20 (128 mg, 0.50 mmol) in DME (4 mL), (Ph$_3$P)$_4$Pd (58 mg, 0.05 mmol), and 2 M aqueous Na$_2$CO$_3$ (0.8 mL) on coupling at reflux for 18.7 h, workup, and chromatography (16−33% EtOAc/hexane) gave 246 mg (99%) of 27 as a cream solid, mp 49−52 °C. IR 2903, 1711, 1477, 1232, 1141 cm^{-1}. ^{1}H NMR δ 1.35 (t, J = 7.3 Hz, 3H, OCH$_2$CH$_3$), 1.75 (bs, 6H, AdCH$_2$), 2.07 (bs, 3H,

AdCH), 2.20 (bs, 6H, AdCH$_2$), 4.28 (q, J = 7.3 Hz, 2H, OCH$_2$CH$_3$), 5.18 (s, 2H, ArCH$_2$), 6.91 (d, J = 15.9 Hz, 1H, CH=CHCO), 7.04 (d, J = 8.5 Hz, 1H, 5′-ArH), 7.29−7.44 (m, 4H, 3ArH, 6′-ArH), 7.46 (d, J = 8.5 Hz, 1H, 3-ArH), 7.48−7.53 (m, 3H, 2ArH, 2′-ArH), 7.72 (d, J = 15.9 Hz, 1H, CH=CHCO), 7.86 (d, J = 2.4 Hz, 8.5 Hz, 1H, 4-ArH), 8.86 ppm (d, J = 2.4 Hz, 1H, 6-ArH). HRMS calcd C$_{33}$H$_{35}$NO$_3$ [M + H]$^+$, 494.2690; found, 494.2687.

Ethyl (E)-3-{6-[3′-(1-Adamantyl)-4′-benzyloxyphenyl]-3-pyridinyl}-2-propenoate (28). Compound 21 (2.12 g, 8.30 mmol) in DME (50 mL), (Ph$_3$P)$_4$Pd (1.15 g, 1.00 mmol), and 2 M aqueous Na$_2$CO$_3$ (10 mL) after coupling at reflux for 20 h, workup, and chromatography (12−25% EtOAc/hexane) gave 4 g (97%) of 28 as a pale-yellow solid, mp 60−63 °C. IR 2901, 1710, 1234, 1176 cm^{-1}. ^{1}H NMR δ 1.39 (t, J = 7.2 Hz, 3H, OCH$_2$CH$_3$), 1.77 (bs, 6H, AdCH$_2$), 2.10 (bs, 3H, AdCH), 2.25 (bs, 6H, AdCH$_2$), 4.32 (q, J = 7.2 Hz, 2H, OCH$_2$CH$_3$), 5.22 (s, 2H, ArCH$_2$), 6.53 (d, J = 16.2 Hz, 1H, CH=CHCO), 7.07 (d, J = 8.7 Hz, 1H, 5′-ArH), 7.28−7.57 (m, 5H, ArH), 7.72 (d, J = 16.2 Hz, 1H, CH=CHCO), 7.75 (d, J = 8.4 Hz, 1H, 5-ArH), 7.85 (dd, J = 8.4 Hz, 2.4 Hz, 1H, 6′-ArH), 7.90 (dd, J = 8.7 Hz, 2.7 Hz, 1H, 4-ArH), 8.03 (d, J = 2.4 Hz, 1H, 2′-ArH), 8.81 ppm (d, J = 2.7 Hz, 1H, 2-ArH). HRMS calcd C$_{33}$H$_{35}$NO$_3$ [M + H]$^+$, 494.2690; found, 494.2687.

Ethyl (E)-3-[2-(3′-(1-Adamantyl)-4′-benzyloxyphenyl)-5-pyrazinyl]-2-propenoate (29). Compound 22 (278 mg, 1.08 mmol) in DME (8 mL), (Ph$_3$P)$_4$Pd (151 mg, 0.13 mmol), and 2 M aqueous Na$_2$CO$_3$ (1.5 mL) after coupling at reflux for 19.5 h, workup, and chromatography (10−25% EtOAc/hexane) gave 488 mg (91%) of 29 as a yellow solid, mp 145−148 °C. IR 2899, 1710, 1238 cm^{-1}. ^{1}H NMR δ 1.35 (t, J = 7.3 Hz, 3H, OCH$_2$CH$_3$), 1.73 (bs, 6H, AdCH$_2$), 2.06 (bs, 3H, AdCH), 2.20 (bs, 6H, AdCH$_2$), 4.29 (q, J = 7.3 Hz, 2H, OCH$_2$CH$_3$), 5.19 (s, 2H, C$_6$H$_5$CH$_2$), 6.98 (d, J = 15.9 Hz, 1H, CH=CHCO), 7.04 (d, J = 8.5 Hz, 1H, 5′-ArH), 7.28−7.52 (m, 5H, C$_6$H$_5$), 7.72 (d, J = 15.9 Hz, 1H, CH=CHCO), 7.84 (dd, J = 8.5 Hz, 2.4 Hz, 1H, 6′-ArH), 8.02 (d, J = 2.4 Hz, 1H, 2′-ArH), 8.63 (d, J = 1.24 Hz, 1H, 3-ArH), 8.99 ppm (d, J = 1.24 Hz, 1H, 6-ArH). HRMS calcd C$_{32}$H$_{34}$N$_2$O$_3$ [M + H]$^+$, 495.2642; found, 495.2659.

Ethyl (E)-3-[2-(3′-(1-Adamantyl)-4′-benzyloxyphenyl)-5-pyrimidinyl]-2-propenoate (30). Compound 23 (1.76 g, 8.30 mmol) in DME (50 mL), (Ph$_3$P)$_4$Pd (1.15 g, 1.00 mmol), and 2 M aqueous Na$_2$CO$_3$ (10 mL) on coupling at reflux for 18 h, workup, and chromatography (9−14% EtOAc/hexane) gave 3.98 g (96%) of 30 as a yellow solid, mp 164−167 °C. IR 2903, 1710, 1432, 1225 cm^{-1}. ^{1}H NMR δ 1.40 (t, J = 7.2 Hz, 3H, OCH$_2$CH$_3$), 1.77 (bs, 6H, AdCH$_2$), 2.11 (bs, 3H, AdCH), 2.26 (bs, 6H, AdCH$_2$), 4.33 (q, J = 7.2 Hz, 2H, OCH$_2$CH$_3$), 5.24 (s, 2H, CH$_2$), 6.59 (d, J = 16.2 Hz, 1H, CH=CHCO), 7.08 (d, J = 8.7 Hz, 1H, 5′-ArH), 7.35−7.58 (m, 5H, C$_6$H$_5$), 7.65 (d, J = 16.2 Hz, 1H, CH=CHCO), 8.33 (dd, J = 8.7 Hz, 2.1 Hz, 1H, 6′-ArH), 8.47 (d, J = 2.1 Hz, 1H, 2′-ArH), 8.91 ppm (s, 2H, 4-ArH, 6-ArH). HRMS calcd C$_{32}$H$_{34}$N$_2$O$_3$ [M + H]$^+$, 495.2642; found, 495.2636.

Ethyl (E)-3-{6-[3′-(1-Adamantyl)-4′-benzyloxyphenyl]-3-pyridazinyl]-2-propenoate (31). Compound 24 (165 mg, 0.776 mmol) in DME (5 mL), (Ph$_3$P)$_4$Pd (115 mg, 0.10 mmol), and 2 M aqueous Na$_2$CO$_3$ (1 mL) on coupling at reflux for 20 h, workup, and chromatography (14−20% EtOAc/hexane) gave 59 mg (15%) of 31 as a yellow solid, mp 134−136 °C. IR 2912, 1710, 1578, 1230 cm^{-1}. ^{1}H NMR δ 1.39 (t, J = 7.2 Hz, 3H, OCH$_2$CH$_3$), 1.77 (bs, 6H, AdCH$_2$), 2.09 (bs, 3H, AdCH), 2.24 (bs, 6H, AdCH$_2$), 4.34 (q, J = 7.2 Hz, 2H, OCH$_2$CH$_3$), 5.24 (s, 2H, ArCH$_2$), 7.02 (d, J = 15.9 Hz, 1H, CH=CHCO), 7.11 (d, J = 9.0 Hz, 1H, 5′-ArH), 7.34−7.51 (m, 3H, ArH), 7.52−7.57 (m, 2H, ArH), 7.65 (d, J = 8.7 Hz, 1H, 4-ArH), 7.86 (d, J = 9.0 Hz, 1H, 5-ArH), 7.92 (d, J = 15.9 Hz, 1H, CH=CHCO), 7.96 (dd, J = 8.7 Hz, 2.1 Hz, 1H, 6′-ArH), 8.15 ppm (d, J = 2.1 Hz, 1H, 2′-ArH). HRMS calcd C$_{32}$H$_{34}$N$_2$O$_3$ [M + H]$^+$, 495.2642; found, 495.2630.

2-[3′-(1-Adamantyl)-4′-benzyloxyphenyl]-5-nitropyrimidine (49). 2-Chloro-5-nitropyrimidine (45) (320 mg, 2.00 mmol) in MePh (15 mL), (Ph$_3$P)$_4$Pd (347 mg, 0.30 mmol), NaHCO$_3$ (336 mg, 4.00 mmol), and degassed H$_2$O (3 mL) after coupling at reflux for 24 h,

workup, and chromatography (3% EtOAc/hexane) gave 165 mg (19%) of **49** as a yellow solid, mp 206 °C (dec.). IR 2902, 1405, 1179 cm^{-1}. ^{1}H NMR δ 1.76 (bs, 6H, AdCH$_2$), 2.09 (bs, 3H, AdCH), 2.22 (m, 6H, AdCH$_2$), 5.24 (s, 2H, C$_6$H$_5$CH$_2$), 7.07 (d, J = 8.7 Hz, 1H, 5′-ArH), 7.34−7.53 (m, 5H, C$_6$H$_5$), 8.40 (dd, J = 8.7 Hz, 2.4 Hz, 1H, 6′-ArH), 8.51 (d, J = 2.4 Hz, 1H, 2′-ArH), 9.46 ppm (s, 2H, 4-ArH, 6-ArH). HRMS calcd C$_{27}$H$_{27}$N$_3$O$_3$ [M + H]$^+$, 442.2125; found, 442.2137.

3′-(1-Adamantyl)-4′-benzyloxy-2-chloro-4-nitro-1,1′-biphenyl (51). 2-Chloro-4-nitrophenyl trifluoromethanesulfonate (**47**) (721 mg, 2.36 mmol) in DME (16 mL), (Ph$_3$P)$_4$Pd (307 mg, 0.26 mmol), and K$_3$PO$_4$ (450 mg, 2.12 mmol) after coupling at reflux for 4.5 h, workup, and chromatography (7% EtOAc/hexane) gave 908 mg (81%) of **51** as a yellow solid, mp 52−54 °C. IR 2911, 1342, 1208 cm^{-1}. ^{1}H NMR δ 1.77 (bs, 6H, AdCH$_2$), 2.09 (bs, 3H, AdCH), 2.21 (m, 6H, AdCH$_2$), 5.21 (s, 2H, C$_6$H$_5$CH$_2$), 7.06 (d, J = 8.7 Hz, 1H, 5-ArH), 7.31−7.48 (m, 3H, C$_6$H$_5$, 2H, 6-ArH, 2-ArH), 7.52−7.56 (m, 2H, C$_6$H$_5$, 1H, 6′-ArH), 8.16 (dd, J = 8.7 Hz, 2.4 Hz, 1H, 5′-ArH), 8.37 ppm (d, J = 2.4 Hz, 1H, 3′-ArH).

3′-(1-Adamantyl)-4′-benzyloxy-2-chloro-4-hydroxy-1,1′-biphenyl (53). 4-Bromo-3-chlorophenol (**48**) (207 mg, 1.00 mmol) in DME (5 mL), (Ph$_3$P)$_4$Pd (115 mg, 0.10 mmol), and 2 M aqueous Na$_2$CO$_3$ (1.75 mL) after coupling at reflux for 21 h, workup, and chromatography (16% EtOAc/hexane) gave 316 mg (71%) of **53** as a light-gray solid, mp 56−58 °C. IR 3351, 2901, 1507, 1215 cm^{-1}. ^{1}H NMR δ 1.73 (bs, 6H, AdCH$_2$), 2.05 (bs, 3H, AdCH), 2.18 (bs, 6H, AdCH$_2$), 5.07 (s, 1H, OH), 5.17 (s, 2H, C$_6$H$_5$CH$_2$), 6.79 (dd, J = 8.7 Hz, 2.4 Hz, 1H, 5-ArH), 6.98 (d, J = 2.4 Hz, 1H, 3-ArH), 7.00 (d, J = 8.4 Hz, 1H, 5′-ArH), 7.22 (d, J = 8.7 Hz, 1H, 6-ArH), 7.23 (dd, J = 8.4 Hz, 2.4 Hz, 1H, 6′-ArH), 7.32 (d, J = 2.4 Hz, 1H, 2′-ArH), 7.32−7.56 ppm (m, 5H, C$_6$H$_5$). HRMS calcd C$_{29}$H$_{29}$ClO$_2$ [M + Na]$^+$, 467.1748; found, 467.1736.

Ethyl 2-[3′-(1-Adamantyl)-4′-benzyloxy-2-chloro-1,1′-biphenyl-4-ylthio]acetate (65). Ethyl 2-(4-bromo-3-chlorophenylthio)acetate (**60**) (173 mg, 0.560 mmol) in DMF (4 mL), (Ph$_3$P)$_4$Pd (65 mg, 0.07 mmol), and K$_3$PO$_4$ (297 mg, 1.40 mmol) after coupling at reflux for 6 h, workup, and chromatography (2% EtOAc/hexane) gave 164 mg (63%) of **65** as a cream-colored solid, mp 104−106 °C. IR 2901, 1734, 1229 cm^{-1}. ^{1}H NMR δ 1.28 (t, J = 7.2 Hz, 3H, OCH$_2$CH$_3$), 1.73 (bs, 6H, AdCH$_2$), 2.05 (bs, 3H, AdCH), 2.18 (bs, 6H, AdCH$_2$), 3.68 (s, 2H, CH$_2$CO$_2$), 4.22 (q, J = 7.2 Hz, 2H, OCH$_2$CH$_3$), 5.17 (s, 2H, C$_6$H$_5$CH$_2$), 6.99 (d, J = 8.7 Hz, 1H, 5′-ArH), 7.25 (dd, J = 8.7 Hz, 2.4 Hz, 1H, 6-ArH), 7.30−7.46 (m, 3H, C$_6$H$_5$, 2H, 3, 5-ArH, 1H, 6′-ArH), 7.50−7.56 ppm (m, 2H, C$_6$H$_5$, 1H, 2′-ArH). HRMS calcd C$_{33}$H$_{35}$ClO$_3$S [M + H]$^+$, 547.2068; found, 547.2061.

Ethyl 3-[4-(3′-(1-Adamantyl)-4′-benzyloxy)-3-chlorophenyl]propanoate (67). Ethyl 3-(4-Bromo-3-chlorophenyl) propanoate (**61**) (242 mg, 0.83 mmol) in DME, (Ph$_3$P)$_4$Pd (96 mg, 0.08 mmol), and 2 M aqueous Na$_2$CO$_3$ after coupling at reflux for 20 h, workup, and chromatography (2−7% EtOAc/hexane) gave 328 mg (62%) of **67** as a white solid, mp 109−110 °C. IR 2908, 1734, 1229 cm^{-1}. ^{1}H NMR δ 1.29 (t, J = 7.2 Hz, 3H, OCH$_2$CH$_3$), 1.75 (bs, 6H, AdCH$_2$), 2.06 (bs, 3H, AdCH), 2.20 (bs, 6H, AdCH$_2$), 2.67 (t, J = 7.8 Hz, 2H, CH$_2$CH$_2$CO), 2.98 (t, J = 7.8 Hz, 2H, CH$_2$CH$_2$CO), 4.18 (q, J = 7.2 Hz, 2H, OCH$_2$CH$_3$), 5.18 (s, 2H, ArCH$_2$), 7.02 (d, J = 8.4 Hz, 1H, 5′-ArH), 7.16 (d, J = 7.8 Hz, 1H, 6-ArH), 7.27 (dd, J = 1.4, 8.4 Hz, 1H, 6′-ArH), 7.32 (d, J = 7.8 Hz, 1H, 5-ArH), 7.34 (s, 1H, 2-ArH), 7.36 (d, J = 1.4 Hz, 1H, 2′-ArH), 7.35−7.58 ppm (m, 5H, C$_6$H$_5$). HRMS calcd C$_{34}$H$_{37}$ClO$_3$ [M + H]$^+$, 529.2504; found, 529.2479.

Ethyl 6-[3′-(1-Adamantyl)-4′-benzyloxyphenyl]-1H-indole-2-carboxylate (81). Ethyl 6-bromoindole-2-carboxylate (**80**) (80 mg, 0.30 mmol) in MePh (1 mL), EtOH (1 mL), (Ph$_3$P)$_4$Pd (35 mg, 0.03 mmol), saturated aqueous NaHCO$_3$ (0.65 mL) on coupling at reflux for 18.5 h, workup, and chromatography (10% EtOAc/hexane) gave 136 mg (90%) of **81** as a pale-yellow solid, mp 200−202 °C. IR 3315, 2903, 1686, 1272, 1214 cm^{-1}. ^{1}H NMR δ 1.46 (t, J = 7.2 Hz, 3H, OCH$_2$CH$_3$), 1.78 (bs, 6H,

AdCH$_2$), 2.10 (bs, 3H, AdCH), 2.26 (bs, 6H, AdCH$_2$), 4.45 (q, J = 7.2 Hz, 2H, OCH$_2$CH$_3$), 5.21 (s, 2H, C$_6$H$_5$CH$_2$), 7.06 (d, J = 8.4 Hz, 1H, 5′-ArH), 7.27 (m, 1H, 7-InH), 7.34−7.51 (m, 5H, 5-InH, 6′-ArH, 3H from C$_6$H$_5$), 7.54−7.58 (m, 2H, C$_6$H$_5$), 7.59 (d, J = 2.4 Hz, 1H, 2′-ArH), 7.61 (s, 1H, 3-InH), 7.75 (d, J = 8.1 Hz, 1H, 4-InH), 8.91 ppm (bs, 1H, NH). HRMS calcd C$_{34}$H$_{35}$NO$_3$ [M + H]$^+$, 506.2690; found, 506.2687.

General Procedures for Deprotection of Benzyl Ethers 26−31, 62−67, 81, 91, 92, and 94. To Give Phenols 32−37, 68−73, 82, and 95−97, Respectively. *Method A for Preparing* ***32***−***37****,* ***68****,* ***69****,* ***71****−****73****,* ***82****, and* ***95****−****97****.* To a stirred solution of the benzyl ether (1 mmol) in CH$_2$Cl$_2$ (13 mL) at −78 °C under argon was added slowly 1.0 M boron tribromide (4.0 mmol) in CH$_2$Cl$_2$ (4.0 mL). The mixture was stirred at −78 °C for 2 h, quenched with water (50 mL), and extracted with EtOAc. The extract was washed (brine) and dried. After solvent removal at reduced pressure, flash chromatography of the residue yielded the phenol.

Method B for Preparing ***70****.* To a stirred solution of the benzyl ether (335 mg, 0.630 mmol) in anhydrous EtOH (5 mL) was added 10% palladium on carbon (50 mg). The reaction mixture was stirred vigorously under H$_2$ for 5.5 h, diluted with EtOAc (100 mL), and filtered through Celite (EtOAc rinse). After solvent removal at reduced pressure, the residue was chromatographed to give the phenol.

Method A: Ethyl (E)-3-{2-[3′-(1-Adamantyl)-4′-hydroxyphenyl]-3-chloro-5-pyridinyl}-2-propenoate (32). Compound **26** (72 mg, 0.14 mmol) after treatment, workup, and chromatography (13−25% EtOAc/hexane) gave 36 mg (61%) of **32** as a yellow solid, mp 260−261 °C. IR 3373, 2905, 1712, 1411, 1183 cm^{-1}. ^{1}H NMR δ 1.39 (t, J = 7.2 Hz, 3H, OCH$_2$CH$_3$), 1.82 (bs, 6H, AdCH$_2$), 2.12 (bs, 3H, AdCH), 2.20 (bs, 6H, AdCH$_2$), 4.33 (q, J = 7.2 Hz, 2H, OCH$_2$CH$_3$), 5.21 (s, 1H, OH), 6.57 (d, J = 15.9 Hz, 1H, CH=CHCO), 6.77 (d, J = 8.4 Hz, 1H, 5′-ArH), 7.58 (dd, J = 1.5, 8.4 Hz, 1H, 6′-ArH), 7.67 (d, J = 15.9 Hz, 1H, CH=CHCO), 7.71 (d, J = 1.5, 1H, 2′-ArH), 7.96 (s, 1H, 4-ArH), 8.71 ppm (s, 1H, 6-ArH). HRMS calcd C$_{26}$H$_{28}$ClNO$_3$ [M + H]$^+$, 438.2830; found, 438.1826.

Ethyl (E)-3-{5-[3′-(1-Adamantyl)-4′-hydroxyphenyl]-2-pyridinyl}-2-propenoate (33). Compound **27** (225 mg, 0.46 mmol) after treatment, workup, and chromatography (14−66% EtOAc/hexane) gave 168 mg (91%) of **33** as a yellow solid, mp 197−199 °C. IR 3352, 2903, 1714, 1603, 1299 cm^{-1}. ^{1}H NMR δ 1.35 (t, J = 7.3 Hz, 3H, OCH$_2$CH$_3$), 1.80 (bs, 6H, AdCH$_2$), 2.11 (bs, 3H, AdCH), 2.18 (bs, 6H, AdCH$_2$), 4.28 (q, J = 7.3 Hz, 2H, OCH$_2$CH$_3$), 5.31 (bs, 1H, OH), 6.78 (d, J = 8.5 Hz, 1H, 5′-ArH), 6.91 (d, J = 15.9 Hz, 1H, CH=CHCO), 7.32 (dd, J = 2.4 Hz, 8.5 Hz, 1H, 6′-ArH), 7.45 (d, J = 2.4 Hz, 1H, 2′-ArH), 7.47 (d, J = 7.9 Hz, 1H, 3-ArH), 7.73 (d, J = 15.9 Hz, 1H, CH=CHCO), 7.85 (dd, J = 2.4 Hz, 7.9 Hz, 1H, 4-ArH), 8.85 ppm (d, J = 2.4 Hz, 1H, 6-ArH). HRMS calcd C$_{26}$H$_{29}$NO$_3$ [M + H]$^+$, 404.2220; found, 404.2223.

Ethyl (E)-3-{6-[3′-(1-Adamantyl)-4′-hydroxyphenyl]-3-pyridinyl}-2-propenoate (34). Compound **28** (2.49 g, 5.04 mmol) after treatment, workup, and chromatography (14−33% EtOAc/hexane) gave 2.0 g (98%) of **34** as a yellow solid, mp 215−217 °C; purity (HPLC): ≥ 96%. IR 3406, 2899, 1707, 1478, 1589, 1250 cm^{-1}. ^{1}H NMR δ 1.39 (t, J = 7.2 Hz, 3H, OCH$_2$CH$_3$), 1.83 (bs, 6H, AdCH$_2$), 2.14 (bs, 3H, AdCH), 2.22 (bs, 6H, AdCH$_2$), 4.32 (q, J = 7.2 Hz, 2H, OCH$_2$CH$_3$), 5.50 (br s, 1H, OH), 6.53 (d, J = 15.9 Hz, 1H, CH=CHCO), 6.78 (d, J = 8.1 Hz, 1H, 5′-ArH), 7.71 (d, J = 8.4 Hz, 1H, 5-ArH), 7.73 (d, J = 15.9 Hz, 1H, CH=CHCO), 7.75 (dd, J = 8.4 Hz, 2.1 Hz, 1H, 6′-ArH), 7.89 (dd, J = 8.4 Hz, 2.4 Hz, 1H, 4-ArH), 7.98 (d, J = 2.1 Hz, 1H, 2′-ArH), 8.79 ppm (d, J = 2.4 Hz, 1H, 2-ArH). HRMS calcd C$_{26}$H$_{29}$NO$_3$ [M + H]$^+$, 404.2220; found, 404.2219.

Ethyl (E)-3-[5-(3′-(1-Adamantyl)-4′-hydroxyphenyl)-2-pyrazinyl]-2-propenoate (35). Compound **29** (477 mg, 0.96 mmol) after treatment, workup, and chromatography (20−33% EtOAc/hexane) gave 367 g (94%) of **35** as a yellow solid, mp 212−215 °C. IR 3352, 2843, 1686 cm^{-1}. ^{1}H NMR δ 1.35 (t, J = 7.3 Hz, 3H, OCH$_2$CH$_3$), 1.79 (bs,

6H, AdCH$_2$), 2.10 (bs, 3H, AdCH), 2.18 (bs, 6H, AdCH$_2$), 4.29 (q, J = 7.3 Hz, 2H, OCH$_2$CH$_3$), 5.32 (s, 1H, OH), 6.77 (d, J = 8.5 Hz, 1H, 5′-ArH), 6.97 (d, J = 15.9 Hz, 1H, CH═CHCO), 7.71 (d, J = 15.9 Hz, 1H, CH═CHCO), 7.75 (dd, J = 8.5 Hz, 2.4 Hz, 1H, 6′-ArH), 7.98 (d, J = 2.4 Hz, 1H, 2′-ArH), 8.62 (d, J = 1.2 Hz, 1H, 6-ArH), 8.97 ppm (d, J = 1.2 Hz, 1H, 3-ArH). HRMS calcd C$_{25}$H$_{28}$N$_2$O$_3$ [M + H]$^+$, 405.2173; found, 405.2181.

Ethyl (E)-3-[2-(3′-(1-Adamantyl)-4′-hydroxyphenyl)-5-pyrimidinyl]-2-propenoate (**36**). Compound **30** (2.30 g, 4.65 mmol) after treatment, workup, and chromatography (16—20% EtOAc/hexane) gave 1.8 g (95%) of **36** as a pale-yellow solid, mp 226—228 °C. IR 3345, 2856, 1715, 1456 cm^{-1}. ^{1}H NMR δ 1.39 (t, J = 7.2 Hz, 3H, OCH$_2$CH$_3$), 1.83 (bs, 6H, AdCH$_2$), 2.13 (bs, 3H, AdCH), 2.24 (bs, 6H, AdCH$_2$), 4.33 (q, J = 7.2 Hz, 2H, OCH$_2$CH$_3$), 5.38 (bs, 1H, OH), 6.59 (d, J = 16.2 Hz, 1H, CH═CHCO), 6.79 (d, J = 8.1 Hz, 1H, 5′-ArH), 7.65 (d, J = 16.2 Hz, 1H, CH═CHCO), 8.22 (dd, J = 8.1 Hz, 2.1 Hz, 1H, 6′-ArH), 8.44 (d, J = 2.1 Hz, 1H, 2′-ArH), 8.90 ppm (s, 2H, 4-ArH, 6-ArH). HRMS calcd C$_{25}$H$_{28}$N$_2$O$_3$ [M + H]$^+$, 405.2173; found, 405.2191.

Ethyl (E)-3-{6-[3′-(1-Adamantyl)-4′-hydroxyphenyl]-3-pyridazinyl}-2-propenoate (**37**). Compound **31** (53 mg, 0.11 mmol) after treatment, workup, and chromatography (14—33% EtOAc/hexane) gave 36 mg (84%) of **37** as a yellow solid, mp 246—248 °C. IR 3360, 2907, 1714, 1568, 1227 cm^{-1}. ^{1}H NMR (acetone-d_6) 1.36 (t, J = 7.5 Hz, 3H, OCH$_2$CH$_3$), 1.86 (bs, 6H, AdCH$_2$), 2.13 (bs, 3H, AdCH), 2.30 (bs, 6H, AdCH$_2$), 4.30 (q, J = 7.5 Hz, 2H, OCH$_2$CH$_3$), 7.03 (d, J = 8.4 Hz, 1H, 5′-ArH), 7.06 (d, J = 15.9 Hz, 1H, CH═CHCO), 7.91 (d, J = 15.9 Hz, 1H, CH═CHCO), 7.96 (dd, J = 8.4 Hz, 2.1 Hz, 1H, 6′-ArH), 8.06 (d, J = 9.0 Hz, 1H, 4-ArH), 8.17 (d, J = 9.0 Hz, 1H, 5-ArH), 8.20 (d, J = 2.1 Hz, 1H, 2′-ArH), 8.96 ppm (s, 1H, OH). HRMS calcd C$_{25}$H$_{28}$N$_2$O$_3$ [M + H]$^+$, 405.2173; found, 405.2174.

2-[3′-(1-Adamantyl)-4′-hydroxyphenyl]-5-(carbethoxymethylamino)-pyrimidine (**68**). Compound **62** (51 mg, 0.10 mmol) after treatment, workup, and chromatography (20% EtOAc/hexane) gave 41.6 mg (99%) of **68** as a pale-tan solid, mp 190 °C (dec.). IR 3432, 2904, 1708, 1211 cm^{-1}. ^{1}H NMR δ 1.32 (t, J = 7.2 Hz, 3H, OCH$_2$CH$_3$), 1.79 (bs, 6H, AdCH$_2$), 2.09 (bs, 3H, AdCH), 2.21 (m, 6H, AdCH$_2$), 4.30 (q, J = 7.2 Hz, 2H, OCH$_2$CH$_3$), 4.60 (m, 1H, NH), 4.72 (s, 2H, NHCH$_2$CO), 5.85 (s, 1H, OH), 6.71 (d, J = 8.4 Hz, 1H, 5′-ArH), 8.03 (dd, J = 8.4 Hz, 2.1 Hz, 1H, 6′-ArH), 8.27 (d, J = 2.1 Hz, 1H, 2′-ArH), 8.45 ppm (s, 2H, 4-ArH, 6-ArH). HRMS calcd C$_{24}$H$_{29}$N$_3$O$_3$ [M + H]$^+$, 408.2287; found, 408.2291.

Ethyl 2-[3′-(1-Adamantyl)-2-chloro-4′-hydroxy-1,1′-biphenyl-4-ylami-no]acetate (**69**). Compound **63** (256 mg, 0.48 mmol) after treatment, workup, and chromatography (25% EtOAc/hexane) gave 138 mg (65%) of **69** as a pale-tan solid, mp 184 °C (dec.). IR 3342, 2903, 1712, 1210 cm^{-1}. ^{1}H NMR δ 1.33 (t, J = 7.2 Hz, 3H, OCH$_2$CH$_3$), 1.78 (m, 6H, AdCH$_2$), 2.09 (m, 3H, AdCH), 2.16 (m, 6H, AdCH$_2$), 3.92 (d, J = 5.4 Hz, 2H, NHCH$_2$CO), 4.28 (q, J = 7.2 Hz, 3H, OCH$_2$CH$_3$), 4.39 (t, J = 5.4 Hz, 1H, NHCH$_2$CO), 4.80 (s, 1H, OH), 6.56 (dd, J = 8.4 Hz, 2.4 Hz, 1H, 5-ArH), 6.67 (d, J = 8.4 Hz, 1H, 5′-ArH), 6.69 (d, J = 2.4 Hz, 1H, 3-ArH), 7.12 (dd, J = 8.1 Hz, 2.1 Hz, 1H, 6′-ArH), 7.16 (J = 8.1 Hz, 1H, 6-ArH), 7.26 (d, J = 2.1 Hz, 1H, 2′-ArH). HRMS calcd C$_{26}$H$_{30}$ClNO$_3$ [M + H]$^+$, 440.1987; found, 440.1985.

Ethyl 2-[3′-(1-Adamantyl)-2-chloro-4′-hydroxy-1,1′-biphenyl-4-ylthio]-acetate (**71**). Compound **65** (54 mg, 0.10 mmol) after treatment, workup, and chromatography (4% EtOAc/hexane) gave 45 mg (94%) of **71** as a pale-yellow solid, mp 95—97 °C. IR 3433, 2901, 1712, 1472, 1284 cm^{-1}. ^{1}H NMR δ 1.29 (t, J = 7.2 Hz, 3H, OCH$_2$CH$_3$), 1.80 (bs, 6H, AdCH$_2$), 2.10 (bs, 3H, AdCH), 2.16 (bs, 6H, AdCH$_2$), 3.69 (s, 2H, SCH$_2$), 4.23 (q, J = 7.2 Hz, 2H, OCH$_2$CH$_3$), 5.04 (bs, 1H, OH), 6.71 (d, J = 8.4 Hz, 1H, 5′-ArH), 7.15 (dd, J = 8.1 Hz, 2.1 Hz, 1H, 6-ArH), 7.26 (d, J = 8.1 Hz, 1H, 5-ArH), 7.29 (d, J = 2.1 Hz, 1H, 2-ArH), 7.34 (dd, J = 8.4 Hz, 1.8 Hz, 1H, 6′-ArH), 7.52 ppm (d, J = 1.8 Hz, 1H, 2′-ArH). HRMS calcd C$_{26}$H$_{29}$ClO$_3$S [M + H]$^+$, 457.1599; found, 457.1596.

Ethyl 2-[3′-(1-Adamantyl)-2-chloro-4′-hydroxy-1,1′-biphenyl-4-yl-sulfonyl]acetate (**72**). Compound **66** (35 mg, 0.060 mmol) after

treatment, workup, and chromatography (4% EtOAc/hexane) gave 26 mg (89%) of **72** as an off-white solid, mp 170—172 °C. IR 3455, 2908, 1740, 1325, 1151 cm^{-1}. ^{1}H NMR δ 1.29 (t, J = 7.2 Hz, 3H, OCH$_2$CH$_3$), 1.82 (bs, 6H, AdCH$_2$), 2.13 (bs, 3H, AdCH), 2.18 (bs, 6H, AdCH$_2$), 4.19 (s, 2H, S(O)$_2$CH$_2$), 4.24 (q, J = 7.2 Hz, 2H, OCH$_2$CH$_3$), 5.09 (s, 1H, OH), 6.77 (d, J = 8.1 Hz, 1H, 5′-ArH), 7.22 (dd, J = 8.1 Hz, 2.1 Hz, 1H, 6′-ArH), 7.35 (d, J = 2.1 Hz, 1H, 2′-ArH), 7.57 (d, J = 8.1 Hz, 3-ArH), 7.88 (dd, J = 8.1 Hz, 1.8 Hz, 1H, 5-ArH), 8.07 ppm (d, J = 1.8 Hz, 1H, 6-ArH). HRMS calcd C$_{26}$H$_{29}$ClO$_5$S [M + H]$^+$, 489.1497; found, 489.1495.

Ethyl 3-[4-(3′-(1-Adamantyl)-4′-hydroxy)-3-chlorophenyl]propanoate (**73**). Compound **67** (322 mg, 0.61 mmol) after treatment, workup, and chromatography (5% to 20% EtOAc/hexane) gave 250 mg (93%) of **73** as a white solid, mp 46—47 °C. IR 3380, 2903, 1710, 1251 cm^{-1}. ^{1}H NMR δ 1.29 (t, J = 7.2 Hz, 3H, OCH$_2$CH$_3$), 1.81 (bs, 6H, AdCH$_2$), 2.12 (bs, 3H, AdCH), 2.18 (bs, 6H, AdCH$_2$), 2.68 (t, J = 7.8 Hz, 2H, CH$_2$CH$_2$CO), 2.98 (t, J = 7.8 Hz, 2H, CH$_2$CH$_2$CO), 4.18 (q, J = 7.2 Hz, 2H, OCH$_2$CH$_3$), 5.03 (s, 1H, OH), 6.73 (d, J = 8.1 Hz, 1H, 5′-ArH), 7.15 (dd, J = 1.2 Hz, 8.1 Hz, 1H, 6-ArH), 7.18 (dd, J = 1.8 Hz, 7.8 Hz, 1H, 6′-ArH), 7.28 (d, J = 7.8 Hz, 1H, 5-ArH), 8.32 (d, J = 1.8 Hz, 1H, 2′-ArH), 8.33 ppm (d, J = 1.2 Hz, 1H, 2-ArH). HRMS calcd C$_{27}$H$_{31}$ClO$_3$ [M + H]$^+$, 439.2034; found, 439.2032.

Ethyl 6-[3′-(1-Adamantyl)-4′-hydroxyphenyl]-1H-indole-2-carbox-ylate (**82**). Compound **81** (70.0 mg, 0.138 mmol) after treatment, workup, and chromatography (20% EtOAc/hexane) gave 48 mg (84%) of **82** as a pale-yellow solid, mp 216—217 °C. IR 3367, 2902, 1681, 1514, 1274, 1208 cm^{-1}. ^{1}H NMR δ 1.46 (t, J = 7.2 Hz, 3H, OCH$_2$CH$_3$), 1.84 (bs, 6H, AdCH$_2$), 2.14 (bs, 3H, AdCH), 2.23 (bs, 6H, AdCH$_2$), 4.45 (q, J = 7.2 Hz, 2H, OCH$_2$CH$_3$), 4.97 (bs, 1H, OH), 6.78 (d, J = 8.1 Hz, 1H, 5′-ArH), 7.26 (d, J = 0.9 Hz, 1H, 7-InH), 7.36 (dd, J = 8.1 Hz, 2.1 Hz, 1H, 6′-ArH), 7.41 (dd, J = 0.9 Hz, 8.4 Hz, 1H, 5-InH), 7.54 (d, J = 2.1 Hz, 1H, 2′-ArH), 7.57 (s, 1H, 3-InH), 7.73 (d, J = 8.4 Hz, 1H, 4-InH), 8.91 ppm (bs, 1H, NH). HRMS calcd C$_{27}$H$_{29}$NO$_3$ [M + H]$^+$, 416.2220; found, 416.2219.

Ethyl (E)-3-{1-[3′-(1-Adamantyl)-4′-hydroxyphenyl]piperidin-4-yl}-2-propenoate (**95**). Compound **91** (59 mg, 0.12 mmol) after treatment, workup, and chromatography (14—20% EtOAc/hexane) gave 37 mg (77%) of **95** as an off-white solid, mp 67—69 °C. IR 3362, 2907, 1701, 1172 cm^{-1}. ^{1}H NMR δ 1.33 (t, J = 7.2 Hz, 3H, OCH$_2$CH$_3$), 1.68 (m, 2H, N(CH$_2$CH$_2$)$_2$CH), 1.80 (bs, 6H, AdCH$_2$), 1.87 (m, 2H, N(CH$_2$CH$_2$)$_2$CH), 2.11 (bs, 3H, AdCH), 2.14 (bs, 6H, AdCH$_2$), 2.23 (m, 1H, N(CH$_2$CH$_2$)$_2$CH), 2.69 (m, 2H, N(CH$_2$CH$_2$)$_2$CH), 3.53 (m, 2H, N(CH$_2$CH$_2$)$_2$CH), 4.23 (q, J = 7.2 Hz, 2H, OCH$_2$CH$_3$), 4.54 (bs, 1H, OH), 5.87 (d, J = 15.6 Hz, 1H, CH═CHCO), 6.59 (d, J = 7.8 Hz, 1H, 6′-ArH), 6.69 (d, J = 7.8 Hz, 1H, 5′-ArH), 6.92 (s, 1H, 2′-ArH), 7.0 ppm (dd, J = 15.6 Hz, 6.9 Hz, 1H, CH═CHCO). HRMS calcd C$_{26}$H$_{35}$NO$_3$ [M + H]$^+$, 410.2690; found, 410.2686.

Ethyl 3-[4-(3′-(1-Adamantyl)-4′-hydroxyphenyl)piperazinyl]propionate (**96**). Compound **92** (206 mg, 0.410 mmol) after treatment, workup, and chromatography (33—66% EtOAc/hexane) gave 111 mg (66%) of **96** as an off-white solid, mp 162—163 °C. IR 3356, 2903, 1732, 1501, 1175 cm^{-1}. ^{1}H NMR δ 1.29 (t, J = 7.2 Hz, 3H, OCH$_2$CH$_3$), 1.79 (bs, 6H, AdCH$_2$), 2.10 (bs, 3H, AdCH), 2.13 (bs, 6H, AdCH$_2$), 2.57 (t, J = 7.5 Hz, 2H, NCH$_2$CH$_2$CO), 2.66 (bs, 4H, ArN(CH$_2$CH$_2$)$_2$N), 2.79 (t, J = 7.5 Hz, 2H, NCH$_2$CH$_2$CO), 3.10 (bs, 4H, ArN(CH$_2$CH$_2$)$_2$N), 4.18 (q, J = 7.2 Hz, 2H, OCH$_2$CH$_3$), 4.74 (s, 1H, OH), 6.58 (d, J = 8.7 Hz, 1H, 5′-ArH), 6.66 (d, J = 8.7 Hz, 1H, 6′-ArH), 6.90 ppm (s, 1H, 2′-ArH). HRMS calcd C$_{25}$H$_{36}$N$_2$O$_3$ [M + H]$^+$, 413.2799; found, 413.2802.

Ethyl 3-{4-[3′-(1-Adamantyl)-4′-hydroxyphenyl]-3-oxopiperazin-1-yl}-3-oxopropionate (**97**). Compound **94** (91 mg, 0.17 mmol) after treatment, workup, and chromatography (MeOH/EtOAc/hexane, 0:2.5:1—1:9:0) gave 76 mg (100%) of **97** as a white solid, mp 217—219 °C. IR 3319, 2903, 1737, 1647, 1423 cm^{-1}. ^{1}H NMR δ 1.34 (t, J = 7.5 Hz, 3H, OCH$_2$CH$_3$), 1.79 (bs, 6H, AdCH$_2$), 2.11 (bs, 9H, AdCH, AdCH$_2$), 3.56

(s, 2H, COCH$_2$CO$_2$), 3.73 (t, J = 6 Hz, 2H, ArNCH$_2$CH$_2$N), 4.02 (t, J = 6 Hz, 2H, ArNCH$_2$CH$_2$N), 4.26 (q, J = 7.5 Hz, 2H, OCH$_2$CH$_3$), 4.30 (s, 2H, NCOCH$_2$N), 5.38 (s, 1H, OH), 6.62 (d, J = 8.4 Hz, 1H, 5′-ArH), 7.08 (dd, J = 8.4, 2.7 Hz, 1H, 6′-ArH), 7.13 ppm (d, J = 2.7 Hz, 1H, 2′-ArH). HRMS calcd C$_{25}$H$_{32}$N$_2$O$_5$ [M + H]$^+$, 441.2384; found, 441.2379.

Method B. Ethyl 2-[3′-(1-Adamantyl)-2-chloro-4′-hydroxy-1,1′-bi-phenyl-4-yloxo]acetate (70). To a solution of ethyl 2-[3′-(1-adamantyl)-4′-benzyloxy-2-chloro-1,1′-biphenyl-4-yloxo]acetate (64) (335 mg, 0.630 mmol) after treatment for 5.5 h, workup, and chromatography (16% EtOAc/hexane) gave 264 mg (95%) of 70 as a white solid, mp 195−197 °C. IR 3374, 2865, 1734, 1215 cm^{-1}. ^{1}H NMR δ 1.33 (t, J = 7.2 Hz, 3H, OCH$_2$CH$_3$), 1.79 (m, 6H, AdCH$_2$), 2.09 (bs, 3H, AdCH), 2.16 (m, 6H, AdCH$_2$), 4.31 (q, J = 7.2 Hz, 2H, OCH$_2$CH$_3$), 4.65 (s, 2H, OCH$_2$CO), 4.94 (s, 1H, OH), 6.70 (d, J = 8.1 Hz, 1H, 5′-ArH), 6.86 (dd, J = 8.4 Hz, 2.7 Hz, 1H, 5-ArH), 7.02 (d, J = 2.7 Hz, 1H, 3-ArH), 7.12 (dd, J = 8.1 Hz, 2.1 Hz, 1H, 6′-ArH), 7.25 (d, J = 8.4 Hz, 1H, 6-ArH), 7.26 ppm (d, J = 2.1 Hz, 1H, 2′-ArH). HRMS calcd C$_{26}$H$_{29}$ClO$_4$ [M + H]$^+$, 441.1827; found, 441.1815.

General Procedure for Hydrolysis of Ethyl Esters 33−37 to Carboxylic Acids 39−43, Respectively, with Aqueous Sodium Hydroxide. To a solution of the ethyl ester (1.0 mmol) in MeOH (10 mL) was added 5 M aqueous NaOH (1 mL, 5 mmol). This mixture was heated at reflux under argon for 1 h, cooled to room temperature, acidified with 2 N HCl (22 mL), and extracted with EtOAc (100, 50, and 20 mL portions). The extract was washed (brine) and dried. The yellow solid obtained by concentration was chromatographed or triturated to afford the carboxylic acid.

(E)-3-{5-[3′-(1-Adamantyl)-4′-hydroxyphenyl]-2-pyridinyl}-2-pro-penoic Acid (39). Compound 33 (130 mg, 0.32 mmol) after hydrolysis, workup, and trituration (hexane, CH$_2$Cl$_2$, and CHCl$_3$) afforded 121 mg (100%) of 39 as a yellow solid, mp >260 °C (dec.); purity (HPLC): 100%. IR 3217, 2903, 1695, 1601, 1219 cm^{-1}. ^{1}H NMR (C^{2}H$_3$O^{2}H) δ 1.84 (bs, 6H, AdCH$_2$), 2.09 (bs, 3H, AdCH), 2.23 (bs, 6H, AdCH$_2$), 6.92 (d, J = 8.5 Hz, 1H, 5′-ArH), 7.07 (d, J = 15.9 Hz, 1H, CH═CHCO), 7.53 (dd, J = 2.4, 8.5 Hz, 1H, 6′-ArH), 7.57 (d, J = 2.4 Hz, 1H, 2′-ArH), 7.77 (d, J = 15.9 Hz, 1H, CH═CHCO), 8.32 (d, J = 8.5 Hz, 1H, 3-ArH), 8.70 (dd, J = 1.8, 8.5 Hz, 1H, 4-ArH), 9.00 ppm (d, J = 1.8 Hz, 1H, 6-ArH). HRMS calcd C$_{24}$H$_{25}$NO$_3$ [M + H]$^+$, 376.1907; found, 376.1908.

(E)-3-{2-[3′-(1-Adamantyl)-4′-hydroxyphenyl]-5-pyridinyl}-2-pro-penoic Acid (40). Compound 34 (1.92 g, 4.75 mmol) after hydrolysis, workup, and trituration (hexane, CH$_2$Cl$_2$, and CHCl$_3$) afforded 1.69 g (94%) of 40 as a yellow solid, mp 316 °C (dec.); purity (HPLC): ≥ 98%. IR 3363, 2900, 1648, 1589, 1412 cm^{-1}. ^{1}H NMR ((C^{2}H$_3$)$_2$SO) δ 1.77 (bs, 6H, AdCH$_2$), 2.08 (bs, 3H, AdCH), 2.15 (bs, 6H, AdCH$_2$), 6.68 (d, J = 15.9 Hz, 1H, CH═CHCO), 6.88 (d, J = 8.4 Hz, 1H, 5′-ArH), 7.64 (d, J = 15.9 Hz, 1H, CH═CHCO), 7.80 (dd, J = 8.4, 2.4 Hz, 1H, 6′-ArH), 7.88 (d, J = 8.4 Hz, 1H, 3-ArH), 7.98 (d, J = 2.4 Hz, 1H, 2′-ArH), 8.16 (dd, J = 8.4, 2.1 Hz, 1H, 4-ArH), 8.85 (d, J = 2.1 Hz, 1H, 6-ArH), 9.78 (s, 1H, OH), 12.31 ppm (bs, 1H, CO$_2$H). HRMS calcd C$_{24}$H$_{25}$NO$_3$ [M + H]$^+$, 376.1907; found, 376.1916.

(E)-3-[5-(3′-(1-Adamantyl)-4′-hydroxyphenyl]-2-pyrazinyl]-2-pro-penoic Acid (41). Compound 35 (310 mg, 0.77 mmol) after hydrolysis, workup, and trituration (hexane and CH$_2$Cl$_2$) afforded 254 mg (88%) of 41 as a yellow powder, mp 296 °C (dec.); purity (HPLC): 97%. IR 3208, 2903, 1696, 1600, 1219 cm^{-1}. ^{1}H NMR (C^{2}H$_3$O^{2}H/C^{2}HCl$_3$) δ 1.65 (bs, 6H, AdCH$_2$), 1.95 (bs, 3H, AdCH), 2.06 (bs, 6H, AdCH$_2$), 6.72 (d, J = 8.5 Hz, 1H, 5′-ArH), 6.78 (d, J = 15.9 Hz, 1H, CH═CHCO), 7.55 (d, J = 15.9 Hz, 1H, CH═CHCO), 7.57 (dd, J = 8.5, 2.4 Hz, 1H, 6′-ArH), 7.77 (d, J = 2.4 Hz, 1H, 2′-ArH), 8.49 (s, 1H, 6-ArH), 8.82 ppm (s, 1H, 3-ArH). HRMS calcd C$_{23}$H$_{24}$N$_2$O$_3$ [M + H]$^+$, 377.1860; found, 377.1859.

(E)-3-[2-(3′-(1-Adamantyl)-4′-hydroxyphenyl)-5-pyrimidinyl]-2-propenoic Acid (42). Compound 36 (1.8 g, 4.4 mmol) after hydrolysis, workup, and trituration (hexane, CH$_2$Cl$_2$, and CHCl$_3$) afforded 1.52 g (91%) of 42 as a yellow powder, mp 290−292 °C (dec.); purity

(HPLC): 98%. IR 3315, 2847, 1673, 1435, 1265 cm^{-1}. ^{1}H NMR (C^{2}H$_3$O^{2}H) δ 1.86 (bs, 6H, AdCH$_2$), 2.10 (bs, 3H, AdCH), 2.25 (m, 6H, AdCH$_2$), 6.72 (d, J = 16.2 Hz, 1H, CH═CHCO), 6.84 (d, J = 8.1 Hz, 1H, 5′-ArH), 7.64 (d, J = 16.2 Hz, 1H, CH═CHCO), 8.12 (dd, J = 8.1 Hz, 1.8 Hz, 1H, 6′-ArH), 8.34 (d, J = 2.1 Hz, 1H, 2′-ArH), 8.98 ppm (s, 2H, 4-ArH, 6-ArH). HRMS calcd C$_{23}$H$_{24}$N$_2$O$_3$ [M + H]$^+$, 377.1860; found, 377.1875.

(E)-3-{6-[3′-(1-Adamantyl)-4′-hydroxyphenyl]-3-pyridazinyl}-2-propenoic Acid (43). Compound 37 (28 mg, 0.07 mmol) on hydrolysis, workup, and trituration (hexane and CHCl$_3$) afforded 23 mg (88%) of 43 as a yellow solid, mp 181 °C (dec.); purity (HPLC): ≥ 96%. IR 3373, 2900, 1693, 1543 cm^{-1}. ^{1}H NMR (C^{2}H$_3$O^{2}H) δ 1.87 (bs, 6H, AdCH$_2$), 2.12 (bs, 3H, AdCH), 2.27 (m, 6H, AdCH$_2$), 6.91 (d, J = 8.4 Hz, 1H, 5′-ArH), 6.98 (d, J = 16.2 Hz, 1H, CH═CHCO), 7.80 (dd, J = 8.4 Hz, 2.1 Hz, 1H, 6′-ArH), 7.88 (d, J = 16.2 Hz, 1H, CH═CHCO), 8.00 (d, J = 2.1 Hz, 1H, 2′-ArH), 8.03 (d, J = 9.0 Hz, 1H, 4-ArH), 8.11 ppm (d, J = 9.0 Hz, 1H, 5-ArH). HRMS calcd C$_{23}$H$_{24}$N$_2$O$_3$ [M + H]$^+$, 377.1860; found, 377.1873.

3-[4-(3′-(1-Adamantyl)-4′-hydroxy)-3-chlorophenyl]propionic Acid (79). To a solution of 73 (245 mg, 0.56 mmol) in EtOH (1.5 mL) was added 8.5 N aqueous NaOH (263 μL, 2.23 mmol). This reaction mixture was stirred under argon for 1.3 h, quenched with 2 N HCl (15 mL), and extracted with EtOAc (50 and 30 mL). The combined extract was washed (brine) and dried. The residue obtained after concentration at reduced pressure was washed with hexane (3×) and dried to give 218 mg (95%) of 79 as a cream solid, mp 135−137 °C; purity (HPLC): 96%. IR 3340, 2904, 1707, 1249 cm^{-1}. ^{1}H NMR (DMSO-d_6) δ 1.74 (bs, 6H, AdCH$_2$), 2.04 (bs, 3H, AdCH), 2.10 (bs, 6H, AdCH$_2$), 2.58 (t, J = 7.2 Hz, 2H, CH$_2$CH$_2$CO), 2.85 (t, J = 7.2 Hz, 2H, CH$_2$CH$_2$CO), 6.83 (d, J = 8.1 Hz, 1H, 5′-ArH), 7.08 (dd, J = 2.1 Hz, 8.1 Hz, 1H, 6′-ArH), 7.12 (d, J = 2.1 Hz, 1H, 2′-ArH), 7.23 (dd, J = 1.5 Hz, 7.8 Hz, 1H, 6-ArH), 7.28 (d, J = 7.8 Hz, 1H, 5-ArH), 7.39 (d, J = 1.5 Hz, 1H, 2-ArH), 9.48 (s, 1H, OH), 12.12 ppm (bs, 1H, COOH). HRMS calcd C$_{25}$H$_{27}$ClO$_3$ [M + Na]$^+$, 433.1541; found, 433.1542.

General Procedure for Hydrolysis of Ethyl Esters 32, 68−72, 82, and 95−97 to Carboxylic Acids 38, 74−78, 83, and 98−100, Respectively, Using Aqueous Lithium Hydroxide. To a solution of the ethyl ester (1.0 mmol) in THF/MeOH/H$_2$O (3:2:1, 16 mL) at room temperature unless specified to be 0 °C was added LiOH·H$_2$O (6.0 mmol). This mixture was stirred at room temperature or 0 °C under argon for 1.5−6 h, quenched to pH 2−4 with 2 N HCl, and extracted with EtOAc (40 and 20 mL). The extract was washed (brine) and dried. The residue obtained by concentration was chromatographed or triturated to afford the carboxylic acid.

(E)-3-{2-[3′-(1-Adamantyl)-4′-hydroxyphenyl]-3-chloro-5-pyridi-nyl}-2-propenoic Acid (38). Compound 32 (32 mg, 0.073 mmol) on hydrolysis at 0 °C for 5 h, workup, and trituration afforded 26 mg (87%) of 38 as a yellow solid, mp 186−188 °C; purity (HPLC): 96%. IR 3377, 2901, 1688, 1412 cm^{-1}. ^{1}H NMR (C^{2}H$_3$O^{2}H) δ 1.85 (bs, 6H, AdCH$_2$), 2.09 (bs, 3H, AdCH), 2.24 (bs, 6H, AdCH$_2$), 6.69 (d, J = 15.9 Hz, 1H, CH═CHCO), 6.84 (d, J = 8.4 Hz, 1H, 5′-ArH), 7.46 (dd, J = 8.4, 2.1 Hz, 1H, 6′-ArH), 7.58 (d, J = 2.1 Hz, 1H, 2′-ArH), 7.69 (d, J = 15.9 Hz, 1H, CH═CHCO), 8.26 (s, 1H, 4-ArH), 8.70 ppm (s, 1H, 2-ArH). HRMS calcd C$_{24}$H$_{24}$ClNO$_3$ [M + H]$^+$, 410.1517; found, 410.1515.

2-[3′-(1-Adamantyl)-4′-hydroxyphenyl]-5-(carboxymethylamino) pyrimidine (74). Compound 68 (41.6 mg, 0.100 mmol) on hydrolysis for 6 h, workup, and chromatography (20% EtOAc/hexane) gave 38 mg (98%) of 74 as a pale-tan solid, mp 235 °C (dec.); purity (HPLC): 97%. IR 3420, 2902, 1691, 1215 cm^{-1}. ^{1}H NMR ((C^{2}H$_3$)SO) δ 1.73 (bs, 6H, AdCH$_2$), 2.04 (bs, 3H, AdCH), 2.10 (m, 6H, AdCH$_2$), 4.15 (bs, 1H, NH), 4.43 (s, 2H, NHCH$_2$CO), 6.85 (d, J = 8.4 Hz, 1H, 5′-ArH), 7.91 (d, J = 8.4 Hz, 1H, 6′-ArH), 8.12 (s, 1H, 2′-ArH), 8.40 (s, 2H, 4-ArH, 6-ArH), 9.93 ppm (s, 1H, OH). HRMS calcd C$_{22}$H$_{25}$N$_3$O$_3$ [M + H]$^+$, 380.1974; found, 380.1975.

2[3′-(1-Adamantyl)-2-chloro-4′-hydroxy-1,1′-biphenyl-4-ylamino]-acetic Acid (75). Compound **69** (134 mg, 0.300 mmol) on hydrolysis for 5 h, workup, and chromatography (EtOAc/hexane/MeOH, 5:5:1−1:1:1) gave 88 mg (70%) of **75** as a pale-tan solid, mp 220 °C (dec.); purity (HPLC): ≥ 97%. IR 3314, 2909, 1691, 1228 cm^{-1}. ^{1}H NMR ((C^{2}H$_3$)SO) δ 1.72 (m, 6H, AdCH$_2$), 2.02 (m, 3H, AdCH), 2.08 (m, 6H, AdCH$_2$), 3.48 (s, 2H, NHCH$_2$CO), 5.76 (bs, 1H, NHCH$_2$CO), 6.55 (dd, *J* = 8.4 Hz, 2.4 Hz, 1H, 5-ArH), 6.62 (d, *J* = 2.4 Hz, 1H, 3-ArH), 6.77 (d, *J* = 8.4 Hz, 1H, 5′-ArH), 6.97 (dd, *J* = 8.1 Hz, 2.1 Hz, 1H, 6′-ArH), 7.03 (*J* = 8.1 Hz, 1H, 6-ArH), 7.05 (d, *J* = 2.1 Hz, 1H, 2′-ArH). HRMS calcd C$_{24}$H$_{26}$ClNO$_3$ [M + H]$^+$, 412.1674; found, 412.1666.

2-[3′-(1-Adamantyl)-2-chloro-4′-hydroxy-1,1′-biphenyl-4-yloxo]-acetic Acid (76). Compound **70** (153 mg, 0.350 mmol) on hydrolysis for 6 h, workup, and chromatography (EtOAc/hexane/MeOH, 5:5:1−1:1:1) gave 125 mg (87%) of **76** as a pale-tan solid, mp 216 °C (dec.); purity (HPLC): ≥ 96%. IR 3401, 2893, 1705, 1209, 1137 cm^{-1}. ^{1}H NMR ((C^{2}H$_3$)SO) δ 1.72 (bs, 6H, AdCH$_2$), 2.02 (bs, 3H, AdCH), 2.09 (m, 6H, AdCH$_2$), 4.24 (s, 2H, OCH$_2$CO), 6.79 (d, *J* = 8.1 Hz, 1H, 5′-ArH), 6.82 (dd, *J* = 8.4 Hz, 2.4 Hz, 1H, 5-ArH), 6.89 (d, *J* = 2.4 Hz, 1H, 3-ArH), 7.00 (dd, *J* = 8.1 Hz, 2.1 Hz, 1H, 6′-ArH), 7.06 (d, *J* = 2.1 Hz, 1H, 2′-ArH), 7.20 ppm (d, *J* = 8.4 Hz, 1H, 6-ArH). HRMS calcd C$_{24}$H$_{25}$ClO$_4$ [M + Na]$^+$, 435.1333; found, 435.1321.

2-[3′-(1-Adamantyl)-2-chloro-4′-hydroxy-1,1′-biphenyl-4-ylthio] acetic Acid (77). Compound **71** (40 mg, 0.087 mmol) on hydrolysis for 6 h, workup, and chromatography (EtOAc/hexane/MeOH, 1:1:0−10:10:3) gave 23 mg (61%) of **77** as a cream-colored solid, mp 176−178 °C; purity (HPLC): 97%. IR 3430, 2901, 1710, 1586, 1405 cm^{-1}. ^{1}H NMR (C^{2}H$_3$O^{2}H) δ 1.84 (bs, 6H, AdCH$_2$), 2.07 (bs, 3H, AdCH), 2.20 (m, 6H, AdCH$_2$), 3.73 (s, 2H, SCH$_2$CO), 6.78 (d, *J* = 8.1 Hz, 1H, 5′-ArH), 7.06 (dd, *J* = 8.4 Hz, 2.4 Hz, 1H, 6′-ArH), 7.19 (d, *J* = 2.4 Hz, 1H, 2′-ArH), 7.26 (d, *J* = 8.1 Hz, 1H, 6-ArH), 7.34 (dd, *J* = 8.1 Hz, 2.1 Hz, 1H, 5-ArH), 7.49 ppm (d, *J* = 2.1 Hz, 1H, 3-ArH). HRMS calcd C$_{24}$H$_{25}$ClO$_3$S [M + Na]$^+$, 451.1105; found, 451.1105.

2-[3′-(1-Adamantyl)-2-chloro-4′-hydroxy-1,1′-biphenyl-4-ylsulfonyl]acetic Acid (78). Compound **72** (24 mg, 0.049 mmol) on hydrolysis for 6 h, workup, and chromatography (EtOAc/hexane/MeOH, 1:1:0−1:0:1) gave 18 mg (81%) of **78** as an off-white solid, mp 270 °C (dec.); purity (HPLC): ≥ 95%. IR 3436, 2900, 1686, 1598, 1150 cm^{-1}. ^{1}H NMR (C^{2}H$_3$O^{2}H) δ 1.84 (bs, 6H, AdCH$_2$), 2.08 (bs, 3H, AdCH), 2.20 (bs, 6H, AdCH$_2$), 4.90 (s, 2H, S(O)$_2$CH$_2$), 6.83 (d, *J* = 8.1 Hz, 1H, 5′-ArH), 7.15 (dd, *J* = 8.1 Hz, 1.8 Hz, 1H, 6′-ArH), 7.24 (d, *J* = 1.8 Hz, 1H, 2′-ArH), 7.55 (d, *J* = 8.1 Hz, 6-ArH), 7.92 (dd, *J* = 8.1 Hz, 1.5 Hz, 1H, 5-ArH), 8.08 ppm (d, *J* = 1.5 Hz, 1H, 3-ArH). HRMS calcd C$_{24}$H$_{25}$ClO$_5$S [M + Na]$^+$, 483.1003; found, 483.1006.

6-[3′-(1-Adamantyl)-4′-hydroxyphenyl]-1H-indole-2-carboxylic Acid (83). Compound **82** (38 mg, 0.09 mmol) on hydrolysis for 21.7 h, workup, and chromatography (EtOAc/hexane/MeOH, 1:1:0−1:0:1) gave 33 mg (94%) of **83** as a tan solid, mp 228 °C (dec.); purity (HPLC): 100%. IR 3397, 2899, 1665, 1521, 1409 cm^{-1}. ^{1}H NMR (C^{2}H$_3$O^{2}H) δ 1.86 (bs, 6H, AdCH$_2$), 2.10 (bs, 3H, AdCH), 2.25 (bs, 6H, AdCH$_2$), 6.79 (d, *J* = 7.8 Hz, 1H, 5′-ArH), 7.09 (d, *J* = 0.9 Hz, 1H, 7-InH), 7.28 (dd, *J* = 7.8 Hz, 2.4 Hz, 1H, 6′-ArH), 7.29 (dd, *J* = 8.4, 0.9 Hz, 1H, 5-InH), 7.44 (d, *J* = 2.4 Hz, 1H, 2′-ArH), 7.56 (s, 1H, 3-InH), 7.6 ppm (d, *J* = 8.4 Hz, 1H, 4-InH). HRMS calcd C$_{25}$H$_{25}$NO$_3$ [M + H]$^+$, 388.1907; found, 388.1907.

(E)-3-{1-[3′-(1-Adamantyl)-4′-hydroxyphenyl]piperidin-4-yl}-2-propenoic Acid (98). Compound **95** (34 mg, 0.083 mmol) on hydrolysis at 0 °C for 1.5 h, workup, and chromatography (11−25% MeOH/CH$_2$Cl$_2$) gave 12 mg (38%) of **98** as a brown solid, mp 200 °C (dec.); purity (HPLC): ≥ 96%. IR 3316, 2904, 1658, 1598, 1174 cm^{-1}. ^{1}H NMR (C^{2}H$_3$O^{2}H) δ 1.68 (m, 2H, N(CH$_2$CH$_2$)$_2$CH), 1.86 (bs, 6H, AdCH$_2$), 1.89 (m, 2H, N(CH$_2$CH$_2$)$_2$CH), 2.10 (bs, 3H, AdCH), 2.25 (bs, 6H, AdCH$_2$), 2.21 (m, 1H, N(CH$_2$CH$_2$)$_2$CH), 2.78 (m, 2H, N(CH$_2$CH$_2$)$_2$CH), 3.53 (m, 2H, N(CH$_2$CH$_2$)$_2$CH), 5.52 (s, 1H, 2′-

ArH), 5.88 (d, *J* = 16.2 Hz, 1H, CH=CHCO), 6.82 (d, *J* = 2.4 Hz, 1H, 6′-ArH), 6.86 (dd, *J* = 16.2 Hz, 6.6 Hz, 1H, CH=CHCO), 7.01 ppm (d, *J* = 2.4 Hz, 1H, 5′-ArH). HRMS calcd C$_{24}$H$_{31}$NO$_3$ [M + H]$^+$, 382.2377; found, 382.2340.

3-[4-(3′-(1-Adamantyl)-4′-hydroxyphenyl)piperazinyl]propionic Acid (99). Compound **96** (30 mg, 0.073 mmol) on hydrolysis at 0 °C for 5.8 h, workup, and trituration (hexane and CH$_2$Cl$_2$) gave 14 mg (50%) of **99** as a brown solid, mp 191 °C (dec.); purity (HPLC): ≥ 95%. IR 3352, 2901, 1710, 1439, 1221 cm^{-1}. ^{1}H NMR (C^{2}H$_3$CN) δ 1.83 (bs, 6H, AdCH$_2$), 2.09 (bs, 3H, AdCH), 2.15 (bs, 6H, AdCH$_2$), 2.82 (t, *J* = 7.5 Hz, 2H, NCH$_2$CH$_2$CO), 3.13 (m, 6H, ArN(CH$_2$CH$_2$)$_2$N, NCH$_2$CH$_2$CO), 3.28 (t, *J* = 5.1 Hz, 4H, ArN(CH$_2$CH$_2$)$_2$N), 6.69 (dd, *J* = 8.4 Hz, 2.7 Hz, 1H, 6′-ArH), 6.73 (d, *J* = 8.4 Hz, 1H, 5′-ArH), 6.87 ppm (d, *J* = 2.7 Hz, 1H, 2′-ArH). HRMS calcd C$_{23}$H$_{32}$N$_2$O$_3$ [M + H]$^+$, 385.2486; found, 385.2484.

3-{4-[3′-(1-Adamantyl)-4′-hydroxyphenyl]-3-oxopiperazin-1-yl}-3-oxopropionic Acid (100). Compound **97** (74 mg, 0.17 mmol) on hydrolysis at 0 °C for 4 h was quenched with H$_2$O (3 mL) and 2 N HCl (6 mL) and then washed with EtOAc (40 mL and 3 × 30 mL) to remove 4 mg of an impurity. The white solid found in the aqueous layer was collected by filtration, washed with H$_2$O (2 ×), and dried to give 25 mg (42%) of **100** as a white solid, mp 195 °C (dec.); purity (HPLC): 100%. IR 3398, 2927, 1641, 1625, 1215 cm^{-1}. ^{1}H NMR ((C^{2}H$_3$)SO) δ 1.74 (bs, 6H, AdCH$_2$), 2.06 (bs, 9H, AdCH, AdCH$_2$), 3.52 (s, 2H, COCH$_2$CO), 3.59 (t, *J* = 6 Hz, 2H, ArNCH$_2$CH$_2$N), 3.81 (t, *J* = 6 Hz, 2H, ArNCH$_2$CH$_2$N), 4.15 (s, 2H, NCOCH$_2$N), 6.77 (d, *J* = 8.4 Hz, 1H, 5′-ArH), 6.93 (dd, *J* = 8.4, 2.7 Hz, 1H, 6′-ArH), 6.98 (d, *J* = 2.7 Hz, 1H, 2′-ArH), 9.46 (s, 1H, OH), 12.51 ppm (bs, 1H, CO$_2$H). HRMS calcd C$_{23}$H$_{28}$N$_2$O$_5$ [M + H]$^+$, 413.2071; found, 413.2067.

(E)-3-{2-[3′-(1-Adamantyl)-4′-acetoxyphenyl]-5-pyridinyl}-2-propionic Acid (44). To a solution of **40** (50 mg, 0.13 mmol) in THF was added Ac$_2$O (25 μL, 0.27 mmol) and DMAP (33 mg, 0.27 mmol). The mixture was stirred at room temperature under argon for 27 h, quenched with H$_2$O (10 mL), and extracted with EtOAc (40 and 30 mL). The extract was washed (brine) and dried. After solvent removal at reduced pressure, the residue was chromatographed (EtOAc/hexane/MeOH, 1:1:0−10:5:1) to give 47 mg (84%) of **44** as a pale-yellow solid, mp >260 °C (dec.); purity (HPLC): 100%. IR 2900, 1754, 1690, 1204 cm^{-1}. ^{1}H NMR ((C^{2}H$_3$)$_2$SO) δ 1.77 (bs, 6H, AdCH$_2$), 2.03 (bs, 6H, AdCH$_2$), 2.10 (bs, 3H, AdCH), 2.38 (s, 3H, CH$_3$CO), 6.74 (d, *J* = 15.9 Hz, 1H, CH=CHCO), 7.18 (d, *J* = 8.4 Hz, 1H, 5′-ArH), 7.67 (d, *J* = 15.9 Hz, 1H, CH=CHCO), 7.98 (d, *J* = 8.4 Hz, 1H, 6′-ArH), 8.03 (d, *J* = 8.7 Hz, 1H, 3-ArH), 8.16 (s, 1H, 2′-ArH), 8.25 (d, *J* = 8.7 Hz, 1H, 4-ArH), 8.93 (d, 1H, 6-ArH), 12.43 ppm (bs, 1H, CO$_2$H). HRMS calcd C$_{26}$H$_{27}$NO$_4$ [M + H]$^+$, 418.2013; found, 418.2016.

2-Chloro-4-nitrophenyl Trifluoromethanesulfonate (47). To a solution of 2-chloro-4-nitrophenol (**46**) (1.58 g, 9.12 mmol) and pyridine (redistilled from KOH, 1.60 mL, 20.5 mmol) in CH$_2$Cl$_2$ (20 mL) under argon at 0 °C was slowly added Tf$_2$O (2.07 mL, 12.3 mmol). The resulting solution was allowed to warm to room temperature, stirred for 7 h, diluted with CH$_2$Cl$_2$ (270 mL), washed (2 N HCl, water, and brine), and dried. After solvent removal at reduced pressure, the residue was purified on silica gel (12.5% EtOAc/hexane) to give 2.73 g (97%) of **47** as a yellow oil. ^{1}H NMR δ 7.59 (d, *J* = 9 Hz, 1H, 6-ArH), 8.26 (dd, *J* = 9 Hz, 2.7 Hz, 1H, 5-ArH), 8.45 ppm (d, *J* = 2.7 Hz, 1H, 3-ArH).

General Procedure for Reduction of Aryl Nitro Groups of 49 and 51 To Give Arylamines 50 and 52, Respectively. A suspension of the nitro-arene (1.0 mmol) and stannous(II) chloride dihydrate (10 mmol) in anhydrous EtOH (4.5 mL) was heated at reflux, cooled to room temperature, and diluted with H$_2$O (10 mL). After adjustment of the pH to 7−8 by addition of 2 N NaOH and 5% NaHCO$_3$, the mixture was stirred for 1 h and then extracted (EtOAc). After solvent removal at reduced pressure, flash chromatography of the residue yielded the arylamine.

*5-Amino-2-[3′-(1-adamantyl)-4′-benzyloxyphenyl]pyrimidine (**50**).* Compound **49** (163 mg, 0.37 mmol) after reduction for 3.3 h, workup, and flash chromatography (25% EtOAc/hexane) gave 53 mg (35%) of **50** as a light-purple solid, mp 216−219 °C. IR 3424, 2900, 1182 cm^{-1}. ^{1}H NMR 1.76 (bs, 6H, AdCH$_2$), 2.08 (bs, 3H, AdCH), 2.24 (m, 6H, AdCH$_2$), 3.74 (bs, 2H, NH$_2$), 5.21 (s, 2H, C$_6$H$_5$CH$_2$), 7.04 (d, J = 8.7 Hz, 1H, 5′-ArH), 7.34−7.56 (m, 5H, C$_6$H$_5$), 8.13 (dd, J = 8.7 Hz, 2.4 Hz, 1H, 6′-ArH), 8.28 (d, J = 2.4 Hz, 1H, 2′-ArH), 8.43 ppm (s, 2H, 4-ArH, 6-ArH). HRMS calcd C$_{27}$H$_{29}$N$_3$O [M + H]$^+$, 412.2389; found, 412.2391.

*3′-(1-Adamantyl)-4′-benzyloxy-2-chloro-1,1′-biphenyl-4-ylamine (**52**).* Compound **51** (2.08 g, 4.40 mmol) after reduction for 2.5 h, workup, and flash chromatography (28% EtOAc/hexane) gave 1.77 g (90%) of **52** as a white solid, mp 154−155 °C. IR 3322, 2901, 1192 cm^{-1}. ^{1}H NMR δ 1.73 (m, 6H, AdCH$_2$), 2.05 (m, 3H, AdCH), 2.18 (m, 6H, AdCH$_2$), 3.73 (bs, 2H, NH$_2$), 5.16 (s, 2H, C$_6$H$_5$CH$_2$), 6.62 (dd, J = 8.1 Hz, 2.4 Hz, 1H, 5-ArH), 6.80 (d, J = 2.4 Hz, 1H, 3-ArH), 6.97 (d, J = 8.4 Hz, 1H, 5′-ArH), 7.15 (d, J = 8.4 Hz, 1H, 6-ArH), 7.35 (dd, J = 8.7 Hz, 2.4 Hz, 1H, 6′-ArH), 7.32−7.46 (m, 3H, C$_6$H$_5$, 1H, 2′-ArH), 7.51−7.55 ppm (m, 2H, C$_6$H$_5$). HRMS calcd C$_{29}$H$_{30}$ClNO [M + H]$^+$, 444.2089; found, 444.2096.

*4-Bromo-3-chlorobenzenethiol (**55**)*[33]. A reported procedure[33] was followed. To a slurry of 4-bromo-3-chloroaniline (**54**) (3.0 g, 14 mmol), concentrated HCl (4 mL), and ice (7.0 g) at −5 to 0 °C was slowly added a solution of NaNO$_2$ (1.038 g, 14.56 mmol) in H$_2$O (7 mL). The resulting cold diazonium salt solution was added dropwise into a stirred solution of potassium *O*-ethyl xanthate (4.5 g, 28 mmol) in H$_2$O (7 mL) at 75 °C (oil bath). After it was stirred at 75 °C for 1.5 h, the reaction mixture was cooled to room temperature, adjusted to pH 8 with saturated NaHCO$_3$, and extracted with ether (4 × 250 mL). The extract was washed (H$_2$O), dried, and concentrated.

To the residue obtained was added a solution of KOH (3.6 g, 64 mmol) in EtOH (25 mL). This mixture was heated at reflux for 17 h under argon and then concentrated. The residue was diluted with H$_2$O (50 mL) and washed with ether (45 mL). The aqueous layer was acidified to pH 1−2 by the slow addition of 3 N H$_2$SO$_4$ (50 mL) and then extracted with CH$_2$Cl$_2$ (3 × 190 mL). The extract was washed (H$_2$O) and dried. After solvent removal at reduced pressure, the residue was chromatographed (hexane) to give 2.22 g of **55** (71%) as a light-yellow liquid. IR 3246, 3049, 1453, 640 cm^{-1}. ^{1}H NMR δ 3.5 (s, 1H, SH), 7.02 (dd, J = 8.4 Hz, 2.1 Hz, 1H, 6-ArH), 7.38 (d, J = 2.1 Hz, 1H, 2-ArH), 7.46 ppm (d, J = 8.4 Hz, 1H, 5-ArH), in agreement with that reported.[75]

*4-Bromo-3-chlorobenzonitrile (**57**)*[76]. A literature procedure[76] was modified. To a solution of CuBr$_2$ (6.60 g, 29.55 mmol), CH$_3$CN (66 mL), and *tert*-butylnitrile (4.70 mL, 35.46 mmol) at 0 °C was slowly added 4-amino-3-chlorobenzonitrile (**56**) (3.00 g, 19.70 mmol). The mixture was stirred at 0 °C for 50 min and at room temperature for 5 h, quenched with 1 N HCl (60 mL), and extracted with EtOAc (150 and 80 mL). The extract was washed (brine) and dried. After solvent removal at reduced pressure, the residue was chromatographed (2−5% EtOAc/hexane) to give 4.13 g (99%) of **57** as a white solid, mp 80−82 °C (lit: 80−81 °C).[76] IR 2929, 2234, 1545, 1157 cm^{-1}. ^{1}H NMR δ 7.43 (dd, J = 2.1 Hz, 8.1 Hz, 1H, 6-ArH), 7.77 (d, J = 2.1 Hz, 1H, 2-ArH), 7.85 ppm (d, J = 8.1 Hz, 1H, 5-ArH).

*Ethyl 3-(4-Bromo-3-chlorophenyl)propanoate (**61**).* To a solution of **59** (250 mg, 0.86 mmol) in EtOAc was added 10% Pd(C) (28 mg). The mixture was stirred under H$_2$ for 23 h and then filtered through Celite (EtOAc rinse). After solvent removal at reduced pressure, the residue was chromatographed (2−9% EtOAc/hexane) to give 252 mg (100%) of **61** as a colorless liquid. IR 2958, 1728, 1181 cm^{-1}. ^{1}H NMR δ 1.26 (t, J = 7.2 Hz, 3H, OCH$_2$CH$_3$), 2.62 (t, J = 7.2 Hz, 2H, CH$_2$CH$_2$CO), 2.92 (t, J = 7.2 Hz, 2H, CH$_2$CH$_2$CO), 4.15 (q, J = 7.2 Hz, 2H, OCH$_2$CH$_3$), 6.99 (dd, J = 1.8 Hz, 8.4 Hz, 1H, 6-ArH), 7.33 (d, J = 1.8 Hz, 1H, 2-ArH),

7.54 ppm (d, J = 8.4 Hz, 1H, 5-ArH). HRMS calcd C$_{11}$H$_{12}$BrClO$_2$ [M + H]$^+$, 290.9787; found, 290.9785.

General Procedure for Alkylation of Arylamines 50 and 52, Phenol 53, and Thiophenol 55. A reported procedure[77] was used. To a suspension of the arylamine, phenol, or thiophenol (1.0 mmol) and K$_2$CO$_3$ (1.2−4.2 mmol) in acetone was added ethyl bromoacetate (1.1−4.0 mmol). This mixture was heated at reflux under argon and then cooled to room temperature. After removal of acetone at reduced pressure, the residue was diluted with water (20 mL) and extracted with EtOAc (150 mL). The extract was washed (water and brine) and dried. After solvent removal at reduced pressure, flash chromatography of the residue yielded the product.

*Ethyl 2-(4-Bromo-3-chlorophenylthio)acetate (**60**).* Compound **55** (1.00 g, 4.47 mmol) after reaction for 18 h, workup, and flash chromatography (5% EtOAc/hexane) gave 668 mg (48%) of **60** as a cream-colored liquid. IR 2977, 1731, 1019 cm^{-1}. ^{1}H NMR δ 1.27 (t, J = 7.2 Hz, 3H, OCH$_2$CH$_3$), 3.64 (s, 2H, SCH$_2$), 4.20 (q, J = 7.2 Hz, 2H, OCH$_2$CH$_3$), 7.16 (dd, J = 2.1 Hz, 8.4 Hz, 1H, 6-ArH), 7.50 (d, J = 2.1 Hz, 1H, 2-ArH), 7.53 ppm (d, J = 8.4 Hz, 1H, 5-ArH). HRMS calcd C$_{10}$H$_{10}$BrClO$_2$S [M + Na]$^+$, 330.9166; found, 330.9171.

*2-[3′-(1-Adamantyl)-4′-benzyloxyphenyl]-5-(carbethoxymethyl-amino)pyrimidine (**62**).* Compound **50** (49 mg, 0.12 mmol) after reaction for 19 h, workup, and flash chromatography (14% EtOAc/hexane) gave 53 mg (89%) of **62** as a pale-tan solid, mp 153−156 °C. IR 3455, 2901, 1710, 1179 cm^{-1}. ^{1}H NMR δ 1.33 (t, J = 7.2 Hz, 3H, OCH$_2$CH$_3$), 1.75 (bs, 6H, AdCH$_2$), 2.07 (bs, 3H, AdCH), 2.24 (m, 6H, AdCH$_2$), 4.31 (q, J = 7.2 Hz, 2H, OCH$_2$CH$_3$), 4.60 (m, 1H, NH), 4.73 (s, 2H, NHCH$_2$CO), 5.20 (s, 2H, C$_6$H$_5$CH$_2$), 7.03 (d, J = 8.4 Hz, 1H, 5′-ArH), 7.32−7.55 (m, 5H, C$_6$H$_5$), 8.17 (dd, J = 8.4 Hz, 2.1 Hz, 1H, 6′-ArH), 8.32 (d, J = 2.1 Hz, 1H, 2′-ArH), 8.46 ppm (s, 2H, 4-ArH, 6-ArH). HRMS calcd C$_{31}$H$_{35}$N$_3$O$_3$ [M + H]$^+$, 498.2757; found, 498.2762.

*Ethyl 2-[3′-(1-Adamantyl)-4′-benzyloxy-2-chloro-1,1′-biphenyl-4-ylamino]acetate (**63**).* Compound **52** (426 mg, 0.960 mmol) after reaction for 20 h, workup, and flash chromatography (20% EtOAc/hexane) gave 261 mg (51%) of **63** as a pale-tan solid, mp 158−159 °C. IR 3213, 2902, 1715, 1219 cm^{-1}. ^{1}H NMR δ 1.33 (t, J = 7.2 Hz, 3H, OCH$_2$CH$_3$), 1.73 (m, 6H, AdCH$_2$), 2.05 (m, 3H, AdCH), 2.18 (m, 6H, AdCH$_2$), 3.93 (s, 2H, NHCH$_2$CO), 4.28 (q, J = 7.2 Hz, 3H, OCH$_2$CH$_3$), 4.39 (bs, 1H, NHCH$_2$CO), 5.16 (s, 2H, C$_6$H$_5$CH$_2$), 6.57 (d, J = 7.8 Hz, 1H, 5-ArH), 6.70 (s, 1H, 3-ArH), 6.98 (d, J = 7.8 Hz, 1H, 5′-ArH), 7.16−7.46 (m, 3H, C$_6$H$_5$, 1H, 6-ArH, 1H, 6′-ArH, 1H, 2′-ArH), 7.50−7.55 (m, 2H, ArH). HRMS calcd C$_{33}$H$_{36}$ClNO$_3$ [M + H]$^+$, 530.2456; found, 530.2453.

*Ethyl 2-[3′-(1-Adamantyl)-4′-benzyloxy-2-chloro-1,1′-biphenyl-4-yloxo]acetate (**64**).* Compound **53** (316 mg, 0.710 mmol) after reaction for 6.5 h, workup, and flash chromatography (9% EtOAc/hexane) gave 335 mg (89%) of **64** as an off-white solid, mp 102−104 °C. IR 2889, 1738, 1210 cm^{-1}. ^{1}H NMR δ 1.33 (t, J = 7.2 Hz, 3H, OCH$_2$CH$_3$), 1.73 (m, 6H, AdCH$_2$), 2.05 (m, 3H, AdCH), 2.18 (m, 6H, AdCH$_2$), 4.31 (q, J = 7.2 Hz, 2H, OCH$_2$CH$_3$), 4.65 (s, 2H, OCH$_2$CO), 5.17 (s, 2H, C$_6$H$_5$CH$_2$), 6.87 (dd, J = 8.7 Hz, 2.4 Hz, 1H, 5-ArH), 6.99 (d, J = 8.4 Hz, 1H, 5′-ArH), 7.03 (d, J = 2.4 Hz, 1H, 3-ArH), 7.23 (dd, J = 8.4 Hz, 2.4 Hz, 1H, 6′-ArH), 7.28 (d, J = 8.7 Hz, 1H, 6-ArH), 7.32 (d, J = 2.4 Hz, 1H, 2′-ArH), 7.32−7.55 ppm (m, 5H, C$_6$H$_5$). HRMS calcd C$_{33}$H$_{35}$ClO$_4$ [M + H]$^+$, 531.2297; found, 531.2288.

*Ethyl 2-[3′-(1-Adamantyl)-4′-benzyloxy-2-chloro-1,1′-biphenyl-4-ylsulfonyl]acetate (**66**).* A solution of ethyl 2-[3′-(1-adamantyl)-4′-benzyloxy-2-chloro-1,1′-biphenyl-4-ylthio]acetate (**65**) (54 mg, 0.098 mmol) and 3-chloroperbenzoic acid (56 mg, 0.25 mmol) in CH$_2$Cl$_2$ (2 mL) was stirred overnight and then extracted with CH$_2$Cl$_2$ (60 mL). The extract was washed (5% aqueous Na$_2$S$_2$O$_3$, saturated NaHCO$_3$, and brine) and dried. After solvent removal at reduced pressure, the residue was chromatographed (16% EtOAc/hexane) to give 46 mg (81%) of **66**

as a viscous oil. IR 2902, 1741, 1498, 1157 cm^{-1}. ^{1}H NMR δ 1.29 (t, J = 7.2 Hz, 3H, OCH$_2$CH_3), 1.76 (bs, 6H, AdCH$_2$), 2.09 (bs, 3H, AdCH), 2.19 (bs, 6H, AdCH$_2$), 4.19 (s, 2H, S(O)$_2$CH$_2$), 4.24 (q, J = 7.2 Hz, 2H, OCH_2CH$_3$), 5.21 (s, 2H, C$_6$H$_5$CH_2), 7.06 (d, J = 8.4 Hz, 1H, 5'-ArH), 7.33 (dd, J = 8.4 Hz, 2.4 Hz, 1H, 6'-ArH), 7.40 (d, J = 2.4 Hz, 1H, 2'-ArH), 7.40−7.57 (m, 5H, C$_6$H$_5$), 7.59 (d, J = 8.1 Hz, 6-ArH), 7.89 (dd, J = 2.1 Hz, 8.1 Hz, 1H, 5-ArH), 8.08 ppm (d, J = 2.1 Hz, 1H, 3-ArH). HRMS calcd C$_{33}$H$_{35}$ClO$_5$S [M + H]$^+$, 579.1966; found, 579.1966.

*3-(1-Adamantyl)-4-benzyloxyphenyl Iodide (**88**).* A solution of 4-iodophenol (11.1 g, 50 mmol), 1-adamantanol (7.69 g, 50 mmol), and MeSO$_3$H (2.5 mL) in CH$_2$Cl$_2$ (30 mL) was heated at reflux (55 °C oil bath) for 5 h, cooled to room temperature, and then stirred for 16 h. The reaction mixture was diluted with H$_2$O (40 mL) and extracted with CHCl$_3$ (150 mL). The extract was washed (5% NaHCO$_3$ and brine). After solvent removal at reduced pressure, the residue was chromatographed (5% EtOAc/hexane) to give 12.48 g (71%) of 2-(1-adamantyl)-4-iodophenol as a yellow solid, mp 131−133 °C. IR 3268, 2906, 1190 cm^{-1}. ^{1}H NMR δ 1.77 (bs, 6H, AdCH$_2$), 2.08 (bs, 9H, AdCH, AdCH$_2$), 4.82 (s, 1H, OH), 6.44 (d, J = 8.4 Hz, 6-ArH), 7.34 (dd, J = 8.4, 2.1 Hz, 1H, 5-ArH), 7.46 ppm (d, J = 2.1 Hz, 3-ArH). HRMS calcd C$_{16}$H$_{19}$IO [M + H]$^+$, 355.0559; found, 355.0556.

To a solution of 2-(1-adamantyl)-4-iodophenol (4.0 g, 11.3 mmol) in acetone (20 mL) was added a solution of BnBr (2.0 g, 11.8 mmol) in acetone (15 mL) followed by K$_2$CO$_3$ (1.9 g, 13.9 mmol). This mixture was stirred at reflux under argon for 18 h. After removal of acetone at reduced pressure, the residue was acidified with 1 N HCl (40 mL) and extracted with EtOAc (200 mL). The extract was washed (H$_2$O and brine). After solvent removal at reduced pressure, the residue was chromatographed (1% EtOAc/hexane) to give 4.9 g (97%) of **88** as a yellow solid, mp 99−101 °C. IR 2901, 1191 cm^{-1}. ^{1}H NMR δ 1.72 (bs, 6H, AdCH$_2$), 2.04 (bs, 3H, AdCH), 2.11 (bs, 6H, AdCH$_2$), 5.09 (s, 2H, ArCH$_2$), 6.69 (d, J = 8.4 Hz, 5-ArH), 7.30−7.47 ppm (m, 5H, C$_6$H$_5$), 7.45 (dd, J = 8.4, 2.1 Hz, 1H, 6-ArH), 7.49 ppm (d, J = 2.1 Hz, 2-ArH). HRMS calcd C$_{23}$H$_{25}$IO [M + H]$^+$, 445.1028; found, 445.1031.

*1-[3'-(1-Adamantyl)-4'-benzyloxyphenyl]piperazin-2-one (**93**).* To a mixture of **88** (444 mg, 1.00 mmol), 2-oxopiperazine (**87**) (120 mg, 1.20 mmol), and K$_3$PO$_4$ (875 mg, 4.00 mmol) in 1,4-dioxane (4 mL) was added CuI (48 mg, 0.25 mmol) and *trans*-N,N'-dimethylcyclohexane-1,2-diamine (65 μL, 0.40 mmol). This mixture was heated at 110 °C (oil bath) with stirring for 23.7 h, then cooled to room temperature, diluted with 28−30% aqueous NH$_4$OH (4 mL) and H$_2$O (10 mL), and extracted with EtOAc (70 and 2 × 40 mL). The extract was washed (brine) and dried. After solvent removal at reduced pressure, the residue was chromatographed (16−33% MeOH/EtOAc) to give 289 mg (69%) of **93** as a pale-yellow solid, mp 164−166 °C. IR 3617, 2905, 1646, 1491, 1222 cm^{-1}. ^{1}H NMR ((C^{2}H$_3$)$_2$SO) δ 1.69 (bs, 6H, AdCH$_2$), 2.01 (bs, 3H, AdCH), 2.08 (bs, 6H, AdCH$_2$), 2.77 (bs, 1H, NH), 3.0 (t, J = 5.1 Hz, 2H, NCH$_2$CH_2NH), 3.36 (s, 2H, NCOCH_2NH), 3.55 (t, J = 5.1 Hz, 2H, NCH_2CH$_2$NH), 5.16 (s, 2H, ArCH$_2$), 7.08 (s, 3H, 2',5',6'-ArH), 7.28−7.57 ppm (m, 5H, C$_6$H$_5$). HRMS calcd C$_{27}$H$_{32}$N$_2$O$_2$ [M + Na]$^+$, 417.2536; found, 417.2547.

General Procedure for Syntheses of Phenylpiperidine 89 and Phenylpiperazine 92. A reported method[35] was adapted. To a suspension of 2-(1-adamantyl)-1-benzyloxy-4-bromobenzene (**86**)[6] (1.0 mmol), piperidinecarboxylate (**84**) (1.1 mmol), or ethyl 3-(piperazin-1-yl)-propionate (**85**) (1.2 mmol), 2,2'-bis(diphenylphosphino)-1,1'-binaphthyl (7.5% mmol), and Pd(OAc)$_2$ (10% mmol) in MePh (0.17 M) was added Cs$_2$CO$_3$ (1.5 mmol). This mixture was heated at 111 °C (oil bath) for 19−23 h, cooled to room temperature, and filtered through Celite (EtOAc rinse). After solvent removal at reduced pressure, the residue was chromatographed to afford the product.

*Ethyl 1-[3'-(1-Adamantyl)-4'-benzyloxyphenyl]piperidine-4-carboxylate (**89**).* Compound **84** (1.2 g, 3.0 mmol) after reaction for 19.5 h, workup, and chromatography (10% EtOAc/hexane) gave 1.12 g

(78%) of **89** as an off-white solid, mp 75−76 °C. IR 2904, 1729, 1219, 1169 cm^{-1}. ^{1}H NMR δ 1.30 (t, J = 7.2 Hz, 3H, CH$_2$CH_3), 1.75 (bs, 6H, AdCH$_2$), 1.96 (m, 2H, N(CH$_2$CH_2)$_2$CH), 2.06 (bs, 3H, AdCH), 2.06 (m, 2H, N(CH$_2$CH_2)$_2$CH), 2.17 (bs, 6H, AdCH$_2$), 2.42 (m, 1H, N(CH$_2$CH$_2$)$_2$CH), 2.73 (m, 2H, N(CH_2CH$_2$)$_2$CH), 3.52 (m, 2H, N(CH_2CH$_2$)$_2$CH), 4.19 (q, J = 7.2 Hz, 2H, CH_2CH$_3$), 5.10 (s, 2H, ArCH$_2$), 6.75 (dd, J = 8.7 Hz, 3.0 Hz, 1H, 6'-ArH), 6.89 (d, J = 8.7 Hz, 1H, 5'-ArH), 6.97 (d, J = 3.0 Hz, 1H, 2'-ArH), 7.28−7.57 ppm (m, 5H, ArH). HRMS calcd C$_{31}$H$_{39}$NO$_3$ [M + H]$^+$, 474.3003; found, 474.3009.

*Ethyl 3-[4-(3'-(1-Adamantyl)-4'-benzyloxyphenyl)piperazinyl]propionate (**92**).* Compound **85** (300 mg, 0.75 mmol) after reaction for 23 h, workup, and chromatography (25−33% EtOAc/hexane) gave 245 mg (65%) of **92** as a pale-gray solid, mp 79−81 °C. IR 2902, 1730, 1498, 1169 cm^{-1}. ^{1}H NMR δ 1.30 (t, J = 7.2 Hz, 3H, OCH$_2$CH_3), 1.75 (bs, 6H, AdCH$_2$), 2.06 (bs, 3H, AdCH), 2.16 (bs, 6H, AdCH$_2$), 2.57 (t, J = 7.5 Hz, 2H, NCH$_2$CH_2CO), 2.67 (t, J = 4.5 Hz, 4H, ArN(CH$_2$CH_2)$_2$N), 2.80 (t, J = 7.5 Hz, 2H, NCH_2CH$_2$CO), 3.13 (t, J = 4.5 Hz, 4H, ArN(CH_2CH$_2$)$_2$N), 4.18 (q, J = 7.2 Hz, 2H, OCH_2CH$_3$), 5.10 (s, 2H, ArCH$_2$), 6.74 (dd, J = 8.7 Hz, 3.0 Hz, 1H, 6'-ArH), 6.89 (d, J = 8.7 Hz, 1H, 5'-ArH), 6.97 (d, J = 3.0 Hz, 1H, 2'-ArH), 7.28−7.57 ppm (m, 5H, C$_6$H$_5$). HRMS calcd C$_{32}$H$_{42}$N$_2$O$_3$ [M + H]$^+$, 503.3268; found, 503.3262.

*1-[3'-(1-Adamantyl)-4'-benzyloxyphenyl]-4-piperidinecarboxaldehyde (**90**).* To a solution of **89** (459 mg, 0.970 mmol) in CH$_2$Cl$_2$ (15 mL) at −78 °C was added 1.0 M DIBAL (2.91 mmol) in hexane (3.0 mL). The solution was stirred at −78 °C for 1 h, then quenched with 2 N HCl (20 mL), and extracted with CHCl$_3$ (120 mL). The extract was washed (water and brine) and dried. After solvent removal at reduced pressure, the residue was chromatographed (14−25% EtOAc/hexane, CHCl$_3$/hexane/Et$_3$N, 25:25:1) to give 86 mg (25%) of **90** as a light-brown gum. IR 2901, 1735, 1221 cm^{-1}. ^{1}H NMR δ 1.75 (bs, 6H, AdCH$_2$), 1.88 (m, 2H, N(CH$_2$CH_2)$_2$CH), 2.07 (bs, 5H, AdCH), 2.07 (m, 2H, N(CH$_2$CH_2)$_2$CH), 2.17 (bs, 6H, AdCH$_2$), 2.39 (m, 1H, N(CH$_2$CH$_2$)$_2$CH), 2.82 (m, 2H, N(CH_2CH$_2$)$_2$CH), 3.50 (m, 2H, N(CH_2CH$_2$)$_2$CH), 5.10 (s, 2H, ArCH$_2$), 6.75 (dd, J = 8.7 Hz, 3.0 Hz, 1H, 6'-ArH), 6.89 (d, J = 8.7 Hz, 1H, 5'-ArH), 6.97 (d, J = 3.0 Hz, 1H, 2'-ArH), 7.28−7.57 ppm (m, 5H, ArH). HRMS calcd C$_{29}$H$_{35}$NO$_2$ [M + H]$^+$, 4302740; found, 430.2733.

*Ethyl 3-{4-[3'-(1-Adamantyl)-4'-benzyloxyphenyl]-3-oxopiperazin-1-yl}-3-oxopropionate (**94**).* A mixture of **93** (88 mg, 0.21 mmol), ethyl 3-chloro-3-oxopropionate (53 μL, 0.42 mmol), and Et$_3$N (88 μL, 0.63 mmol) in CH$_2$Cl$_2$ (2 mL) was stirred under argon overnight, diluted with 0.5 N HCl (10 mL), and extracted with EtOAc (50 and 30 mL). The extract was washed (brine) and dried. After solvent removal at reduced pressure, the residue was chromatographed (66−80% EtOAc/hexane) to give 107 mg (95%) of **94** as a white solid, mp 61−63 °C. IR 2911, 1736, 1657, 1216 cm^{-1}. ^{1}H NMR δ 1.34 (t, J = 7.5 Hz, 3H, OCH$_2$CH_3), 1.74 (bs, 6H, AdCH$_2$), 2.07 (bs, 3H, AdCH), 2.15 (bs, 6H, AdCH$_2$), 3.56 (s, 2H, COCH$_2$CO), 3.75 (t, J = 6 Hz, 2H, ArNCH$_2$CH_2N), 4.03 (t, J = 6 Hz, 2H, ArNCH_2CH$_2$N), 4.26 (q, J = 7.5 Hz, 2H, OCH_2CH$_3$), 4.30 (s, 2H, NCOCH$_2$N), 5.15 (s, 2H, ArCH$_2$), 6.97 (d, J = 8.7 Hz, 1H, 5'-ArH), 7.08 (dd, J = 8.7, 2.7, 1H, 6'-ArH), 7.13 (d, J = 2.7 Hz, 1H, 2'-ArH), 7.33−7.53 ppm (m, 5H, C$_6$H$_5$). HRMS calcd C$_{32}$H$_{38}$N$_2$O$_5$ [M + H]$^+$, 531.2853; found, 531.2851.

NMR Binding Studies. GST-SHP was expressed in *E. coli* BL21-(DE3) and purified using glutathione-Sepharose 4B beads (Amersham, GE Healthcare Ltd., NJ), as we previously described.[78] GST-SHP fusion protein was incubated with glutathione-Sepharose 4B beads overnight at 4 °C. After the protein-bound beads were washed with PBS, specifically bound GST-SHP protein was eluted from the beads at 4 °C using 50 mM Tris·HCl, pH 8.0, containing 15 mM reduced glutathione. One-dimensional ^{1}H NMR spectra were recorded with 128 transients and a sweep width of 12,376 Hz using a Bruker Avance 600-MHz NMR spectrometer equipped with a TCI cryoprobe. The repetition time was 3 s. Spectra were obtained on 11 °C solutions of each compound

(100 μM) in the bead elution buffer containing 61% D_2O and 2% DMSO-d_6 alone or plus GST-SHP (10 nM).

Docking Experiments. The three-dimensional model used for docking was that derived by homology modeling of the USP LBD–phospholipids complex crystal structure (PDB: 1g2n).[34] Docking of **6** and analogues into the putative LBP of this model was performed using BioMed Cache 6.2 (Fujitsu Limited, Beaverton, OR). After setting the diaryl dihedral (torsion) angle (C6′–C1′–C4–C5) at 50° on the basis of molecular dynamics studies on **3**,[5] the resulting conformer was energetically minimized to give optimized geometry. The binding pocket site was derived by selecting all neighboring residues within 4 Å (radius) of the USP ligand 1-stearoyl-2-palmitoylglycero-3-phosphoethanolamine, which had been docked to the SHP model.[34] This distance was large enough to encompass the putative binding pocket. Each analogue was docked into a 15 Å × 15 Å × 15 Å box located at the center of the active site using a united atom potential for mean force with a genetic algorithm that ran for 600 generations. Other parameters were left at their respective default values. Both the ligand and the side chains of the pocket residues were allowed to be flexible during the docking process. Final docking poses as shown in Figure 6 were analyzed by measuring interatom distances after overlaying the docked structures by superposing the backbone of the SHP model structure.

Aqueous Solubility Determination. Standard curves at the UV λ_{max} were determined using 0.245, 0.163, 0.049, and 0.025 mM **6** and 0.380, 0.178, 0.053, and 0.027 mM **40** and **42**, which were prepared from 1.0% (wt/vol) compound stocks in Me_2SO. Absorbances were measured at the λ_{max} values for **6**, **40**, and **42**, which were 330, 350, and 345 nm, respectively. Calibration curves demonstrating linearity of response are shown in Figure S2 in the Supporting Information. Measurements for maximum solubilities in distilled water (pH 5) and phosphate-buffered saline (PBS, pH 7.2) at 22 °C were made by UV absorbance using solutions obtained after saturation at higher temperatures, overnight incubation at 22 °C, and centrifugation to remove undissolved material.

Biologic Studies. *Cell Culture.* KG-1 AML cells were obtained from Dr. H. Phillip Koeffler (UCLA, Cedars-Sinai Medical Center, Los Angeles, CA) and grown in RPMI-1640 medium supplemented with 5% heat-inactivated fetal bovine serum (FBS) and gentamycin (100 μg/mL). Retinoid-resistant HL-60R myeloid leukemia cells were obtained from Dr. Steve Collins (University of Washington, Seattle) and grown under the same conditions. MDA-MB-231 and SKBR-3 breast cancer and HeLa cervical cancer cells (ATCC, Manassas, VA) were seeded in DMEM/F-12 medium supplemented with 10% FBS and gentamycin (25 μg/mL). Cells were incubated for 24 h before treatment with compound (0.1% Me_2SO final concentration) for 24, 48, or 72 h. A549 lung adenocarcinoma, HT29 colon adenorcacinoma, and PC-3 prostate cancer cell lines (ATCC) were cultured in DMEM (A549 and HT29) or RPMI (PC-3) supplemented with 10% heat-inactivated FBS and a 1% penicillin–streptomycin mixture in 10 cm dishes at 37 °C in a 10% CO_2 atmosphere and at 90% relative humidity.

Inhibition of Proliferation. Leukemia or cancer cells ($5-10 \times 10^3$/well) were seeded in 96-well plates containing 200 μL medium plus 5 or 10% FBS, respectively, per well and incubated for 24 h. After compounds dissolved in Me_2SO were added, cells were incubated at various concentrations for the specified times and harvested. Cell numbers were determined by a standard 3,4-dimethylthiazol-2-yl)-2,5-diphenyltetrazolium bromide (MTT) assay according to the manufacturer's instructions (Biotek Instruments, Inc., Winooski, VT). Results shown are the averages of three replicates ± standard deviations (SDs), which were <10%.

Cell Apoptosis. Leukemia and cancer cells were seeded and incubated in 6-well plates as described.[5] Apoptotic cells were identified using acridine orange staining for DNA fragmentation as we described.[5] Results shown are the means of four replicates ± SDs, which were <10%.

Cancer Stem Cell (CSC) Assay. MMTV-Wnt1 cancer stem cells were cloned and amplified by growth as tumor spheroids in Matrigel. After dissociation, cells were plated in MSC medium without serum into gelatin-coated 384-well plates and then exposed to the indicated concentrations of compound or vehicle for 3 days. Experiments were performed in triplicate (mean ± SD). Fixed cells were stained with 4,6′-diamidino-2-phenylindole dihydrochloride (DAPI), and cell numbers were determined by analyzing nine images acquired by the IC100 automatic focusing imaging system. Cyteseer software was used to identify and measure the average number of cells/well.

Cell Viability Assay. A549 lung, HT29 colon, and PC-3 prostate cancer cell suspensions (10000 cells in 50 μL medium/well) were added to 384-well white-bottomed Greiner plates, containing various concentrations of compounds, which had been originally dissolved in Me_2SO (0.125% maximum final concentration, which had no effect on cell growth) and then diluted into medium containing 10% FBS. After 72 h of incubation, plates were transferred to room temperature for 15 min. Luciferase assays to determine ATP levels (metabolically active cells) were performed by adding CellTiter-Glo Luminescent Cell Viability Reagent (20 μL per well; Promega, Madison, WI) and 10 min later measuring light emission using a FlexStation 3 Microplate Reader (Molecular Devices, Sunnyvale, CA). Experiments were performed in triplicate (mean ± SD). Cell viability was calculated on the basis of maximum luminescence intensity observed for each cell line in the presence of the Me_2SO vehicle control (100% value). Assay results are displayed graphically in Figure S1 in the Supporting Information.

HeLa cells (1000 per well) in DMEM containing 5% FBS supplemented with antibiotics were plated in poly-L-lysine precoated 96-well plates. At 6 h after plating, **40** in DMSO plus medium was added as above to give final concentrations of 0.5, 1.0, and 2.0 μM. Cells were then cultured for 24, 48, or 72 h with culture medium plus compound or DMSO alone exchanged every 24 h. Viability was determined by measurements of ATP levels, and viability (% control) was calculated relative to cells treated with DMSO alone at same amount used to prepare 2.0 μM **40**, which were considered to be 100% viable. Assays were performed in triplicate (mean ± SD).

Escalating Dose Study. Female ICR-SCIDS mice (two/group) were injected intravenously via the tail vein with compound daily for 7 days beginning at 20 mg/kg of compound in vehicle and increasing daily by 25%. Mice were weighed and observed daily on days 1–8. Average daily body weights for **6**- and **42**-treated mice are depicted graphically in Figure S3 in the Supporting Information.

■ ASSOCIATED CONTENT

ⓢ Supporting Information. Dose–response curves showing the effects of the analogues on ATP levels in A549, HT29, and PC-3 cancer cell lines (Figure S1), calibration curves for **6**, **40**, and **42** demonstrating linearity of response used for determining solubility in PBS and H_2O (Figure S2), daily average weights of mice treated for 7 days with **6** and **42** (Figure S3), HPLC analyses of purity of target compounds in two different and one solvent system, respectively, that would be used for characterization and in biological assays (Tables S1 and S2). This material is available free of charge via the Internet at http://pubs.acs.org.

■ AUTHOR INFORMATION

Corresponding Author

*Fax: 858-646-3197. E-mail: mdawson@burnham.org.

■ ACKNOWLEDGMENT

measurements, and Dr. Roberto Pellicciari, Univ. of Perugia, Italy, for use of the USP LBD-derived homology model of SHP.

ABBREVIATIONS USED

1-Ad, 1-adamantyl; 3-Cl-AHPC, (E)-4-[3′-(1-adamantyl)-4′-hydroxyphenyl]-3-chlorocinnamic acid; 4-HPR, N-(4-hydroxyphenyl) all-trans-retinamide; AHPN, 6-[3′-(1-adamantyl)-4′-hydroxyphenyl]-2-naphthalenecarboxylic acid; AHP3, (E)-3-{2-[3′-(1-adamantyl)-4′-hydroxyphenyl]-5-pyrimidyl}propenoic acid; AHPPyP, (E)-3-{2-[3′-(1-adamantyl)-4′-hydroxyphenyl]-5-pyridyl}propenoic acid; AML, acute myelocytic leukemia; (DR5)$_2$-tk-CAT, synthetic gene of retinoic acid response element of two direct repeats separated by five base pairs linked to the thymidine kinase promoter followed by the base sequence for chloramphenicol acetyl transferase gene; RAR, retinoic acid receptor; RXR, retinoid X receptor; SHP, small heterodimer partner

REFERENCES

(1) Shao, Z. M.; Dawson, M. I.; Li, X. S.; Rishi, A. K.; Sheikh, M. S.; Han., Q. X.; Ordonez, J. V.; Shroot, B.; Fontana, J. A. p53 independent G$_0$/G$_1$ arrest and apoptosis induced by a novel retinoid in human breast cancer cells. Oncogene 1995, 11, 493–504.

(2) Zhang, Y.; Huang, Y.; Rishi, A. K.; Sheikh, M. S.; Shroot, B.; Reichert, U.; Dawson, M. I.; Poirer, G.; Fontana, J. A. Activation of the p38 and JNK/SAPK mitogen-activated protein kinase pathways during apoptosis is mediated by a novel retinoid. Exper. Cell Res. 1999, 247, 233–240.

(3) Dawson, M. I.; Hobbs, P. D.; Peterson, V. J.; Leid, M.; Lange, C. W.; Feng, K.-C.; Chen, G.; Gu, J.; Li, H.; Kolluri, S. K.; Zhang, X.; Zhang, Y.; Fontana, J. A. Apoptosis induction in cancer cells by a novel analogue of 6-[3-(1-adamantyl)-4-hydroxyphenyl]-2-naphthalenecarboxylic acid lacking retinoid receptor transcriptional activation activity. Cancer Res. 2001, 61, 4723–4730.

(4) Zhang, Y.; Dawson, M. I.; Mohammad, R.; Rishi, A. K.; Farhana, L.; Feng, K.-C.; Leid, M.; Peterson, V.; Zhang, X.-K.; Edelstein, M.; Eilander, D.; Biggar, S.; Wall, N.; Reichert, U.; Fontana, J. A. Induction of apoptosis of human B-CLL and ALL cells by a novel retinoid and its nonretinoidal analog. Blood 2002, 100, 2917–2925.

(5) Dawson, M. I.; Harris, D. L.; Liu, G.; Hobbs, P. D.; Lange, C. W.; Jong, L.; Bruey-Sedano, N.; James, S. Y.; Zhang, X.-K.; Peterson, V. J.; Leid, M.; Farhana, L.; Rishi, A. K.; Fontana, J. A. Antagonist analogue of 6-[3′-(1-adamantyl)-4′-hydroxyphenyl]-2-naphthalenecarboxylic acid (AHPN) family of apoptosis inducers that effectively blocks AHPN-induced apoptosis but not cell-cycle arrest. J. Med. Chem. 2004, 47, 3518–3536.

(6) Dawson, M. I.; Xia, Z.; Liu, G.; Fontana, J. A.; Farhana, L.; Patel, B. B.; Arumugarajah, S.; Bhuiyan, M.; Zhang, X.-K.; Han, Y.-H.; Stallcup, W. B.; Fukushi, J.; Mustelin, T.; Tautz, L.; Su, Y.; Harris, D. L.; Waleh, N.; Hobbs, P. D.; Jong, L.; Chao, W.; Schiff, L. J.; Sani, B. P. An adamantyl-substituted retinoid-derived molecule that inhibits cancer cell growth and angiogenesis by inducing apoptosis and binds to small heterodimer partner nuclear receptor: Effects of modifying its carboxylate group on apoptosis proliferation and protein-tyrosine phosphatase activity. J. Med. Chem. 2007, 50, 2622–2639.

(7) Dawson, M. I.; Xia, Z.; Jiang, T.; Ye, M.; Fontana, J. A.; Farhana, L.; Patel, B.; Xue, L.-P.; Bhuiyan, M.; Pellicciari, R.; Macchiarulo, A.; Nuti, R.; Zhang, X.-K.; Han, Y.-H.; Tautz, L.; Hobbs, P. D.; Jong, L.; Waleh, N.; Chao, W.-R.; Feng, G.-S.; Pang, Y.; Su, Y. Adamantyl-substituted retinoid-derived molecules that interact with the orphan nuclear receptor small heterodimer partner: Effects of replacing the 1-adamantyl or hydroxyl group on inhibition of cancer cell growth, induction of cancer cell apoptosis, and inhibition of src homology 2 domain-containing protein tyrosine phosphatase-2 activity. J. Med. Chem. 2008, 51, 5650–5662.

(8) Garattini, E.; Gianni, M.; Terao, M. Retinoid related molecules. An emerging class of apoptotic agents with promising potential in oncology: Pharmacological activity and mechanism of action. Curr. Pharm. Des. 2004, 10, 433–448.

(9) Benbrook, D. M.; Turman, M.; Guruswamy, S. Flexible hetero-arotinoids (Flex-Hets) as anti-cancer and other therapeutic agents. World Patent WO 113627, 2006.

(10) Charpentier, B.; Bernardon, J. M.; Eustache, J.; Millois, C.; Martin, B.; Michel, S.; Shroot, B. Synthesis, structure—affinity relationships and biological activities of ligands binding to retinoic acid receptor subtypes. J. Med. Chem. 1995, 38, 4993–5006.

(11) Li, X. S.; Rishi, A. K.; Shao, Z. M.; Dawson, M. I.; Jong, L.; Shroot, B.; Reichert, U.; Ordonez, J.; Fontana, J. A. Posttranscriptional regulation of p21$^{WAF1/CIP1}$ expression in human breast carcinoma cells. Cancer Res. 1996, 56, 5055–5062.

(12) Silverman, A. K.; Ellis, C. N.; Voorhees, J. J. Hypervitaminosis A syndrome: A paradigm of retinoid side effects. J. Am. Acad. Dermatol. 1987, 16, 1027–1039.

(13) Newton, D. L.; Henderson, W. R.; Sporn, M. B. Structure-activity relationships of retinoids in hamster tracheal organ culture. Cancer Res. 1980, 40, 3413–3425.

(14) Verma, A. K.; Shapas, B. G.; Rice, H. M.; Boutwell, R. K. Correlation of the inhibition by retinoids of tumor promoter-induced mouse epidermal ornithine decarboxylase activity and of skin tumor promotion. Cancer Res. 1979, 39, 419–425.

(15) Cincinelli, R.; Dallavalle, S.; Merlini, L.; Penco, S.; Pisano, C.; Carminati, P.; Giannini, G.; Vesci, L.; Gaetano, C.; Illy, B.; Zuco, V.; Supino, R.; Zunino, F. A novel atypical retinoid endowed with pro-apoptotic and antitumor activity. J. Med. Chem. 2003, 46, 909–912.

(16) Strickland, S.; Breitman, T. R.; Frickel, F.; Nürrenbach, A.; Hädicke, E.; Sporn, M. B. Structure-activity relationships of a new series of retinoidal benzoic acid derivatives as measured by induction of differentiation of murine F9 teratocarcinoma cells and human HL-60 promyelocytic leukemia cells. Cancer Res. 1983, 43, 5268–5272.

(17) Boehm, M. F.; Zhang, L.; Badea, B. A.; White, S. K.; Mais, D. E.; Berger, E.; Suto, C. M.; Goldman, M. E.; Heyman, R. A. Synthesis and structure-activity relationships of novel retinoid X receptor-selective retinoids. J. Med. Chem. 1994, 37, 2930–2941.

(18) Boehm, M. F.; Zhang, L.; Zhi, L.; McClurg, M. R.; Berger, E.; Wagoner, M.; Mais, D. E.; Suto, C. M.; Davies, P. J. A.; Heyman, R. A.; Nadzan, A. M. Design and synthesis of potent retinoid X receptor selective ligands that induce apoptosis in leukemia cells. J. Med. Chem. 1995, 38, 3146–3155.

(19) Renaud, J.-P.; Rochel, N.; Ruff, M.; Vivat, V.; Chambon, P.; Gronemeyer, H.; Moras, D. Crystal structure of the RAR-γ ligand-binding domain bound to all-trans retinoic acid. Nature 1995, 378, 681–689.

(20) Keidel, S.; Lemotte, P.; Apfel, C. Different agonist- and antagonist-induced conformational changes in retinoic acid receptors analyzed by protease mapping. Mol. Cell. Biol. 1994, 14, 287–298.

(21) Green, D. R.; Reed, J. C. Mitochondria and apoptosis. Science 1998, 281, 1309–1312.

(22) Li, H.; Kolluri, S. K.; Gu, J.; Dawson, M. I.; Cao, X.; Hobbs, P. D.; Lin, B.; Chen, G.; Lu, J.; Lin, F.; Xie, Z.; Fontana, J. A.; Reed, J. C.; Zhang, X. Cytochrome c release and apoptosis induced by mitochondrial targeting of nuclear orphan receptor TR3. Science 2000, 289, 1159–1164.

(23) Lin, B.; Kolluri, S. K.; Lin, F.; Liu, W.; Han, Y. H.; Cao, X.; Dawson, M. I.; Reed, J. C.; Zhang, X.-K. Conversion of Bcl-2 from protector to killer by interaction with nuclear orphan receptor Nur77/TR3. Cell 2004, 116, 527–540.

(24) Han, Y. H.; Cao, X.; Lin, B.; Lin, F.; Kolluri, S. K.; Stebbins, J.; Reed, J. C.; Dawson, M. I.; Zhang, X.-K. Regulation of Nur77 nuclear export by c-Jun N-terminal kinase and Akt. Oncogene 2006, 25, 2974–2986.

(25) Farhana, L.; Dawson, M. I.; Leid, M.; Wang, L.; Moore, D. D.; Liu, G.; Xia, Z.; Fontana, J. A. Adamantyl-substituted retinoid-related molecules bind small heterodimer partner and modulate the Sin3A repressor. Cancer Res. 2007, 67, 318–325.

(26) Lynch, C. J.; Milner, J. Loss of one p53 allele results in four-fold reduction of p53 mRNA and protein: A basis for p53 haplo-insufficiency. Oncogene 2006, 25, 3463–3470.

(27) Hollstein, M.; Sidransky, D.; Vogelstein, B.; Harris, C. C. p53 mutations in human cancers. *Science* **1991**, *253*, 49–53.

(28) Amstrong, R. B.; Ashenfelter, K. O.; Eckhoff, C.; Levin, A. A.; Shapiro, S. S. General and reproductive toxicology of retinoids. In *The Retinoids, Biology, Chemistry and Medicine*; Sporn, M. B., Roberts, A. B., Goodman, D. S., Eds.; Raven Press: New York, 1994; pp 545–572.

(29) Miyaura, N.; Suzuki, A. Palladium-catalyzed cross-coupling reactions of organoboron compounds. *Chem. Rev.* **1995**, *95*, 2457–2483.

(30) Malik, I.; Hussain, M.; Ali, A.; Toguem, S.-M. T.; Basha, F. Z.; Fischer, C.; Langer, P. Synthesis of 2,3-disubstituted pyrazines and quinoxalines by Heck cross-coupling reactions of 2,3-dichloropyrazine and 2,3-dichloroquinoxaline. Influence of the temperature on the product distribution. *Tetrahedron* **2010**, *66*, 1637–1642.

(31) Dawson, M. I.; Fontana, J. A.; Zhang, X.-K.; Leid, M.; Jong, L.; Hobbs, P. D. Preparation of cinnamic acids for induction of apoptosis in cancer cells. World Patent WO 048101, 2003.

(32) Dawson, M. I.; Hobbs, P.; Derdzinski, K.; Chan, R. L.-S.; Gruber, J.; Chao, W.; Smith, S.; Thies, R. W.; Schiff, L. J. Conformationally restricted retinoids. *J. Med. Chem.* **1984**, *27*, 1516–1531.

(33) Mukherjee, C.; Biehl, E. An efficient synthesis of benzene fused six-, seven-, and eight-membered rings containing nitrogen and sulfur by benzyne ring closure reaction. *Heterocycles* **2004**, *63*, 2309–2318.

(34) Macchiarulo, A.; Rizzo, G.; Costantino, G.; Fiorucci, S.; Pellicciari, R. Unveiling hidden features of orphan nuclear receptors: The case of the small heterodimer partner (SHP). *J. Mol. Graphics Modell.* **2006**, *24*, 362–372.

(35) Torrado, A.; Lamas, C.; Agejas, J.; Jiménez, A.; Díaz, N.; Gilmore, J.; Boot, J.; Findlay, J.; Hayhurst, L.; Wallace, L.; Broadmore, R.; Tomlinson, R. Novel selective and potent 5-HT reuptake inhibitors with 5-HT$_{1D}$ antagonist activity: Chemistry and pharmacological evaluation of a series of thienopyran derivatives. *Bioorg. Med. Chem.* **2004**, *12*, 5277–5295.

(36) Toto, P.; Gesquière, J.-C.; Cousaert, N.; Deprez, B.; Willand, N. UFU ('Ullmann–Finkelstein–Ullmann'): A new multicomponent reaction. *Tetrahedron Lett.* **2006**, *47*, 4973–4978.

(37) Gieseler, F.; Bauer, E.; Nuessler, V.; Clark, V.; Valsamas, S. Molecular effect of topoisomerase II inhibitors in AML cell lines: Correlation of apoptosis with topoisomerase II activity but not with DNA damage. *Leukemia* **1999**, *13*, 1859–1863.

(38) Amico, D.; Barbui, A. M.; Erba, E.; Rambaldi, A.; Introna, M.; Golay, J. Differential response of human acute myeloid leukemia cell to gemtuzumab ozogamicin in vitro: Role of Chk1 and Chk2 phosphorylation and caspase 3. *Blood* **2003**, *101*, 4589–4597.

(39) Kastan, M. B.; Radin, A. I.; Kuerbitz, S. J.; Onyekwere, O.; Wolkow, C. A.; Civin, C. I.; Stone, K. D.; Woo, T.; Ravindranath, Y.; Craig, R. W. Levels of p53 protein increase with maturation in human hematopoietic cells. *Cancer Res.* **1991**, *51*, 4279–4286.

(40) Duong, V.; Licznar, A.; Margueron, R.; Boulle, N.; Busson, M.; Lacroix, M.; Katzenellenbogen, B. S.; Cavaillès, V.; Lazennec, G. ERα and ERβ expression and transcriptional activity are differentially regulated by HDAC inhibitors. *Oncogene* **2006**, *25*, 1799–1806.

(41) Weisz, A.; Basile, W.; Scafoglio, C.; Altucci, L.; Bresciani, F.; Facchiano, A.; Sismondi, P.; Cicatiello, L.; Bortoli, M. D. Molecular identification of ERα-positive breast cancer cells by the expression profile of an intrinsic set of estrogen regulated genes. *J. Cell. Physiol.* **2004**, *200*, 440–450.

(42) Emi, M.; Kim, R.; Tanabe, K.; Uchida, Y.; Toge, T. Targeted therapy against Bcl-2-related proteins in breast cancer cells. *Breast Cancer Res.* **2005**, *7*, R940–R952.

(43) Sala, F.; Zucchetti, M.; Bagnati, R.; D'Incalci, M.; Pace, S.; Capocasa, F.; Marangon, E. Development and validation of a liquid chromatography-tandem mass spectrometry method for the determination of ST1926, a novel oral antitumor agent, adamantyl retinoid dervative, in plasma of patients in a phase I study. *J. Chromatogr. B* **2009**, *877*, 3118–3126.

(44) Swanson, B. N.; Newton, D. L.; Roller, P. P.; Sporn, M. B. Biotransformation and biological activity of *N*-(4-hydroxyphenyl) retinamide derivatives in rodents. *J. Pharmacol. Exp. Ther.* **1981**, *219*, 632–637.

(45) Peng, Y.-M.; Dalton, W. S.; Alberts, D. S.; Xu, M.-J.; Lim, H.; Meyskens, F. L., Jr. Pharmacokinetics of *N*-4-hydroxyphenyl-retinamide and the effect of its oral administration on plasma retinol concentrations in cancer patients. *Int. J. Cancer* **1989**, *43*, 22–26.

(46) Borutinskaite, V. V.; Navakauskiene, R.; Magnusson, K.-E. Retinoic acid and histone deacetylase inhibitor BML-210 inhibit proliferation of human cervical cancer HeLa cells. *Ann. N.Y. Acad. Sci.* **2006**, *1091*, 346–355.

(47) Kuo, H.-S.; Hsu, F.-N.; Chiang, M.-C.; You, S.-C.; Chen, M.-C.; Lo, M.-J.; Lin, H. The role of Cdk5 in retinoic acid-induced apoptosis of cervical cancer cell line. *Chin. J. Physiol.* **2009**, *52*, 23–30.

(48) Doane, A. S.; Danso, M.; Lal, P.; Donaton, M.; Zhang, L.; Hudis, C.; Gerald, W. L. An estrogen receptor-negative breast cancer subset characterized by a hormonally regulated transcriptional program and response to androgen. *Oncogene* **2006**, *25*, 3994–4008.

(49) Lal, P.; Tan, L. K.; Chen, B. Correlation of Her-2 status with estrogen and progesterone receptors and histologic features in 3655 invasive breast carcinomas. *Am. J. Clin. Pathol.* **2005**, *123*, 541–546.

(50) Lacroix, M.; Toillon, R.-A.; Leclercq, G. p53 and breast cancer, an update. *Endocr.-Relat. Cancer* **2006**, *13*, 293–325.

(51) Rishi, A. K.; Gerald, T. M.; Shao, Z.-M.; Li, X.-S.; Baumann, R.-G.; Dawson, M. I.; Fontana, J. A. Regulation of the human retinoic acid receptor α gene in the estrogen receptor negative human breast carcinoma cell lines SKBR-3 and MDA-MB-435. *Cancer Res.* **1996**, *56*, 5246–5252.

(52) Shiau, R.-J.; Chen, K.-Y.; Wen, Y.-D.; Chuang, C.-H.; Yeh, S.-L. Genistein and β-carotene enhance the growth-inhibitory effect of trichostatin in A549 cell. *Eur. J. Nutr.* **2010**, *49*, 19–25.

(53) Liu, J.-P.; Wei, H.-B.; Zheng, Z.-H.; Guo, W.-P.; Fang, J.-F. Celecoxib increases retinoid sensitivity in human colon cancer cell lines. *Cell. Mol. Biol. Lett.* **2010**, *15*, 440–450.

(54) Gediya, L. K.; Khandelwal, A.; Patel, J.; Belosay, A.; Sabnis, G.; Mehta, J.; Purushottamachar, P.; Njar, V. C. Design, synthesis, and evaluation of novel mutual prodrugs (hybrid drugs) of all-*trans*-retinoic acid and histone deacetylase inhibitors with enhanced anticancer activities in breast and prostate cancer cells in vitro. *J. Med. Chem.* **2008**, *51*, 3895–3904.

(55) Jones, H. E.; Eaton, C. L.; Barrow, D.; Dutkowski, C.; Griffiths, K. Response of cell growth and retinoic acid receptor expression to retinoic acid in neoplastic and non-neoplastic prostate cell lines. *Prostate* **1997**, *30*, 174–182.

(56) Farhana, L.; Dawson, M. I.; Dannenberg, J. H.; Xu, L.; Fontana, J. A. SHP and Sin3A expression are essential for adamantyl-substituted retinoid-related molecule-mediated nuclear factor-κB activation, c-Fos/c-Jun expression, and cellular apoptosis. *Mol. Cancer Ther.* **2009**, *8*, 1625–1635.

(57) Farhana, L.; Dawson, M. I.; Xia, Z.; Aboukameel, A.; Xu, L.; Liu, G.; Das, J. K.; Hatfield, J.; Levi, E.; Mohammad, R.; Fontana, J. A. Adamantyl-substituted retinoid-related molecules induce apoptosis in human acute myelogenous leukemia cells. *Mol. Cancer Ther.* **2010**, *9*, 2903–2913.

(58) Dalvit, C; Flocco, M.; Knapp, S.; Mostardini, M.; Perego, R.; Stockman, B. J.; Veronesi, M.; Varasi, M. High-throughput NMR-based screening with competition binding experiments. *J. Am. Chem. Soc.* **2002**, *124*, 7720–7709.

(59) Shortridge, M. D.; Hage, D. S.; Harbison, G. S.; Powers, R. Estimating protein-ligand binding affinity using high-throughput screening by NMR. *J. Comb. Chem.* **2008**, *10*, 948–958.

(60) Scheiner, S.; Kar, T.; Pattanayak, J. Comparison of various types of hydrogen bonds involving aromatic amino acids. *J. Am. Chem. Soc.* **2002**, *124*, 13257–13264.

(61) Kovács, A.; Varga, Z. Halogen acceptors in hydrogen bonding. *Coord. Chem. Rev.* **2006**, *250*, 710–727.

(62) Chao, W.; Hobbs, P. D.; Jong, L.; Zhang, X.-K.; Zhang, Y.; Wu, Q.; Shroot, B.; Dawson, M. I. Effects of receptor class-and subtype-selective retinoids and an apoptosis-inducing retinoid on the adherent growth of the NIH:OVCAR-3 ovarian cancer cell line in culture. *Cancer Lett.* **1997**, *115*, 1–7.

(63) Tzimas, G.; Thiel, R.; Chahoud, I.; Nau, H. The area under the concentration-time curve of all-*trans*-retinoic acid is the most suitable pharmacokinetic correlate to the embryotoxicity of this retinoid in the rat. *Toxicol. Appl. Pharmacol.* **1997**, *143*, 436–444.

(64) Zile, M. H.; Inhorn, R. C.; DeLuca, H. F. Metabolism in vivo of all-*trans*-retinoic acid. *J. Biol. Chem.* **1982**, *257*, 3544–3550.

(65) Disdier, B.; Bun, H.; Placidi, M.; Durand, A. Excretion of oral 9-*cis*-retinoic acid in the rat. *Drug Metab. Dispos.* **1996**, *24*, 1279–1281.

(66) Howell, S. R.; Shirley, M. A.; Grese, T. A.; Neel, D. A.; Wells, K. E.; Ulm, E. H. Bexarotene metabolism in rat, dog, and human, synthesis of oxidative metabolites, and in vitro activity at retinoid receptors. *Drug Metab. Dispos.* **2001**, *29*, 990–998.

(67) Gorman, G. S.; Coward, L.; Kerstner-Wood, C.; Cork, L.; Kapetanovic, I. M.; Brouillette, W. J.; Muccio, D. D. In vitro metabolic characterization, phenotyping, and kinetic studies of 9cUAB30, a retinoid X receptor-specific retinoid. *Drug Metab. Dispos.* **2007**, *35*, 1157–1164.

(68) Mizojiri, K.; Okabe, H.; Sugeno, K.; Misaki, A.; Ito, M.; Kominami, G.; Esumi, Y.; Takaichi, M.; Harada, T.; Seki, H.; Inaba, A. Studies on the metabolism and disposition of the new retinoid 4-[(5,6,7,8-tetrahydro-5,5,8,8-tetramethyl-2-naphthyl)carbamoyl]benzoic acid. 4th communication: Absorption, metabolism, excretion and plasma protein binding in various animals and man. *Arzneimittelforschung* **1997**, *47*, 259–269.

(69) Hashimoto, S.; Mizobuchi, M.; Kuroda, T.; Okabe, H.; Mizojiri, K.; Takahashi, S.; Kikuchi, J.; Terui, Y. Biotransformation of a new synthetic retinoid, 4-[(5,6,7,8-tetrahydro-5,5,8,8-tetramethyl-2-naphthyl)carbamoyl]benzoic acid (Am-80), in the rat. Structure elucidation of the metabolites by mass and NMR spectrometry. *Xenobiotica* **1994**, *24*, 1177–1193.

(70) Adamas, D. H.; Whittaker, V. P. The characterization of the esterases of human plasma. *Biochem. J.* **1949**, *44*, 62–70.

(71) Ognyanov, V. I.; Balan, C.; Bannon, A. W.; Bo, Y.; Dominguez, C.; Fotsch, C.; Gore, V. K.; Klionsky, L.; Ma, V. V.; Qian, Y.-X.; Tamir, R.; Wang, X.; Xi, N.; Xu, S.; Zhu, D.; Gavva, N. R.; Treanor, J. J. S.; Norman, M. H. Design of potent, orally available antagonists of the transient receptor potential vanilloid 1. Structure—activity relationships of 2-piperazin-1-yl-1*H*-benzimidazoles. *J. Med. Chem.* **2006**, *49*, 3719–3742.

(72) Goodman, A. J.; Stanforth, S. P.; Tarbit, B. Desymmetrization of dichloroazaheterocycles. *Tetrahedron* **1999**, *55*, 15067–15070.

(73) Murugesan, N.; Gu, Z.; Fadnis, L.; Tellew, J. E.; Baska, R. A. F.; Yang, Y.; Beyer, S. M.; Monshizadegan, H.; Dickinson, K. E.; Valentine, M. T.; Humphreys, W. G.; Lan, S.-J.; Ewing, W. R.; Carlson, K. E.; Kowala, M. C.; Zahler, R.; Macor, J. E. Dual angiotensin II and endothelin A receptor antagonists: Synthesis of 2′-substituted *N*-3-isoxazolyl biphenylsulfonamides with improved potency and pharmacokinetics. *J. Med. Chem.* **2005**, *48*, 171–179.

(74) van den Heuvel, M.; van den Berg, T. A.; Kellogg, R. M.; Choma, C. T.; Feringa, B. L. Synthesis of a non-heme template for attaching four peptides: An approach to artificial iron(II)-containing peroxidases. *J. Org. Chem.* **2004**, *69*, 250–262.

(75) Goodacre, S. C.; Williams, K.; Price, S.; Dyke, H. J.; Montana, J. G.; Stanley, M. S.; Bao, L.; Lee, W. Aza-indolyl compounds and methods of use. World Patent WO 067481, 2008.

(76) Patrick, D. A.; Bakunov, S. A.; Bakunova, S. M.; Kumar, E. V. K. S.; Lombardy, R. J.; Jones, S. K.; Bridges, A. S.; Zhirnov, O.; Hall, J. E.; Wenzler, T.; Brun, R.; Tidwell, R. R. Synthesis and in vitro antiprotozoal activities of dicationic 3,5-diphenylisoxazoles. *J. Med. Chem.* **2007**, *50*, 2468–2485.

(77) Touzeau, F.; Arrault, A.; Guillaumet, G.; Scalbert, E.; Pfeiffer, B.; Rettori, M.-C.; Renard, P.; Mérour, J.-Y. Synthesis and biological evaluation of new 2-(4,5-dihydro-1*H*-imidazol-2-yl)-3,4-dihydro-2*H*-1,4-benzoxazine derivatives. *J. Med. Chem.* **2003**, *46*, 1962–1979.

(78) Seol, W.; Hanstein, B.; Brown, M.; Moore, D. D. Inhibition of estrogen receptor action by the orphan receptor SHP (short heterodimer partner). *Mol. Endocrinol.* **1998**, *10*, 1551–1557.